

COCHIN UNIVERSITY OF SCIENCE AND
TECHNOLOGY



DOCTORAL THESIS

**Studies on cosmology and
thermodynamics of holographic dark
energy**

Author:

Praseetha P
Department of Physics
CUSAT

Supervisor:

Dr. Titus K Mathew
Associate Professor
Department of Physics
CUSAT

*A thesis submitted in partial fulfilment of the
requirements for the award of the degree of
Doctor of Philosophy in Science*

SEPTEMBER 2015

Declaration

I hereby declare that this thesis titled, “**Studies on cosmology and thermodynamics of holographic dark energy**” and the work presented in it are my own under the supervision of Dr. Titus K Mathew, Associate professor, Department of Physics, Cochin University of Science and Technology, Cochin-22. I hereby confirm that any part of this thesis has not previously been submitted for the award of any degree or any other qualification at this University or any other institution.

Cochin-22

Praseetha P

September 2015

Certificate

Certified that the work presented in this thesis titled “**Studies on cosmology and thermodynamics of holographic dark energy**” authored by Ms.Praseetha P, Department of Physics, Cochin University of Science and Technology, Cochin-22, is a bona fide work done by herself under my supervision, during the period 2011-2015 and is not included in any other previous work for any degree .

Cochin-22
SEPTEMBER 2015

Dr.Titus K Mathew
(Supervising Guide)
Associate Professor
Department of Physics
Cochin University of Science
and Technology, Cochin-22

Certificate

Certified that all the suggestions and modifications raised during the pre-synopsis presentation, conducted on 08-04-2015, recommended by the doctoral committee have been suitably incorporated in the Ph.D thesis entitled “**Studies on cosmology and thermodynamics of holographic dark energy**” by Ms.Praseetha P, who has carried out the research work in the Department of Physics, Cochin University of Science and Technology, under my guidance.

Cochin-22

SEPTEMBER 2015

Dr.Titus K Mathew

(Supervising Guide)

Associate Professor

Department of Physics

Cochin University of Science

and Technology, Cochin-22

Acknowledgments

I express my sincere gratitude to Dr. Titus K Mathew, Associate Professor, Cochin University of Science and Technology for his valuable guidance and unconditional support throughout the course of my work. I am thankful to Dr. S. Jayalekshmi, the Head of the department for her valuable advices during the completion of the work. I would like to thank Dr. Pradeep B, the former Head of the department who has helped in facilitating necessary requirements for the entire period of my work. My deep respect to Prof. V C Kuriakose, who has provided me the facilities to carry out data analysis. I am indebted to Prof. Ramesh Babu T and Prof. M Sabir, for their comments and queries which has helped the upbringing of my work. At this juncture I would like to express my boundless gratitude to Prof. M R Anantharaman, Prof. C Sudha Kartha, Prof. M K Jayaraj, Prof. K P Vijayakumar, Dr. M Junaid Bushiri, Prof. Godfrey Louise and Dr. Raveendranathan.

I am grateful to all non-teaching staff of the department whose attentiveness have made the period of research so sound and smooth.

I am thankful to all my teachers and friends. I have enjoyed the

friendly association with my junior labmates Athira Sasidharan, Paxy George and M.Phil scholar Elizabeth. They are very helpful at needs and a mere thanks will not suffice. I also thank Dintomon joy, research scholar of theory division for his friendly co-operation.

I mention my hearty thanks to my room mate, Ancy Issac, with whom I have shared a very memorable companionship.

The efforts of my mother, father, sisters and grand mother which inspired and enthused me in completing this work are boundless. I express my heartfelt love to all of them.

Praseetha P

Preface

Cosmology deals with the studies on the structure and evolution of the universe. The model of the universe formulated by Friedmann, Lemaitre, Robertson and Walker known as the standard model (FLRW model) of the universe, which is based on the Einstein's theory of gravity, turned out to be the accepted model because of the various observational supports. The major observational supports to this model are the explanation for the Hubble's law, primordial nucleosynthesis, microwave back ground radiation etc.

Recent observations on Type Ia supernovae by teams led by S Perlmutter, Brian P Schmidt and Adam G Riess led to the discovery that the present universe is expanding in an accelerated manner. The exotic form of matter which causes the acceleration is termed as dark energy which produce negative pressure. Understanding the nature and evolution of dark energy is a challenge for the cosmologists. In addition to the evidences from supernovae, the anisotropy in CMBR spectra, large scale structures and Baryon acoustic oscillations are also supporting the discovery.

To explain dark energy, various theoretical models have been proposed. One such model is the Λ CDM model, in which the universe is assumed to be composed of dark energy and dark matter. In this

model, Einstein's cosmological constant is considered as dark energy. It has a constant equation of state, $\omega_\Lambda = \frac{p_\Lambda}{\rho_\Lambda} = -1$. The model predicts the values of cosmological parameters such as the Hubble parameter, transition redshift and present deceleration parameter, having a very good agreement with the observational constraints. But this model has two major flaws, which are:

1. Cosmological constant problem:- Theoretically predicted value of dark energy density as the vacuum constant Λ is, $\rho_\Lambda \sim 10^{74}\text{GeV}^4$, while the observed value is $\rho_\Lambda \sim 10^{-47}\text{GeV}^4$. The predicted value is greater than the observed value by 120 orders of magnitude. This discrepancy between the theoretical and observational values is known as the cosmological constant problem.
2. Cosmological coincidence problem:- Energy densities of dark energy and dark matter are found to be of the same order even though their evolutionary nature are different. This is known as the coincidence problem which is not explained by the Λ CDM model.

These led to the proposals of dynamical dark energy models by considering that the equation of state parameter is evolving with the expanding universe. Scalar models of dark energy such as Quintessence, K-essence, Phantom model, Chaplygin gas model and holographic

dark energy model are examples of dynamic dark energy models.

Holographic dark energy model is based on the holographic principle developed by Susskind and 't Hooft. The principle says that the degrees of freedom of a system resides on its surface rather than in its volume. The total energy inside a region of size L must not exceed the mass of a black hole of the same size. The holographic dark energy density can then be formulated as,

$$\rho_{\Lambda} = 3c^2 M_{pl}^2 L^{-2} \quad (1)$$

where $3c^2$ is a numerical constant, $M_{pl}^{-2} = 8\pi G$ is the reduced Planck mass. Possible choices for L , the IR cut-off, are Hubble horizon, particle horizon and event horizon. The choices for the IR cut-off whether it be Hubble horizon or particle horizon will not support an accelerating universe, while the third choice, the event horizon, violates causality. Another alternative for the IR cut-off is the Ricci scalar, which was first introduced by Gao et al. Later modified holographic Ricci dark energy was proposed by Granda and Oliveros.

In the present thesis, the modified Ricci dark energy is studied by considering its interaction with the dark matter present in the universe. Owing to the lack of knowledge about the microscopic origin of such an interaction, phenomenological interaction forms of non-gravitational nature is assumed.

The modified Ricci dark energy density is given by,

$$\rho_{de} = (2\dot{H} + 3\alpha H^2)/(\alpha - \beta) \quad (2)$$

where α and β are parameters of the model. Interaction is defined through the conservation equations for the entities inside the universe given by

$$\dot{\rho}_{de} + 3H(\rho_{de} + p_{de}) = -Q \quad (3)$$

$$\dot{\rho}_m + 3H(\rho_m) = Q \quad (4)$$

where Q is the interaction term with forms, $Q = 3bH(\rho_{de} + \rho_m)$, $Q = 3bH\rho_m$, and $Q = 3bH\rho_{de}$, where b is the interaction parameter, $b > 0$ implies dark energy decaying into dark matter. The evolution of the interacting modified holographic Ricci dark energy(IMHRDE) and also the thermodynamics are studied, especially the status of the Generalized second law(GSL) both at the apparent horizon and event horizon of the universe.

The objectives of the thesis are the following:

1. To study the cosmology and thermodynamics of the modified holographic Ricci dark energy model which is in interaction with the dark matter corresponding to the three interaction forms.
2. To constrain the parameters of the model and hence to extract the Hubble parameter using the Type Ia supernovae data.

3. To check how the model solves the Cosmological constant problem.
4. To check how the model explain Cosmological coincidence.
5. To study the evolution of the entropy of the dark energy.
6. To study the status of GSL under both thermal equilibrium and non equilibrium conditions by taking apparent horizon and also event horizon as the boundary of the universe.

By solving the Friedmann equations using the equation for interacting Ricci dark energy, the evolutions of Hubble parameter and dark energy density can be studied. Subsequently the evolutions of the equation of state parameter and decelerations parameter can be obtained. From the Hubble parameter, the distance moduli of the supernovae at respective redshifts are obtained and are compared with the observational data, which is further checked for fitting of the theory with observation. Statistical χ^2 analysis were done to evaluate the parameters of the model including the present value of the Hubble parameter. These values can be used to generate the evolutionary behavior of various cosmological parameters.

The comparison of the IMHRDE model with other models, especially the Λ CDM model were carried out by diagnosing the model with statefinder (r, s) parameters.

The entropy of the dark energy is evaluated and its evolution is studied. The validity of the GSL is studied taking apparent horizon as well as event horizon as the boundary of the universe. The Gibb's relation is used to calculate the entropy of the dark energy and dark matter and Bekenstein's relation is used to obtain the entropy of the horizon. The entropy evolutions were studied under thermal equilibrium and non-equilibrium conditions.

The present work entitled "Studies on the cosmology and thermodynamics of holographic dark energy" is organized into nine chapters. The first chapter is a general introduction to the basic area of the cosmology and FLRW model.

The second chapter details different dark energy models like Λ CDM model, Scalar field models such as Quintessence, K-essence, Phantom model, fluid model like Chaplygin gas model, and Holographic dark energy model. Their advantages and disadvantages are discussed in this chapter.

The third chapter encompasses the history leading to the formation of holographic dark energy model.

Fourth chapter describes the non-interacting modified holographic Ricci dark energy model. Its cosmology is discussed. The merits and de-merits of the model are pointed out here.

In Fifth chapter the interacting model is considered with interaction term $Q = 3bH(\rho_{de} + \rho_m)$, termed as IMHRDE1 model. Co-evolution of dark energy and dark matter is studied for interaction parameter $b = 0.001$. The cosmology of the model is studied. The validity of GSL, which states that the total entropy of the fluid contents inside the universe when added with the entropy of the cosmological horizon must always increase, is checked under thermal equilibrium and non-equilibrium conditions for a universe bounded by apparent horizon and event horizon. The entropy evolution is studied assuming a dark energy dominated universe. It is analyzed that the entropy of the dark energy decreases as the universe expands while the entropy of the horizon and the total entropy of the universe increase as the universe expands.

In sixth chapter, the cosmology of second interaction model IMHRDE2 with interaction term $Q = 3bH\rho_m$ is analyzed. Co-evolution of dark energy and dark matter is explained for interaction parameter $b = 0.003$. Validity of GSL is checked under thermal equilibrium condition and non-equilibrium conditions for a universe bounded by apparent horizon and event horizon. The entropy evolution of the dark energy is studied. The entropy of the dark energy is found to be decreasing as the universe expands, the increase in the horizon entropy compensates this loss resulting in the increase of total entropy

as the universe expands implying the validity of the GSL.

Chapter seven details the cosmology and thermodynamics of the third interaction model IMHRDE3 with $Q = 3bH\rho_{de}$. Co-evolution of dark energy and dark matter is analyzed for interaction parameter $b = 0.009$. The characteristics of the equation of state parameter and deceleration parameter are studied. The validity of GSL is checked under thermal equilibrium condition and non-equilibrium conditions for a universe limited by apparent horizon and event horizon. Evolution of entropy of dark energy under a dark energy dominated case is studied.

Chapter eight comprises statistical analysis. The Chi square minimum method is used to extract the best fit parameters of the model. Confidence contours are drawn in order to estimate errors in the best fit parameters. Error plots are drawn comparing the theoretical and observation values of the distance modulus.

Chapter nine incorporates conclusions and discussions.

Important findings of the study are:

1. A flat universe consisting two interacting components, the dark matter and holographic Ricci dark energy are considered. The evolution characteristics of the Hubble parameter, equation of state parameter and deceleration parameter are obtained.

2. Statistical χ^2 analysis is done using the Type Ia supernovae data to constrain the parameters of the model and obtained the present value of the Hubble parameter. Cosmological parameters are also obtained and are in close agreement with the observational values.
3. It is found that the model is free from Cosmological constant problem.
4. The model also explained the cosmological coincidence of the densities of dark matter and dark energy.
5. Study of thermodynamics showed apparent horizon as the thermodynamic boundary of the universe.
6. The model with the interaction term $Q \propto \rho_{de}$ is having a poor fit with the Type Ia observational data when compared to other types of interaction.

The inferences from the present work are that the IMHRDE model predicts the cosmological parameters which are in close agreement with the observational values from WMAP observation. IMHRDE1 ($Q \propto \rho_m$) and IMHRDE2 ($Q \propto \rho_{de} + \rho_m$) are fitting with the observational data when compared to IMHRDE3 ($Q \propto \rho_{de}$). The advantages of the model are that the model solves cosmological constant problem and explains the cosmological coincidence.

The works presented in this thesis are partially published as research articles in the international journals as given below:

1. Praseetha P and Titus K Mathew, "Interacting modified holographic Ricci dark energy model and statefinder diagnosis in flat universe", *Int. J. Mod. Phys. D*, **23**, 1450024 ,(2014). (arXiv no: 1309.3136)
2. Titus K Mathew and Praseetha P, "Holographic dark energy and generalized second law", *Mod.Phys.Lett.A*, **29**, 1450023, (2014). (arXiv no: 1311.4661)
3. Praseetha P and Titus K Mathew, "Entropy of holographic dark energy and the generalized second law", *Class. Quant. Grav.*, **31**, 185012, (2014). (arXiv no: 1401.8117)
4. Praseetha P and Titus K Mathew, "Evolution of holographic dark energy with interaction term $Q \propto H\rho_{de}$ and generalized second law", *Pramana-J.Phys.*(accepted for publication), (2015).

Dedicated to my sisters, Prasia and Natasha

Contents

Acknowledgements	vi
Preface	viii
Table of Contents	xxi
List of Figures	xxvii
List of Tables	xxxvii
1 Introduction to Cosmology	1
1.1 Introduction	1
1.2 FLRW model of the universe	4
1.3 Friedmann equations	5
1.4 Friedmann model with Cosmological constant . .	10
1.5 Solutions of the Friedmann equations	11
1.6 Observational Parameters of the Friedmann uni- verse	13
1.7 Accelerating Universe	17
2 Dark Energy	25
2.1 Dark energy	25
2.1.1 Cosmological constant	25

2.1.2	Quintessence Model	27
2.1.3	K-essence model	29
2.1.4	Phantom model	30
2.1.5	Chaplygin gas model	30
2.1.6	An alternative model based on holographic principle	32
3	Holographic Dark Energy Model	35
3.1	Holographic Dark energy Model	35
3.1.1	Black hole thermodynamics and general- ized second law of thermodynamics	36
3.1.2	UV/IR connection	38
3.1.3	Possible candidates for L , the IR cut-off .	39
4	Holographic Ricci Dark Energy Model	43
4.1	Holographic Ricci dark energy model	43
4.2	Non-interacting modified holographic Ricci dark energy model	46
5	Interacting modified holographic Ricci dark energy model	51

5.1	Interacting modified holographic Ricci dark energy model	51
5.2	Interacting modified holographic Ricci dark energy model with $Q = 3bH(\rho_{de} + \rho_m)$ -IMHRDE1	53
5.3	Thermodynamics of IMHRDE1 model	64
5.3.1	GSL validity under thermal equilibrium conditions	65
5.3.2	GSL validity under thermal non-equilibrium conditions	73
5.4	Entropy evolution of IMHRDE1	74
5.5	Conclusions	76
6	Interacting modified holographic Ricci dark energy model with interaction term $Q \propto H\rho_m$ -IMHRDE2	79
6.1	Interacting modified holographic Ricci dark energy model with interaction term $Q \propto H\rho_m$ - IMHRDE2	79
6.2	Study of the thermodynamics of IMHRDE2	89
6.2.1	Analysis of IMHRDE2 under thermal equilibrium	90

6.2.2	Analysis of IMHRDE2 under thermal non-equilibrium condition	96
6.3	Conclusion	99
7	Interacting modified holographic Ricci dark energy model with interaction term	
	$Q \propto H\rho_{de}$ -IMHRDE3	103
7.1	Interacting modified holographic Ricci dark energy model with interaction term $Q \propto H\rho_{de}$ -IMHRDE3	103
7.2	Thermodynamics of the IMHRDE3 model	112
7.2.1	Analyzing the case of thermal equilibrium	114
7.2.2	Analyzing the case of thermal non-equilibrium	120
7.3	Conclusion	123
8	Extracting the model parameters	127
8.1	Statistical Methods	128
8.1.1	Determining the best fit parameters using Union2 compilation-SNLS+ESSENCE data	128
8.1.2	Confidence Contours	130

8.1.3	Drawing confidence regions and error estimation for IMHRDE best fit model parameters	131
8.1.4	Variation of distance modulus- comparison of theory and observation	134
8.2	Conclusion	135
9	Conclusion	139
9.1	Major findings and conclusion	139
9.2	Scope for further study	146
	References	149
	Appendix	159

List of Figures

1.1	[Luminosity distance in units of H_0^{-1} for a universe with non-relativistic matter and cosmological constant ($\omega_\Lambda = -1$). Plots A,B,C,D corresponds to $\Omega_\Lambda = 0, 0.3, 0.7, 1$ respectively. Courtesy [20]]	21
1.2	[Prediction of CMBR anisotropy [21, 22]. Courtesy [23].]	23
4.1	[Evolution of equation of state parameter ω_{de} with redshift z for best fit values $(\alpha, \beta) = (1.01, 0.15)$.]	48
4.2	[Evolution of deceleration parameter q for best fit model parameters $(\alpha, \beta) = (1.01, 0.15)$.]	49
5.1	[Evolution of IMHRDE1 in comparison with the cold dark matter, with parameters $(\alpha, \beta) = (1.01, -0.01)$ and $b=0.001$. The continuous line which is deviating represents IMHRDE1 and the other one represents cold dark matter.]	56

- 5.2 [Variation of the equation of state parameter ω_{de} with redshift z for the model parameters $(\alpha, \beta)=(1.2, -0.1)$ -thin continuous, first from the left bottom; $(4/3, -0.05)$ -thick continuous, 2nd from left bottom; $(1.01, -0.01)$ -dotted, 3rd from left bottom; $(1.2, 0.1)$ -large dashed, 4th from left bottom; $(4/3, 0.05)$ -small dashed, 5th from left bottom and $(1.15, 0.15)$ -dot-dashed, 6th from left bottom; all with $b=0.001$.] 57
- 5.3 [Evolution of the q -parameter with redshift. The plots for $(\alpha, \beta)=(1.2, -0.1)$ -thin continuous, first from the bottom of the left side; $(4/3, -0.05)$ -large dashed line, 2nd from the bottom of the left side; $(1.01, -0.01)$ -thick continuous, third from the left bottom; $(4/3, 0.05)$ -dash-dot, 4th from the left bottom; $(1.2, 0.1)$ -dotted line, 5th from the left bottom and $(1.15, 0.15)$ - small dash line, 6th from left bottom, all with coupling constant $b = 0.001$.] 59
- 5.4 [$r-s$ evolutionary trajectories for the model for parameters, $(\alpha, \beta)=(1.2, -0.1)$ -the thin continuous line (extreme left), $(4/3, -0.05)$ -the dashed line (the middle one) and $(1.01, -0.01)$ -the thick continuous line (extreme right), all with $b=0.001$] 61

5.5 [Evolutionary trajectories of $r - s$ plane for parameters $(\alpha, \beta) = (4/3, 0.05)$ -thick continuous, left line; $(1.2, 0.1)$ -thin continuous, middle line and $(1.15, 0.15)$ -dashed, rightmost line; all with $b = 0.001$] 62

5.6 [$r - q$ plots for parameters $(\alpha, \beta) = (1.01, -0.01)$ with interaction constant $b = 0.001$, the diagonal like line representing $r - q$ trajectory of IMHRDE1 and the horizontal line with arrow is for the Λ CDM as comparison] 63

5.7 [The behavior of S' inside the apparent horizon under thermal equilibrium conditions for the parameters $(\alpha, \beta) = (1.2, 0.1)$ (thick continuous line), $(\alpha, \beta) = (1.3, 0.3)$ (thin continuous line), and $(\alpha, \beta) = (1.4, 0.3)$ (dashed line). The interaction coupling constant $b = 0.001$ for all the plots.] 68

5.8 [The behavior of S' inside the apparent horizon under thermal equilibrium conditions for the parameters $(\alpha, \beta) = (1.01, -0.01)$ (thick continuous line), $(\alpha, \beta) = (1.2, -0.1)$ (thin continuous line), and $(\alpha, \beta) = (1.3, -0.05)$ (dashed line). The interaction coupling constant $b = 0.001$ for all the plots.] 69

-
- 5.9 [Plot for the parameters $(\alpha, \beta) = (1.2, 0.1)$ (thick continuous line), $(\alpha, \beta) = (1.3, 0.3)$ (thin continuous line), and $(\alpha, \beta) = (4/3, 0.3)$ (dashed line), with the interaction coupling constant $b = 0.001$ inside the event horizon under thermal equilibrium conditions.] 71
- 5.10 [Plot for the parameters $(\alpha, \beta) = (1.01, -0.01)$ (thick continuous line), $(\alpha, \beta) = (1.2, -0.1)$ (thin continuous line), and $(\alpha, \beta) = (4/3, -0.1)$ (dashed line), with the interaction coupling constant $b = 0.001$ inside the event horizon under thermal equilibrium conditions.] 72
- 5.11 [Evolution of entropy of holographic Ricci dark energy against $x \ln a$] 75
- 5.12 [Evolution of apparent horizon entropy and total entropy against $x = \ln a$. The thick continuous line represents the total entropy S_{tot} while the thin line represents the horizon entropy S_h .] 76
- 6.1 [Evolution of IMHRDE2 model with $Q = 3bH\rho_m$, for parameters, $(\alpha, \beta) = (1.01, -0.01)$ and $b = 0.003$. Continuous line for interacting IMHRDE and dashed line is for dark matter.] 82

6.2 [Behavior of the ω_{de} of IMHRDE2 with $b=0.003$ for parameter $(\alpha, \beta)=(1.2,-0.1)$ -large dashed line, $(4/3,-0.05)$ -small dashed line, $(1.01,-0.01)$ -dotted line, $(1.2,0.1)$ -thin continuous line, $(4/3,0.05)$ -thick continuous line and $(1.15,0.15)$ -dot-dashed line] 83

6.3 [Characteristics of q -parameter of IMHRDE2 with redshift for $(\alpha, \beta)=(1.2,-0.1)$ thin continuous line, $(4/3,-0.05)$ -large dashed line, $(1.01,-0.01)$ -thick continuous line, $(4/3,0.05)$ -dot dashed line, $(1.2,0.1)$ -dotted line and $(1.15,0.15)$ - small dashed line for coupling constant $b = 0.003$.] 84

6.4 [Trajectory of the IMHRDE2 model in the $r - s$ plane $(\alpha, \beta)=(1.2,-0.1)$ -thin continuous, left line; $(4/3, -0.05)$ -dashed, middle line, $(1.01,-0.01)$ -thick continuous, right line, for $b=0.003$. The evolution is from right to left] . . . 87

6.5 [Evolutionary path of IMHRDE2 in $r - s$ plane for parameters $(\alpha, \beta)=(4/3,0.05)$ -thick continuous, left line; $(1.2,0.1)$ -thin continuous, middle line and $(1.15,0.15)$ -dashed, rightmost line; for $b=0.003$] 88

6.6 [Behavior of IMHRDE2 model in the $r - q$ plane for model parameters $(\alpha, \beta) = (1.01, -0.01)$ with $b=0.003$] 89

6.7 [Behavior of S'_{tot} with respect to x for the model parameter $(\alpha, \beta) = (1.01, -0.01)$ for $b = 0.003$.] 92

-
- 6.8 [Behavior of S'_{tot} with respect to x for model parameter $(\alpha, \beta)=(1.2,0.1)$ -first line from the bottom, $(1.2,0.3)$ -second line from the bottom, $(1.3,0.3)$ -third line from the bottom, $(1.4,0.3)$ -topmost line for $b=0.003$.] 93
- 6.9 [Behavior of S'_{tot} in relation to x for the model parameters $(\alpha, \beta)=(1.01,-0.01)$ at the event horizon of the universe with $b=0.003$.] 95
- 6.10 [Behavior of S'_{tot} with respect to x for model parameters $(\alpha, \beta)=(1.2,0.1)$ -thick continuous line, $(1.2,0.3)$ -thin continuous line, $(1.3,0.3)$ -dashed line, $(1.4,0.3)$ -dot-dashed line, for $b=0.003$.] 96
- 6.11 [Behavior of the entropy of dark energy with respect to x for the parameters $(1.2,0.1)$] 98
- 6.12 [Entropy characteristics of apparent horizon in relation to x (bottom line) and total entropy in relation to x (top line) for model parameters $(1.2,0.1)$] 99
- 7.1 [Co-evolution of energy densities of dark energy(IMHRDE3) and dark matter for $(\alpha, \beta) = (1.01, -0.01)$ with $b = 0.009$. The continuous line which deviates represents dark energy and the other line represents dark matter.] 106

7.2 [Evolution of the equation of state parameter of IMHRDE3 with $b=0.009$, for parameters $(\alpha, \beta)=(1.2,-0.1)$ - thin continuous line, first from the left bottom; $(4/3,-0.05)$ - large dashed line, 2nd from left bottom, $(1.01,-0.01)$ - thick continuous line, 3rd from the left bottom; $(4/3,0.05)$ - dot-dashed line, 4th from left bottom; $(1.2,0.1)$ -dotted line, 5th from the left bottom and $(1.15,0.15)$ - small dashed line, 6th from the left bottom.] 107

7.3 [Evolution of the q -parameter with redshift of IMHRDE3. The plots for $(\alpha, \beta)=(1.2,-0.1)$ thin continuous - first from the bottom of the left side, $(4/3,-0.05)$ -large dashed line, 2nd from the bottom of the left side, $(1.01,-0.01)$ - thick continuous, third from the left bottom, $(4/3,0.05)$ - dash-dot, 4th from the left bottom, $(1.2,0.1)$ -dotted line, 5th from the left bottom, $(1.15,0.15)$ - small dash line, 6th from left bottom, all with coupling constant $b = 0.009$.] 109

7.4 [$r - s$ plots of IMHRDE3 for parameters $(\alpha, \beta)=(1.2,-0.1)$ (thin continuous, extreme left trajectory), $(4/3,-0.05)$ (dashed, middle trajectory), $(1.01,-0.01)$ (thick continuous, extreme right trajectory), with $b=0.009$] . . 111

- 7.5 [$r-s$ plots of IMHRDE3 for parameters $(\alpha, \beta)=(4/3, 0.05)$ (thick continuous, extreme left trajectory), $(1.2, 0.1)$ (thin continuous, middle trajectory), and $(1.15, 0.15)$ (dashed, extreme right trajectory) with $b=0.009$] 112
- 7.6 [$r-q$ behavior of the IMHRDE3 for the best fit parameter $(1.01, -0.01)$ with $b=0.009$. The diagonal like line representing the trajectory of IMHRDE3 and the horizontal line representing Λ CDM for comparison.] . 113
- 7.7 [The behavior of S' for the parameters $(\alpha, \beta) = (1.01, -0.01)$ the thick continuous line, $(\alpha, \beta) = (1.2, -0.1)$ the thin continuous line, $(\alpha, \beta) = (4/3, -0.1)$ the large dashed line, $(\alpha, \beta) = (1.2, 0.1)$ the dotted line, $(\alpha, \beta) = (1.2, 0.3)$ the small dashed line, and $(\alpha, \beta) = (4/3, 0.3)$ the dot-dashed line, with the interaction coupling constant $b=0.009$ inside apparent horizon under thermal equilibrium conditions] 117
- 7.8 [The behavior of S' for the parameters $(\alpha, \beta) = (1.2, 0.1)$ thick continuous line, $(\alpha, \beta) = (4/3, 0.1)$ thin continuous line, $(\alpha, \beta) = (1.2, 0.3)$ dashed line, with the interaction coupling constant $b=0.009$ inside event horizon under thermal equilibrium conditions] 119

7.9 [The behavior of S' for the parameters $(\alpha, \beta) = (1.01, -0.01)$ thick continuous line, $(\alpha, \beta) = (1.2, -0.1)$ thin continuous line, $(\alpha, \beta) = (4/3, -0.1)$ dashed line, with the interaction coupling constant $b=0.009$ inside event horizon under thermal equilibrium conditions] 120

7.10 [The behavior of S_{de} against x for the parameters $(\alpha, \beta) = (1.2, 0.1)$ with $k = 1.25$ inside apparent horizon under thermal non-equilibrium condition] 122

7.11 [The behavior of S_h along with S_{total} with x for the parameters $(\alpha, \beta) = (1.2, 0.1)$ inside apparent horizon under thermal non-equilibrium condition. The thick continuous line represents the total entropy S_{tot} and the thin line represents the entropy of the horizon S_h .] 123

8.1 [confidence region of IMHRDE1 best fit parameters, outer contour represent 99.99% confidence region, the immediate next contour represent 97.3% confidence region, the next contour to it represent 95.4% confidence region and the inner most contour represent 68.3% confidence region.] 132

-
- 8.2 [confidence region of IMHRDE2 best fit parameters. Outer contour represent 99.99% confidence region, the immediate next contour represent 97.3% confidence region, the next contour to it represent 95.4% confidence region and the inner most contour represent 68.3% confidence region.] 133
- 8.3 [confidence region of IMHRDE3 best fit parameters. Outer contour represent 99.99% confidence region, the immediate next contour represent 97.3% confidence region, the next contour to it represent 95.4% confidence region and the inner most contour represent 68.3% confidence region.] 134
- 8.4 [IMHRDE1:continuous line represents theory, dots with error bars represent observation] 135
- 8.5 [IMHRDE2:continuous line represents theory, dots with error bars represents observation] 136
- 8.6 [IMHRDE3:continuous line represents theory, dots with error bars represents observation] 137

List of Tables

1.1	values of the cosmological parameters	16
8.1	The $\Delta\chi^2$ value for various confidence limits for two parameters	131

1

Introduction to Cosmology

1.1 Introduction

Cosmology comprises the study of the dynamics of the universe at large scale and it aims at understanding the origin and evolution of the universe. Since the discovery by Edwin Hubble, in 1920's, on the recessional motion of distant galaxies, cosmology is overwhelmed with various observational data which are all supporting the idea of an expanding universe. Friedmann-Lamaitre-Robertson-Walker (FLRW) model of the universe is considered to be the standard model due to its success in explaining the evolution of the universe. This model is effective in predicting the conditions prevailed in the universe after the Planck time, i.e., 10^{-43} seconds after the Big Bang onwards[1]. At large scale the universe is taken to be homogeneous and isotropic.

This is initially taken as an assumption called cosmological principle which is an extension of Copernican principle which states that we are not privileged observers. The original motivation behind this assumption was its simplicity that a homogeneous and isotropic distribution of matter is the simplest possible way using which a model of the universe can be formulated based on either General Relativity or Newton's law. Later observational evidences confirmed this assumption that the universe is in fact homogeneous and isotropic at scales of the order of 100 Mpc or so. However the universe still seems to be inhomogeneous at smaller scales, where it consists of local clustering of masses like stars, galaxies etc. The strongest observational evidence of homogeneity and isotropy came from the Cosmic Microwave Background Radiation(CMBR). The CMBR, the radiation left over from the early stage of the universe, is observed to be the same in every direction to within 1 part in 10^{-5} [2]. Large scale redshift surveys [3] and 2dFGRS[4–6] have all confirmed the homogeneity and isotropy at large scales.

The FLRW model of the universe describes a homogeneous and isotropic universe started with a big-bang hence called as the big-bang model. The FLRW model is considered to be the widely accepted model of the universe. The major observational supports of the model are the prediction of the cosmic microwave background radiation (CMBR),

prediction of the primordial abundance of light nuclei like Hydrogen, Helium, Lithium etc and explanation of the Hubble law about the recessional motion of distant galaxies. The model is also successful in explaining the evolution of the large scale structure in the universe.

Recent observations of the type Ia supernova have revealed that the present universe is accelerating and the acceleration have begun in the recent past of the evolution of the universe[7, 8]. Later, observations on CMBR [9], large scale structures [3, 10] etc have all confirmed this result. In order to explain this recent acceleration of the universe within the frame work of the FLRW model[11–14], one has to introduce some exotic component of fluid which can produce negative pressure that can drive the acceleration of the universe. This exotic form of energy is called dark energy. One of the hopeful model of dark energy which can explain this recent acceleration is called Λ CDM (Lambda-cold dark matter) model, where the main components of the universe are a cosmological constant(equivalent to dark energy) and non-relativistic matter. But this model faces with severe problem that the theoretically predicted value of the cosmological constant is nearly 10^{120} times larger than the observed value. Only with a fine tuning, the model can comply with the observational results. This motivates the introduction of models with time evolving dark energy, where the density of dark energy varies as the universe

expands. In the present thesis we are analyzing such a model of dark energy called the holographic dark energy model and its feasibility in explaining the late time acceleration of the universe. As a first step we are making a review of the FLRW model of the universe in the following section.

1.2 FLRW model of the universe

Gravity is the force that controls the universe at large scales and is most accurately described by Einstein's field equation in General theory of Relativity(a modified theory of gravity)[15],

$$R_{\mu\nu} - \frac{1}{2}Rg_{\mu\nu} \equiv G_{\mu\nu} = 8\pi GT_{\mu\nu}, \quad (1.1)$$

where $G_{\mu\nu}$ is the Einstein tensor, $R_{\mu\nu}$ is the Ricci tensor, R is the Ricci scalar, all representing the curvature of space, $g_{\mu\nu}$ is the space-time metric tensor and $T_{\mu\nu}$ is the energy-momentum tensor of the fluid components in the universe like matter, radiation etc. This equation tells us that the matter-energy component of the universe causes the curvature and thus the geometry of space-time.

The universe at large scale is isotropic and homogeneous. Around the middle of 1920's Edwin Hubble proposed the idea of an expanding universe based on his observations on the redshift of galaxies. However a theoretical model of an expanding universe was proposed by Fried-

mann even before the discovery by Hubble. Friedmann model is popularly known as the Friedmann-Lamaitre-Robertson-Walker (FLRW) model which describes a universe which is homogeneous and isotropic in 3-space and is evolving along time direction. Such a universe is basically described by the FLRW metric,

$$ds^2 = dt^2 - a^2(t) \left(\frac{dr^2}{1 - kr^2} + r^2 d\theta^2 + r^2 \sin^2 \theta d\phi^2 \right), \quad (1.2)$$

where (r, θ, ϕ) are spherically symmetric co-moving co-ordinates which are the co-ordinates carried along with the expansion of the universe so that the real distance between two galaxies can be obtained by multiplying the co-moving co-ordinate distance with the scale factor of expansion $a(t)$, t is the cosmic time and k is the curvature parameter of the 3-space which determines its geometry:

- $k = +1 \Rightarrow$ positive curvature and a closed universe,
- $k = 0 \Rightarrow$ zero curvature and a flat universe,
- $k = -1 \Rightarrow$ negative curvature and an open universe.

1.3 Friedmann equations

The equations describing the dynamics of Friedmann universe can be obtained from the Einstein's field equation by substituting the FLRW

metric and the energy-momentum tensor of the fluid components of the universe. By assuming that the components of the universe are perfect fluids at rest in the co-moving co-ordinate system, one can write the energy-momentum tensor[15] as

$$T_{\mu\nu} = pg_{\mu\nu} + (p + \rho)U_\mu U_\nu, \quad (1.3)$$

where p and ρ are the pressure and density of the fluid respectively and are functions of time, U^μ is the four velocity with components,

$$U^t = 1 \quad U^i = 0. \quad (1.4)$$

The Friedmann equations are then obtained as,

$$\frac{\dot{a}^2}{a^2} + \frac{k}{a^2} = \frac{8\pi G}{3}\rho, \quad (1.5)$$

$$2\frac{\ddot{a}}{a} + \frac{\dot{a}^2}{a^2} + \frac{k}{a^2} = -8\pi Gp \quad (1.6)$$

where over dot represents the derivative with respect to cosmic time.

Combining equations(1.6) and (1.5) one can obtain the equation,

$$\frac{\ddot{a}}{a} = -\frac{4\pi G}{3}(\rho + 3P), \quad (1.7)$$

which gives the acceleration of expansion of the universe in relation to the energy densities of the fluids and it's pressure. The above three equations are generally known as the Friedmann's equations. We can define the critical density as,

$$\rho_c = \frac{3H^2}{8\pi G}, \quad (1.8)$$

which is the total energy density needed to make the universe flat. Its present value is around $\rho_c \approx 1.9 \times 10^{-29} h^2 g/cm^{-3} \approx 8.1 \times 10^{-11} h^2 eV^4 = 8.1 h^2 \times 10^{-47} GeV^4$ where $h = H_0/(100 km/s/Mpc)$ and H_0 is the present value of the Hubble parameter. When $\rho = \rho_c$, $k = 0$ corresponds to flat universe, when $\rho > \rho_c$, $k > 0$ representing a positively curved universe and when $\rho < \rho_c$, $k < 0$ corresponding to a negatively curved universe.

When equation(1.5) is multiplied with a^2 and differentiated with respect to the cosmic time, then combining with equation(1.7), gives

$$\dot{\rho} + 3H(\rho + P) = 0, \quad (1.9)$$

where $H = \dot{a}/a$, the Hubble parameter. The above equation is called the conservation or continuity equation which describes the evolution of energy density of the fluid components as the universe expands. The evolution of the energy density depends on the equation of state parameter defined as

$$\omega_i \equiv \frac{p_i}{\rho_i}, \quad (1.10)$$

where i refers to the possible fluid components of the universe and in general ω is a time dependent quantity. The evolution of energy density of a given component is obtained by integrating the continuity equation(1.9),

$$\rho_i \propto \exp\left(3 \int (1 + \omega_i(z)) d \ln(1 + z)\right). \quad (1.11)$$

For simple fluids where ω is a constant, the energy density become

$$\rho_i \propto a^{-3(1+\omega_i)}. \quad (1.12)$$

For radiation or relativistic particles, $\omega_r = 1/3$, then

$$\rho_r \propto a^{-4}, \quad (1.13)$$

and for non-relativistic matter $\omega_m = 0$, then

$$\rho_m \propto a^{-3}. \quad (1.14)$$

So the radiation density is decreasing faster than the matter density as the universe expands, because unlike matter the radiation suffers a decrease in density due to redshift(stretching of wavelength) also as the universe expands. If one goes back in time the radiation density would be increasing and eventually dominate over that of matter. This means that the early stage of the universe is dominated by radiation, called radiation-dominated era and as the universe expands, due to the faster decrease in the radiation density, the universe will evolve into a later phase where matter is dominated over radiation called matter-dominated era. The evolution of the scale factor with cosmic time can be obtained from the Friedmann equation. For a flat universe (with $k = 0$),

$$H^2 \propto \rho. \quad (1.15)$$

For a radiation-dominated universe, the above equation becomes,

$$H^2 \propto a^{-4}. \quad (1.16)$$

On integrating this, we get the evolution of a with cosmic time in the radiation-dominated universe as,

$$a \propto t^{1/2}. \quad (1.17)$$

Similarly for a matter-dominated universe one can obtain

$$a \propto t^{2/3}. \quad (1.18)$$

The density behavior shows that the early universe was denser and therefore hotter. In the radiation-dominated era $\rho_r \propto a^{-4}$. From Stefan's law the density evolution with temperature follows the relation $\rho_r \propto T^4$. Therefore one can conclude that the temperature of the universe $T \sim a^{-1}$. Hence the early universe was hotter compared to the later phase. Initially the temperature was so great that matter existed in plasma state, the particles were colliding and scattering with one another frequently so that they reached an equilibrium. As the temperature dropped due to the expansion of the universe, the radiation energy decreased below the binding energy of the nuclei and light elements such as deuterium, helium, lithium etc. were formed.

At around 10^{-13} seconds after big bang, the temperature of the radiation was too high to allow the electrons to combine with nuclei to form neutral atoms. After this period, electrons combined with nuclei to form neutral atom and subsequently radiation was decoupled

from matter. It is this radiation leftover from the early stage called as the Background radiation, having temperature around 2.7 Kelvin at present.

1.4 Friedmann model with Cosmological constant

Cosmological constant term was introduced by Einstein basically to create a static model of the universe. The term was abandoned due to the discovery that Hubble made in 1929 of receding galaxies and later the cosmological constant was resurrected after the discovery of the acceleration of the universe. The Friedmann equations with Cosmological constant are,

$$\frac{\dot{a}^2}{a^2} + \frac{k}{a^2} = \frac{8\pi G}{3}\rho + \frac{\Lambda}{3}, \quad (1.19)$$

and

$$\frac{\ddot{a}}{a} = -\frac{4\pi G}{3}(\rho + 3P) + \frac{\Lambda}{3}. \quad (1.20)$$

Cosmological constant gives a positive contribution to the acceleration, so unlike gravity it acts effectively as a repulsive force. An effective energy density corresponding to cosmological constant can be expressed as,

$$\rho_\Lambda = \Lambda/8\pi G. \quad (1.21)$$

The continuity equation for the cosmological constant,

$$\dot{\rho}_\Lambda + 3H(\rho_\Lambda + p_\Lambda) = 0, \quad (1.22)$$

which implies that the corresponding pressure is negative,

$$p_\Lambda = -\rho_\Lambda. \quad (1.23)$$

The physical interpretation of the Cosmological constant is coming from some scalar field theories as vacuum constant or zero-point energy.

1.5 Solutions of the Friedmann equations

The Friedmann equations can be solved for different conditions gives different models, **(i) Closed, open and flat universes:** In the case of matter-dominated universe, the first Friedmann equation can be recast in the form,

$$\left(\frac{\dot{a}}{a}\right)^2 = H_0^2 [\Omega_{m0}a^{-3} + (1 - \Omega_{m0})a^{-2}]. \quad (1.24)$$

This equation can be solved for $k = +1$ in the parametric form,

$$a = \frac{a_{max}}{2} (1 - \cos\theta); \quad a_{max} = a(t_0) \left(\frac{\Omega_{m0}}{\Omega_{m0} - 1} \right), \quad (1.25)$$

and the corresponding time,

$$t = \frac{t_{max}}{\pi} (\theta - \sin\theta); \quad t_{max} = \left(\frac{\Omega_m}{2H_0(\Omega_m - 1)^{3/2}} \right). \quad (1.26)$$

The above equation shows that the universe starts at $\theta = 0$ with big bang, reaches maximum size at $\theta = \pi$ and collapses in a big crunch

at $\theta = 2\pi$. Such a universe is said to be closed universe.

For $k = -1$, the solutions become,

$$a = \frac{a_{max}}{2} (\cosh\theta - 1); \quad a_{max} = a(t_0) \left(\frac{\Omega_{m0}}{\Omega_{m0} - 1} \right), \quad (1.27)$$

and the corresponding time,

$$t = \frac{t_{max}}{\pi} (\sinh\theta - \theta); \quad t_{max} = \left(\frac{\Omega_m}{2H_0(\Omega_m - 1)^{3/2}} \right). \quad (1.28)$$

In this case the universe keeps expanding forever and is called as open universe.

For $k = 0$, the solutions become much simpler that $a \propto t^{2/3}$ and is the critical case where universe will expand forever. The corresponding universe is then called as flat universe. **(ii) de Sitter model:** In this model the universe consists of only cosmological constant, Λ and the Friedmann equation become,

$$\left(\frac{\dot{a}}{a} \right)^2 = \frac{\Lambda}{3}. \quad (1.29)$$

The solution is obtained as

$$a = a_0 e^{\sqrt{\frac{\Lambda}{3}}t}. \quad (1.30)$$

The corresponding universe is eternally accelerating. **(iii) Λ CDM model:** The components of the Λ CDM model are cold dark matter, radiation and the cosmological constant with equation of states, $\omega_m = 0$, $\omega_r = 1/3$ and $\omega_\Lambda = -1$ respectively. The Friedmann equation of

the model is,

$$H^2 = \frac{8\pi G}{3} (\rho_m + \rho_r + \rho_\Lambda). \quad (1.31)$$

This is the simplest model that provides a reasonably good account of the existence of CMBR, large scale structures and distribution of galaxies, abundance of light elements like Hydrogen, Helium, Lithium etc. in the universe and also the recent acceleration of the universe. Even though this is considered as the concordance cosmological model, it is faced with the severe problems of cosmic coincidence and cosmological constant problem when one tries to understand the recent acceleration of the universe.

1.6 Observational Parameters of the Friedmann universe

Different cosmological models were constrained by the observational values of the parameters defined in such models. The most commonly used parameters are: the Hubble parameter, the age of the universe, mass-density parameters like Ω_m , corresponding to non-relativistic matter, Ω_r , corresponding to radiation, Ω_Λ , corresponding to cosmological constant, Ω_{de} , corresponding to dark energy, equation of state parameter for different components of the universe, ω_i , deceleration parameter q characterizing the speed up in the expansion of the universe.

The Hubble parameter H which gives the rate of expansion of the

universe basically defined by the Hubble's law, $v = Hd$, where v is the velocity of the galaxies receding from the observer and d is the physical distance towards the galaxy. It is usually parameterized by its present value as,

$$H_0 = 100hKms^{-1}Mpc^{-1}, \quad (1.32)$$

where h is between 0.4 and 1. The present value of the Hubble parameter is around 72 ± 3 [3].

One of the important parameter that could be predicted by a cosmological model is the age of the universe. The approximate age can be obtained from the Hubble's law. Hubble's law can be written as $d = H^{-1}v$, means that H^{-1} has got the dimension of time. Ignoring the fact that v is changing with respect to time, one can write the age of the universe as $t \sim H_0^{-1}$. By considering the present value of the Hubble parameter, the corresponding age is found to be less than 15 GYr. The latest concordance value of the age of the universe is coming from the observational data of globular clusters and is[3]

$$t_0 = 13.9 \pm 0.6GYr \quad (1.33)$$

The different density parameters specifies the densities of the different components of the universe. The Friedmann equation can be recast

in terms of the energy densities of all possible components as

$$H^2 = \frac{8\pi G}{3} (\rho_m + \rho_r + \rho_\Lambda - k/a^2), \quad (1.34)$$

which can be expressed in terms of the mass-density parameters as

$$1 = [\Omega_m + \Omega_r + \Omega_\Lambda + \Omega_k], \quad (1.35)$$

where

$$\Omega_m = \frac{\rho_m}{\rho_c}, \quad \Omega_r = \frac{\rho_r}{\rho_c}, \quad \Omega_\Lambda = \frac{\rho_\Lambda}{\rho_c}, \quad \Omega_k = -\frac{k}{a^2 H^2}, \quad (1.36)$$

where $\rho_c(t)$ is the critical density given by

$$\rho_c(t) = \frac{8\pi G}{3H^2}. \quad (1.37)$$

Ω_m is the mass-density parameter of non-relativistic matter comprising both baryonic and dark matter, Ω_r is the mass-density parameter of radiation, Ω_Λ is the mass-density parameter corresponding to the cosmological constant and Ω_k is the density parameter corresponding to curvature.

The concordance values of these parameters are given in Table 1 which are obtained from the combined data from SDSS and WMAP [3].

The equation of state parameter characterizes the evolution of the fluid components of the universe and its expression for i^{th} component is

$$\omega_i = \frac{p_i}{\rho_i}. \quad (1.38)$$

Cosmological parameters	Concordance values
Ω_0	1.003 ± 0.010
Ω_{m0}	0.288 ± 0.030
Ω_{de}	0.757 ± 0.020
ω_0	-0.94 ± 0.100
q_0	-0.64 ± 0.030
H_0	72 ± 3

Table 1.1: values of the cosmological parameters

For pressureless non-relativistic matter, $\omega_m = 0$, for radiation with $p = \rho/3$, $\omega_r = 1/3$, and for cosmological constant with $p = -\rho$, $\omega_\Lambda = -1$.

The Hubble parameter gives the idea of rate of expansion of the universe. But the nature of the rate, whether it is increasing or decreasing, can be determined by the deceleration parameter, q defined as

$$q = -\frac{\ddot{a}a}{\dot{a}^2} = -1 - \frac{\dot{H}}{H^2}. \quad (1.39)$$

For $q > 0$, implies a decelerated expansion and $q < 0$ implies accelerated expansion. For the standard Friedmann model, when the universe dominated with radiation the deceleration parameter $q \sim 1$ implies a decelerated universe and when the universe is dominated

with non-relativistic matter, the deceleration parameter $q \sim 0.5$ which also implies a decelerating universe. So for an accelerating universe with $q < 0$ the universe must be dominated with some form of matter different from ordinary matter and radiation, which enable to produce a negative pressure.

1.7 Accelerating Universe

Recent observations on type Ia supernovae(SN Ia) by two teams, High-redshift Supernova Search Team[8] and the Supernova Cosmology Project[7] independently shows that the present universe is accelerating despite the presence of gravity and the acceleration began in the recent past of the universe. The study of the luminosity distance of the type Ia Supernovae led to the above conclusion. This discovery was further supported by the observational data on the anisotropy in Cosmic Microwave Background radiation[16, 17], large-scale structures[10] and Baryon acoustic oscillations(BAO)[18].

Evidence from Supernovae

The supernovae are the exploding stars having high luminosity. Supernovae are mainly classified into two: Type I and Type II. Type II are explosions of high massive stars having hydrogen lines in its absorption spectrum while Type I does not have it. Type I super-

novae again is classified into three: If there is singly ionized Silicon absorption line in the spectrum, then it is Type Ia , If it is a Helium line then Type Ib and Type Ic does not have Silicon or Helium line in its spectrum. Type Ia supernovae are formed from the thermonuclear explosion of a white dwarf in a binary system which when absorbed gas from the companion star so that its mass crosses the Chandrasekhar limit and explodes. Supernovae Ia is consensually named as the "standard Candle" due to its constancy in luminosity at the peak of brightness because of the uniform masses of the exploding white dwarfs. Standard candles such as Cepheid stars whose luminosity varies within a regular cycle used before have the limitation that beyond 30 Mpc[19] they cannot be used. SN Ia have the advantage of perceiving at large distances because of their higher degree of brightness.

The comparison of the redshift and magnitude of Type Ia supernovae provided the evidence for the acceleration in the expansion of the universe. The apparent magnitude estimates the distance while the redshift, which is the stretching of wavelength, corresponds to the expansion. In fact, the magnitude- redshift relation gives the expansion history of the universe. The magnitudes and luminosity of a star

are related through

$$m - M = 5 \log_{10} d_L + 25, \quad (1.40)$$

where the distance is expressed in Megaparsec, m is the apparent magnitude and M is the absolute magnitude of the cosmological object and d_L is the luminosity distance. Since M is same for all SN Ia, $d_L(Z)$ can be calculated using the above expression by knowing m . The corresponding redshift is calculated from the measurement of wavelength of light λ .

In Minkowski space the absolute luminosity L_s of the source and energy flux F at a distance d are related by $L_s/(4\pi d^2)$. By generalizing this to an expanding universe, the luminosity distance d_L is defined as

$$d_L^2 = \frac{L_s}{4\pi F}. \quad (1.41)$$

Let the source is at a comoving distance $\chi = \chi_s$ from the observer at $\chi=0$. The source is emitting energy ΔE_s in a time interval Δt_s , then the absolute luminosity L_s is given by

$$L_s = \frac{\Delta E_s}{\Delta t_s}. \quad (1.42)$$

The corresponding energy received by the observer ΔE_0 during Δt_0 , hence the observed luminosity L_0 is given by

$$L_0 = \frac{\Delta E_0}{\Delta t_0}. \quad (1.43)$$

The energy $\Delta E_s \propto \nu_s$ and $\Delta E_0 \propto \nu_0$ so that

$$\frac{\Delta E_s}{\Delta E_0} = \frac{\nu_s}{\nu_0} = \frac{\lambda_0}{\lambda_s} = (1+z). \quad (1.44)$$

We have $\nu_s \Delta t_s = \nu_0 \Delta t_0$, then

$$L_s = L_0(1+z)^2. \quad (1.45)$$

Since light follows null path the co-moving distance χ_s to the source can be expressed as,

$$\chi_s = \int_0^{\chi} d\chi = \int_t^{t_0} \frac{dt}{a(t)} = \frac{1}{a_0 H_0} \int_0^z \frac{dz}{h(z')}, \quad (1.46)$$

where $h(z) = H(z)/H_0$. The FRW metric using conformal co-ordinate is given as,

$$ds^2 = c^2 dt^2 - a(t)^2 (d\chi^2 + f_k(\chi)^2 (d\theta^2 + \sin^2\theta d\phi^2)). \quad (1.47)$$

Then the area of the sphere at $t = t_0$ is $S = 4\pi (a_0 f_k(\chi_s))^2$ and hence the corresponding flux observed is given by,

$$F = \frac{L_0}{4\pi (a_0 f_k(\chi_s))^2}. \quad (1.48)$$

The luminosity distance now becomes,

$$d_L = a_0 f_k(\chi_s)(1+z) = \frac{1+z}{H_0} \int \frac{dz'}{h(z')}. \quad (1.49)$$

Considering the universe with matter and cosmological constant contributions only, the above equation can be written as,

$$d_L = \frac{1+z}{H_0} \int \frac{dz'}{\sqrt{\Omega_{m0}(1+z)^3 + \Omega_\Lambda}}. \quad (1.50)$$

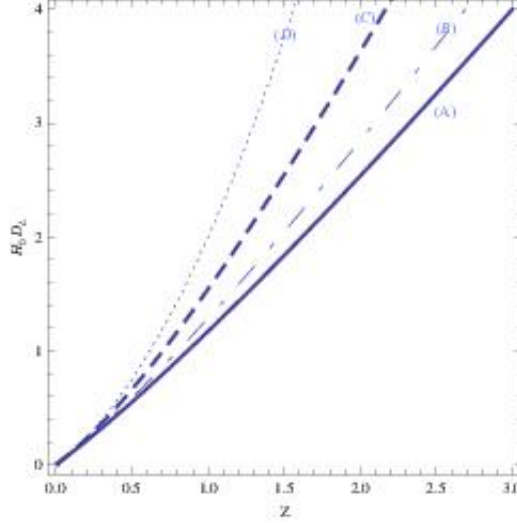


Figure 1.1: [Luminosity distance in units of H_0^{-1} for a universe with non-relativistic matter and cosmological constant ($\omega_\Lambda = -1$). Plots A,B,C,D corresponds to $\Omega_\Lambda = 0, 0.3, 0.7, 1$ respectively. Courtesy [20]]

Then the function $\int_0^z \frac{dz'}{h(z')}$ can be expanded around $z = 0$ as,

$$\int_0^z \frac{dz'}{h(z')} = z - \frac{h'(0)}{2} z^2 + O(z^3). \quad (1.51)$$

Luminosity distance up to second order of redshift is

$$d_L = \frac{cz}{H_0} \left(1 + \left(1 - \frac{3(1 + \Omega_\Lambda)}{2 - \Omega_\Lambda} \right) z \right). \quad (1.52)$$

When $\Omega_\Lambda = 0$, the above relation will be reduced approximately to $d_L \simeq cz/H_0$ for small values of z . A plot of the luminosity distance versus redshift is shown in figure(1.1) From the magnitude relation one can calculate the luminosity distance knowing the apparent and absolute magnitude m and M respectively. This has to be compared

with the theoretical value of luminosity obtained using relation 1.52 with suitable values of Ω_Λ . As an example consider supernovae1997ap at a redshift $z = 0.83$ with $M = -19.09$ and $m = 24.32$. The corresponding luminosity distance from the magnitude relation is found to be around

$$H_0 d_L \simeq 1.16, \text{ for } z = 0.83, \quad (1.53)$$

where $H_0^{-1} = 2998h^{-1}\text{Mpc}$ with $h = 0.72$. The corresponding theoretical estimate of the luminosity distance is

$$H_0 d_L \simeq 0.95, \text{ for } \Omega_{m0} = 1, \quad (1.54)$$

and

$$H_0 d_L \simeq 1.23, \text{ for } \Omega_{m0} = 0.3, \Omega_{\Lambda 0} = 0.7. \quad (1.55)$$

This shows that the theoretical value is satisfying with the observed value only for non-zero values of Ω_Λ , the dark energy.

Evidence from CMBR anisotropy and Large scale structure

Observations on the anisotropy in the temperature of CMBR and large scale structure provide indirect evidence for the existence of dark energy.

The figure 1.2 shows the observed anisotropy in the CMB spectra which was decoupled at an epoch around, $z \simeq 1090$. It was shown that a theoretical prediction of this behavior would need a non-zero

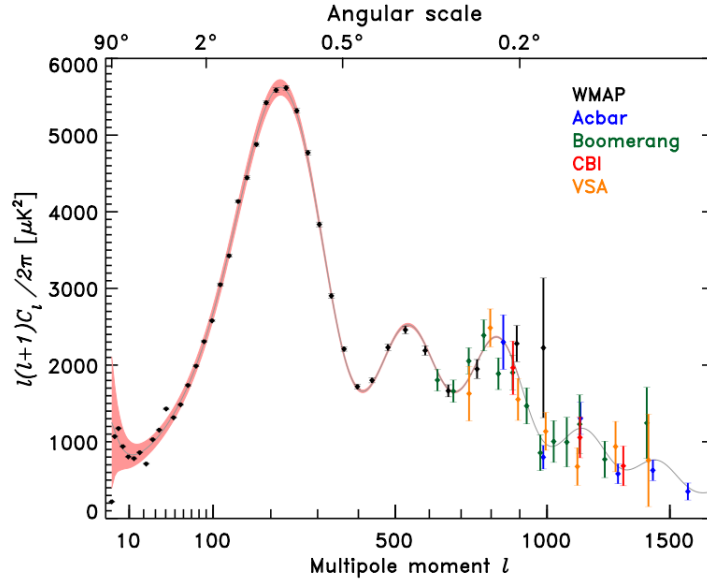


Figure 1.2: [Prediction of CMBR anisotropy[21, 22]. Courtesy [23].]

value for Ω_Λ the dark energy component.

The angular power spectrum of CMBR shown above consist of acoustic peaks that arise from gravity-driven sound waves. These acoustic oscillations are produced by the perturbations in the baryon density which was existed in the early stage of the universe when radiation and matter were in equilibrium. To predict these baryon acoustic oscillations using the standard model of cosmology will need the presence of dark energy. Apart from these there are evidences from the observational data from the age of the universe for the existence of dark energy. From the data of the oldest galactic globular clusters the

age of the universe is constrained to $12Gyr \leq t_0 \leq 15Gyr$ [24]. This is compatible with the standard model of cosmology for $0.2 < \Omega_M < 0.3$.

2

Dark Energy

2.1 Dark energy

The recent acceleration of the universe is caused by an exotic form of energy called dark energy having a negative pressure. Many theoretical models were proposed to understand the nature and evolution of dark energy.

2.1.1 Cosmological constant

The simplest realization of dark energy is through cosmological constant [20, 25, 26] which was first introduced by Einstein[27]. A universe with cosmological constant alone will be eternally accelerating and corresponds to the de Sitter model of the universe. On the other hand the universe consisting of both dark matter and cosmological

constant have an early decelerated epoch followed by an accelerated epoch began in the recent past. This model is often called as the Λ CDM model which almost satisfactorily explaining the recent acceleration of the universe. Theoretically cosmological constant can be realized as the vacuum energy. In spite of its simplicity and success in explaining the recent acceleration, the model faces two severe flaws which are:

(i)Cosmological constant Problem: The value of the cosmological constant can be obtained from the present value of the Hubble parameter, H_0 as[28]

$$\Lambda \approx H_0^2. \quad (2.1)$$

The corresponding critical density of the cosmological constant is,

$$\rho_\Lambda \approx \frac{\Lambda M_{pl}^2}{8\pi} \approx 10^{-47} GeV^4 \approx 10^{-123} M_{pl}^4, \quad (2.2)$$

where $H_0 = 100hKmsec^{-1}Mpc^{-1} = 2.1332h \times 10^{-42}GeV$, $h = 0.7$ and $M_{pl} = 1.22 \times 10^{19}GeV$. In terms of the vacuum energy field of mass m and momentum p , the zero-point energy is $E = \frac{1}{2}\hbar\omega = \frac{1}{2}\sqrt{p^2c^2 + m^2c^4}$, but if $\hbar = c = 1$ and $p = \hbar k$, then $E = \frac{1}{2}\sqrt{k^2 + m^2}$.

When these zero-point energies are summed up to a cut-off scale of $k_{max} \gg m$ (to avoid divergence), the energy density becomes,

$$\rho_{vac} = \int_0^{k_{max}} \frac{d^3k}{(2\pi)^3} \frac{1}{2} \sqrt{k^2 + m^2} = \int_0^{k_{max}} \frac{4\pi k^2 dk}{(2\pi)^3} \frac{1}{2} \sqrt{k^2 + m^2} = \frac{k_{max}^4}{16\pi^2}. \quad (2.3)$$

Within the framework of General Relativity, the $k_{max} = M_{pl} = 1.22 \times 10^{19} GeV$. Hence,

$$\rho_{vac} \simeq 10^{74} GeV^4, \quad (2.4)$$

which is about 10^{121} times greater than the observational value of the cosmological constant given by the equation(2.2). This discrepancy between the observational and theoretical values of the cosmological constant poses a challenge to any model of dark energy.

(ii)Cosmic coincidence Problem: The present value of the energy density of the cosmological constant is found to be around $0.73\rho_c$. [7] On the other hand the present matter density is found to be $0.28\rho_c$. This shows that the dark energy and matter densities are of same order. Any model of dark energy must be able to predict this coincidence of energy densities and is often called the coincidence problem. The Λ CDM model of dark energy failed to explain both the problems.

These drawbacks of the Λ CDM model motivates the introduction of dynamical dark energy models. We will discuss a few of these models in the following sections.

2.1.2 Quintessence Model

In this model[20, 28–31] a scalar field ϕ with a potential $V(\phi)$ is assumed to cause the recent acceleration. The scalar field is coupled

with gravity through a minimal coupling constant. Unlike the cosmological constant, the equation of state of quintessence varies with time hence it is a dynamical dark energy model. The model can be defined by the action,

$$S \equiv \int d^4x \sqrt{-g} \left[\frac{1}{2\kappa^2} R + L_\phi \right] + S_M, \quad (2.5)$$

where L_ϕ is the Lagrangian of the field given by,

$$L_\phi = -\frac{1}{2} g^{\mu\nu} \partial_\mu \phi \partial_\nu \phi - V(\phi), \quad (2.6)$$

$\kappa^2 = 8\pi G$, R is the Ricci scalar and S_M is the said action of matter. For a flat FLRW universe, the variation of the aforesaid action leads to the equation of motion,

$$\ddot{\phi} + 3H\dot{\phi} + \frac{dV}{d\phi} = 0. \quad (2.7)$$

The energy momentum tensor $T_{\mu\nu}$ is obtained from the variation of the action with respect to $g^{\mu\nu}$ and from which the energy density $\rho = -T_0^0$ and the pressure density $p = T_i^i$ can be obtained as,

$$\begin{aligned} \rho &= \frac{1}{2} \dot{\phi}^2 + V(\phi), \\ p &= \frac{1}{2} \dot{\phi}^2 - V(\phi). \end{aligned} \quad (2.8)$$

The Friedmann equations using these expressions for the ρ and p of the field ϕ is obtained as

$$\begin{aligned} H^2 &= \frac{\kappa^2}{3} \left[\frac{1}{2} \dot{\phi}^2 + V(\phi) + \rho_M \right], \\ \frac{\ddot{a}}{a} &= -\frac{\kappa^2}{3} \left[\dot{\phi}^2 - V(\phi) \right]. \end{aligned} \quad (2.9)$$

The above expression indicates that for acceleration to take place $\dot{\phi}^2 < V(\phi)$. The corresponding equation of state will take the form,

$$\omega_\phi = \frac{p}{\rho} = \frac{\frac{1}{2}\dot{\phi}^2 - V(\phi)}{\frac{1}{2}\dot{\phi}^2 + V(\phi)}. \quad (2.10)$$

The physical nature of the quintessence field is not exactly known and hence the nature of interaction with dark matter are also unknown. The coincidence problem can be explained only by choosing suitable values for the coupling constant of the interaction between the quintessence field and dark matter. So the model does not have a natural explanation for the coincidence of dark energy and dark matter.

2.1.3 K-essence model

K-essence is another scalar field model of dark energy[32–34] with a non-canonical form of kinetic energy whose modification accounts for the accelerated expansion and this model is different from the quintessence model where the potential of the scalar field determines the acceleration. The action of the K-essence model is defined to be,

$$S = \int d^4x \sqrt{-g} \left[\frac{1}{2\kappa^2} R + P(\phi, X) \right] + S_M. \quad (2.11)$$

where $P(\phi, X) = f(\phi)P(X)$ is a function relating the scalar field ϕ and its kinetic energy $X = -(1/2)g^{\mu\nu}\partial_\mu\phi\partial_\nu\phi = -(1/2)(\nabla\phi)^2$. In order to explain the coincidence problem, one needs to fine-tune $f(\phi)$ to

be of the order of the present energy density of the universe. Without this fine-tuning the model fails to explain the coincidence.

2.1.4 Phantom model

The recent observations indicating that the equation of state parameter of dark energy is slightly less than -1 . [35, 36] This was theoretically studied by Alam et al. [37] If the equation of state is less than -1 , such models are collectively known as Phantom models. For example, K-essence model with positive energy density gives rise to an equation of state parameter less than -1 . The cosmological evolution of such a field leads to future singularity which results in a Big-Rip [38, 39]. Since the equation of state parameter, $\omega < -1$ for phantom model [40–42], the energy density of dark energy increases with time which is a violation of dominant energy condition [43]. The scale factor of expansion thus blows up, dissociating the bounded system and causes the stripping of the bodies, which eventually leads to the "Big Rip." [44]

2.1.5 Chaplygin gas model

This is a widely studied model [45–47] in explaining dark energy with an exotic equation of state for a perfect fluid in simple terms written

as,

$$p = -\frac{A}{\rho}. \quad (2.12)$$

Later this was generalized known as the generalized Chaplygin gas with an equation of state,

$$p = -\frac{A}{\rho^\alpha}, \quad (2.13)$$

where A is a positive constant and $0 \leq \alpha \leq 1$. In a flat FLRW universe the energy density ρ of the fluid evolve as,

$$\rho = \left(A + \frac{B}{a^{3(1+\alpha)}} \right)^{1/(1+\alpha)}, \quad (2.14)$$

where B is the integration constant. At early epoch when a is very much small,

$$\rho \sim \frac{\sqrt{B}}{a^3}. \quad (2.15)$$

For $\alpha = 1$, the expression implies a universe with pressure-less dust corresponding to the conventional matter-dominated universe. In the late stage of the evolution of the universe, when a is very large, then

$$\rho \sim \sqrt{A}, \quad p = -\rho. \quad (2.16)$$

This implies a behavior similar to a universe dominated with cosmological constant and therefore an accelerating universe. This means that Chaplygin gas acts as non-relativistic matter in the early stage and as cosmological constant in the late stage of the universe. Hence Chaplygin gas provides an interesting possibility for a unified model

for dark energy and dark matter. However the Chaplygin gas with $\alpha = 1$ often called as the standard Chaplygin gas model have been ruled out by many others[48, 49] by contrasting it with cosmological data like Supernovae data, CMB data etc[50]. But generalized gas models with α values other than 1 is also faced with severe drawbacks. The parameter α is severely constrained to produce the late acceleration[51–53]. A much serious problem is regarding the CMB anisotropies. The Jeans instability of perturbations predicted by the generalized Chaplygin gas models behave similar to the cold dark matter fluctuation in the early deceleration phase, but these fluctuations will disappear in the accelerating phase. This will lead to power loss in the CMB anisotropies and hence is incompatible with the observed CMB anisotropy.

2.1.6 An alternative model based on holographic principle

This model represents another dynamic dark energy model. The concept of holographic model was proposed by Gerard 't Hooft[54] while studying black holes thermodynamics which was elaborated and developed by Leonard Susskind[55]. The model is based on the principle of holography says that the degrees of freedom of a system scales with its area rather than with its volume. In other words, Susskind says that the nature can be explained using two-dimensional lattice at the spatial boundaries of the world in the place of a three-dimensional

lattice[55]. The model considers the relation connecting UV and IR cut-off, so that if ρ_Λ is the zero point energy density of a quantum system which is caused by a short-distance cut-off, then the total energy inside the region L should not exceed the mass of the black hole of the same size[56]. The maximum value L can take saturates the inequality,

$$\rho_\Lambda = 3c^2 M_p^2 L^{-2}, \tag{2.17}$$

where c is a dimensionless numerical constant, M_p is the reduced Planck mass such that $M_p^{-2} = 8\pi G$. Considering L to be the size of the present universe the above equation can be taken as the equation for the dark energy density. It is this model which is the subject of our study. In the further chapters we have shown that the model succeeds in explaining the cosmic coincidence and the fine tuning problem to a satisfactory extent compared to other standard models of dark energy.

3

Holographic Dark Energy Model

3.1 Holographic Dark energy Model

The history of the concept of the holographic model way backs to the black hole thermodynamics developed by S W Hawking and J D Bekenstein. The concept of holography was introduced by Gerard 't Hooft, which was later developed as a principle by Leonard Susskind taking into consideration the views of Bekenstein's and t' Hooft's views. Later, holographic principle was applied to cosmology by Fischler and Susskind [57].

3.1.1 Black hole thermodynamics and generalized second law of thermodynamics

The black hole dynamics is explained with the help of thermodynamics. From the study of the black holes, Hawking showed that the area of the black hole event horizon never decreases with time. Even when two black holes merge with each other, the area of the event horizon of the new black hole will be greater than the sum of the event horizon areas of the individual black hole [58, 59]. This property of the black hole area resembles the entropy in thermodynamics. Later Bekenstein proposed that entropy of the black hole is proportional to the area of the event horizon of the black hole and has shown that black hole entropy [60–62] is given by

$$S_{bh} = \frac{A}{4G} \quad (3.1)$$

This was later verified by Hawking [63] [$S_{bh} = K A c^3 / 4G\hbar$].

Ordinary second law of thermodynamics says that the entropy of an isolated system never decreases. Hawking showed that the entropy inside the black hole cannot be determined by an external observer. Since the black hole can accrete mass from the surrounding space it can act as the sink of entropy. Thus the second law of thermodynamics becomes violated. To reconcile the situation, on taking account of the fact that the black hole entropy is proportional to its horizon area,

Bekenstein proposed the generalized second law(GSL) of thermodynamics which says that entropy of the black hole S_{bh} plus entropy of the exterior universe S_{ex} , never decreases, that is

$$\Delta S_{bh} + \Delta S_{ex} \geq 0, \tag{3.2}$$

where ΔS_{bh} and ΔS_{ex} are the change in entropy of the black hole and the change in entropy of the exterior respectively.

This black hole entropy which is characterized by its area later lead to the holographic principle by 't Hooft and Susskind [54, 55]. They proposed that the entropy bound for any form of matter localized in a spherical region is given by

$$S_m \leq \frac{A}{4G} \tag{3.3}$$

where A is the area of the event horizon of the black hole of the same size. Since entropy represents the degrees of freedom measured in Planck units, the complete information regarding a system can be obtained from the degrees of freedom residing in its surface, which is known as the holographic principle. This principle was later used to propose the holographic dark energy in cosmology.

3.1.2 UV/IR connection

The entropy of the black hole is given by

$$S_{bh} = \frac{A}{4G} \quad (3.4)$$

The above relation also holds, as an entropy bound in a spherical region of space, with any kind of matter [47] as

$$S_m \leq \frac{A}{4G} \quad (3.5)$$

This equation implies that the entropy of any material other than black hole have an entropy less than that of the black hole of the same size because black hole is the one which has maximum entropy among the cosmic bodies. Hence the entropy relation above saturates only in the case of a black hole and every other form of matter will be having comparatively a lesser entropy.

In Quantum field theory, a system of size L , with ultraviolet(UV) cut-off Λ will have an entropy scaling extensively as $S = L^3\Lambda^3$ [64]. But from Bekenstein's relation the entropy scales non-extensively. According to Susskind and 't Hooft any form of matter have entropy less than that of the black hole. The system in Quantum field theory have energy density $\rho \sim \Lambda^4$. The total energy of this system given by $E_s = L^3\Lambda^4$, must be less than the total energy of the black hole of the same size give by $E = LM_{pl}^2$. That is,

$$L^3\Lambda^4 \leq LM_{pl}^2 \quad (3.6)$$

In terms of the energy density corresponding to the largest value of L (IR cut-off) which saturates the inequality, the relation becomes

$$\rho_\Lambda = 3c^2 M_{pl}^2 L^{-2} \quad (3.7)$$

where c is a numerical constant. This vacuum energy density is later proposed as the holographic dark energy [47, 65]. The problem then arise is the proper choice of L , the IR cut-off.

3.1.3 Possible candidates for L , the IR cut-off

The possible choices for the IR cut-off are Hubble horizon [65], future event horizon etc. When Hubble horizon is taken as the IR cut-off, the model will not give an accelerating universe. When future event horizon [56] is taken as the IR cut-off, two major problems arose, it violates causality [47, 66] and it also fails to account for the age of the universe. In hope of resolving the above problems, Granda and Oliveros proposed Ricci scalar as the IR cut-off [67] to define the holographic dark energy.

(i) Hubble radius as the IR cut-off: The IR cut-off, $L = 1/H$ where H is the Hubble horizon size. Friedmann equation can be read as

$$H^2 = \frac{8\pi G\rho}{3} = \frac{\rho}{3M_{pl}^2} \quad (3.8)$$

where reduced Planck mass $M_{pl} = (8\pi G)^{-2}$. Hence from the above equation,

$$3M_{pl}^2 H^2 = \rho \quad (3.9)$$

If the universe is assumed to be composed of matter and dark energy, then the total energy density of the universe is given by

$$\rho = \rho_m + \rho_\Lambda \quad (3.10)$$

From equation(3.7), $\rho_\Lambda = 3c^2 M_{pl}^2 L^{-2}$. When size $L = \frac{1}{H}$ is substituted in the expression for the energy density of vacuum, then the above equation can be obtained as

$$\rho_\Lambda = 3c^2 M_{pl}^2 H^2 \quad (3.11)$$

From equation(3.9), we have $\rho_m + \rho_\Lambda = 3M_{pl}^2 H^2$, if the expression for ρ_Λ is substituted from equation(3.11), then the energy density for the matter is obtained as,

$$\rho_m = 3M_{pl}^2 H^2 (1 - c^2) \quad (3.12)$$

Comparing equations(3.11) and (3.12), it can be deduced that ρ_m and ρ_Λ both behave similarly except for the constant factor c . Both ρ_m and ρ_Λ are explicitly proportional to H^2 . From the continuity equation, $\rho_m \sim a^{-3}$, hence it can be assumed that dark energy density also behaves like this. Since matter is pressureless so must be dark energy, then the equation of state for dark energy $\omega_{de} = \frac{p}{\rho} = 0$. But

for an accelerating universe, the pressure must be negative and the equation of state must be $\omega < \frac{-1}{3}$. This implies the holographic dark energy with present IR cut-off will not cause acceleration in the late time of the universe.

Hsu[65] has shown that $\Lambda \sim L^{-2}$ using holographic principle. When the current Hubble size L is chosen as the size of observed universe $L_{today} \sim 10Gyr$, then the cosmological constant is found to be $10^{-10}eV^4$, which is very much near to the today's observed dark energy density. Thus the cosmological constant problem can be resolved. But the corresponding equation of state is found to be zero. This implies the model fails to explain the recent acceleration.

(ii)Future event horizon as the IR cut-off: Another choice for the IR cut-off is future event horizon[56, 66] defined by the expression,

$$R_h = a(t) \int_t^\infty \frac{dt}{a(t)} = a(t) \int_a^\infty \frac{da}{a^2 H} \quad (3.13)$$

It is clear from the above expression that the future event horizon depends upon the future evolution of the scale factor $a(t)$, so it is a global concept. Consider a flat universe, let a sphere of radius R_h have the total energy $4/3\pi R_h^3 \rho_\Lambda$ where ρ_Λ is the energy density inside the sphere. The mass of a black hole of size R_h is $R_h/(2G)$. When these two energies are equated in reference to the holographic principle, the energy density is obtained as

$$\rho_\Lambda = 3c^2 M_{pl}^2 R_h^{-2} \quad (3.14)$$

Adopting the future event horizon as the IR cut-off in calculating the dark energy density, it seems that the present value of the dark energy depends upon the future evolution of the universe[68]. Hence it violates causality.

Another problem in taking event horizon as the IR cut-off is that it is not predicting the age of the universe. The age of the universe can be calculated by the general formula,

$$t = \int_z^\infty \frac{1}{(1+z)H} dz \quad (3.15)$$

Wei and Zhang[69] have calculated the age of the universe by considering event horizon as the IR cut-off of the holographic dark energy. They found that the model fails to predict the age of the universe. Yet another drawback pointed by Li[56] that this model is not explaining the cosmic coincidence of dark energy and dark matter in its full sense. So it seems that taking event horizon as the IR cut-off is no longer a viable solution for explaining the dark energy.

4

Holographic Ricci Dark Energy Model

4.1 Holographic Ricci dark energy model

Holographic dark energy model is formulated in accordance with holographic principle based on the validity of the effective local quantum field theory where a short distance(UV) cut-off is related to a long distance cut-off(IR) due to the limit set by the formation of a black hole [47, 64]. Following this formalism the dark energy density can be expressed as,

$$\rho_{\Lambda} = 3c^2 M_{pl}^2 L^{-2}, \quad (4.1)$$

where $3c^2$ is a convenient numerical constant used[56], M_{pl} is the reduced Planck mass and L is the IR cut-off. Possible choices for IR cut-off include Hubble horizon, particle horizon and future event

horizon[69]. The Hubble horizon and particle horizon as the IR cut-off did not support an accelerating universe [56] while event horizon as the IR cut-off had serious flaws that it violates causality[70] and it could not explain the age of the universe also, however it could explain the late acceleration of the universe.

Following the noted drawbacks of particle horizon and event horizon in using to define the holographic dark energy, Gao et al. proposed a new IR cut-off which is proportional to the local quantities, the Hubble parameter and its time derivative. In their proposal they in fact replaced the future event horizon with the inverse of Ricci scalar curvature $L \sim R^{-1/2}$ [68], which implies that $\rho_\Lambda \propto R$. This model is called as the Ricci dark energy model and is said to be well fitted with the observational data, explained the coincidence problem and the cosmological constant problem. Hence it is said to be a phenomenologically viable model. The age of the universe is explained satisfactorily. The problem of causality violation is avoided in this model. The Ricci scalar curvature is given by

$$R = -6 \left(\dot{H} + 2H^2 + k/a^2 \right), \quad (4.2)$$

where over dot implies the derivative with respect to the cosmic time.

In the study of Gao et al., the co-evolution of dark matter and dark energy is explained neglecting the phase transitions between them. The qualitative study shows that the densities of dark energy and

dark matter are comparable in the past and the acceleration began only recently at lower redshift thus solves the coincidence problem. The model evaluates the evolution of equation of state parameter $\omega = p/\rho$ which is nearly zero at higher redshift where it behaves as non-relativistic dark matter and become -1 when $z \rightarrow 0$. In the far future, the equation of state approaches the value $\omega = -1.12$, which shows that this dark energy evolves to phantom nature in the future evolution of the universe. The study of the deceleration parameter shows that the redshift at which the acceleration began to be $z \simeq 0.55$. Even though holographic dark energy model suffer from failure of predicting the age of the universe, holographic Ricci dark energy model predicts it fairly well.

Later Granda and Oliveros considered the modified form of the new IR cut-off[67] which include square of the Hubble parameter and its time derivative also which is contained in the term Ricci scalar, then the density of holographic dark energy is expressed as,

$$\rho_\Lambda \approx \alpha H^2 + \beta \dot{H}, \quad (4.3)$$

where α and β are the model parameters. Using the Friedmann equation which has an additional term for ρ_Λ , they studied the equation of state which starts from nearly zero at higher redshift to -1 as $z \rightarrow 0$ for $\beta = 0.5$, the evolution of deceleration parameter showed $z = 0.67$ as the redshift at which acceleration began for $\beta = 0.5$. Thus the

theory is consistent with the observational data when β is taken to be closer to 0.5, and when β is fixed at a transition redshift value z_T , the parameter α also gets constrained, since the parameter α can be expressed in terms of β . The transition from deceleration phase to an accelerating phase for the fixed model parameters is shown to be fitting with the observational data. Hence the proponents consider this model viable even though there remains much to evaluate about the form of the IR cut-off which is proportional to the time derivative of Hubble parameter.

The non-interacting and interacting model of holographic Ricci dark energy are discussed in this work. The coming section describes the non-interacting modified holographic Ricci dark energy model.

4.2 Non-interacting modified holographic Ricci dark energy model

In the work [71], the authors have studied the modified holographic Ricci dark energy, without considering its interaction with other cosmic components, in a flat FLRW universe. The evolution of the universe with modified holographic Ricci dark energy is studied by the qualitative analysis of the Hubble parameter, equation of state parameter and deceleration parameter, which characterizes the nature of dark energy. The present value of equation of state parameter and

deceleration parameter and the transition redshift z_T , at which the universe enters the accelerating phase is found. They have used the statefinder diagnostic to distinguish the model from other dark energy models.

In the non-interacting case, the normalized Hubble parameter is given as in [71],

$$h^2 = \Omega_{m0} \exp(-3x) + \frac{\alpha - 1}{1 - \beta} \Omega_{m0} \exp(-3x) + \left[\frac{\alpha - \beta \Omega_{m0}}{\beta - 1} + 1 \right] \exp(-3\beta x), \quad (4.4)$$

where $h = H/H_0$, H_0 is the present value of the Hubble parameter.

The general expression for the equation of state parameter ω_{de} is,

$$\omega_{de} = -1 - \frac{1}{3} \frac{d \ln \Omega_{de}}{dx}, \quad (4.5)$$

where Ω_{de} is the dark energy density parameter. The evolution of the equation of state ω_{de} with respect to redshift z is shown in the figure 4.1. The present values of equation of state parameter is found to be around $\omega_{de0} \simeq -0.70$, for model parameters $(\alpha, \beta) = (1.01, 0.15)$, while WMAP observation value is $\omega_{de0} = -0.93$. The evolution of equation of state showed that ω_{de} starts from nearly zero at higher redshifts implying dark energy behaved like dark matter in the past, and reaching negative values as $z \rightarrow 0$.

The deceleration parameter q , is expressed as

$$q = -\frac{\dot{H}}{H^2} - 1 = -\frac{1}{2h^2} \frac{dh^2}{dx} - 1. \quad (4.6)$$

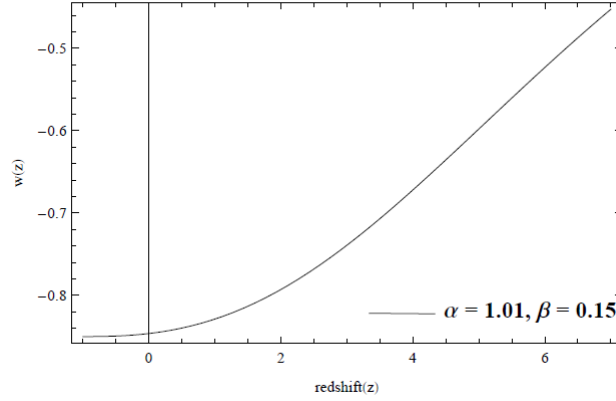


Figure 4.1: [Evolution of equation of state parameter ω_{de} with redshift z for best fit values $(\alpha, \beta) = (1.01, 0.15)$.]

The evolution of the deceleration parameter q with respect to the redshift z is shown in the figure 4.2. The present value of deceleration parameter, and the transition redshift are $q_0 = -0.45$ and $z_T = 0.76$ respectively for model parameters $(\alpha, \beta) = (1.01, 0.15)$, while WMAP observation values are $q_0 = -0.60$ and $z_T = 0.45 - 0.73$. The evolution of deceleration parameter shows that in the remote past it is 0.5, mimicking the nature of cold dark matter, then enters the negative value region such that the acceleration occurs when $z < 1$. Thus it is seen that the predictions of the model is not in good agreement with the observational constraints and at the same time the parameter values are not too far away from them.

The advantage of the model is that the coincidence of the densities of

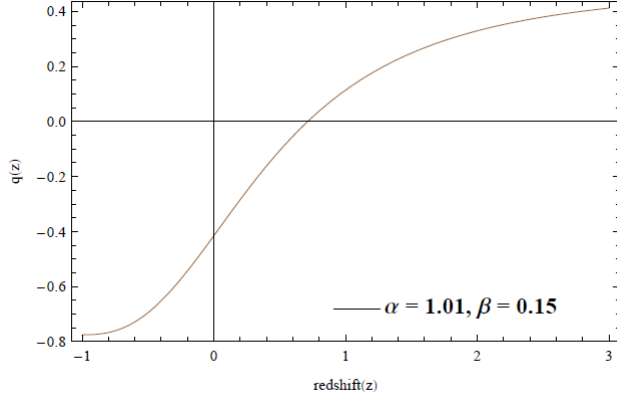


Figure 4.2: [Evolution of deceleration parameter q for best fit model parameters $(\alpha, \beta) = (1.01, 0.15)$.]

dark energy and dark matter is explained for the model parameters $(\alpha, \beta) = (1.01, 0.15)$. The co-evolution of the densities of the dark energy and dark matter is dealt with which has showed that their densities were comparable at the past, and the acceleration began only recently.

Statefinder analysis is carried out employing the statefinder parameters (r, s) introduced by Sahni et al.[72, 73], to discriminate the MHRDE model from other dark energy models. The statefinder parameters are given as

$$r = \frac{\ddot{a}}{aH^3}, \quad s = \frac{r-1}{3(1-q)/2}$$

The analytical expression for the (r, s) parameters in terms of the

weighted Hubble parameter is

$$r = \frac{1}{2h^2} \frac{d^2 h^2}{dx^2} + \frac{3}{2h^2} \frac{dh^2}{dx} + 1 \quad (4.7)$$

and

$$s = -\frac{\frac{1}{2h^2} \frac{d^2 h^2}{dx^2} + \frac{3}{2h^2} \frac{dh^2}{dx}}{\frac{3}{2h^2} \frac{dh^2}{dx} + \frac{9}{2}}. \quad (4.8)$$

From the analysis, they have found that the present position of the universe corresponds to $(r_0, s_0) = (0.59, 0.15)$ in the $r - s$ plane for the model parameters $(\alpha, \beta) = (1.01, 0.15)$. The Λ CDM point have $(r, s) = (1, 0)$, while general quintessence model have $s > 0, r < 1$, for Chaplygin gas $s < 0, r > 1$, and for holographic dark energy with event horizon as the IR cut-off, $s = 2/3, r = 1$. Hence the MHRDE model is distinguished from other models.

It is more logical to expect that the cosmic components might have interacted with each other during the evolution of the universe. So a realistic approach is to consider an interaction between the dark energy and dark matter components. The interaction picture of the model is also studied in many works[74–77].

5

Interacting modified holographic

Ricci dark energy model

5.1 Interacting modified holographic Ricci dark energy model

In this chapter we study the Interacting modified holographic Ricci dark energy(IMHRDE) model[74, 78, 79]. The results presented in this chapter is partly published in the papers[79] and [80]. We have made an analysis of the cosmological parameters. Statefinder diagnostic method is employed to differentiate the IMHRDE model from other dark energy models. The work [80] studies the thermodynamics of the model also. We consider a non-gravitational interaction between Ricci dark energy and dark matter in a flat expanding universe. Since the components, dark energy and dark matter, the cos-

mic fluids, co-exists in the universe, it is logical to expect that they may interact with each other. More over the non-interacting model is not fairly accurate in predicting the cosmological parameters in comparison to the observational results, so it can be expected that the interaction between dark energy and dark matter is plausible to achieve a better the matching of the model with observational results. We assume the nature of interaction in a phenomenological way as given below

$$\dot{\rho}_{de} + 3H(\rho_{de} + p_{de}) = -Q, \quad (5.1)$$

$$\dot{\rho}_m + 3H\rho_m = Q, \quad (5.2)$$

where Q is the interaction term. The Friedmann equation for a flat FLRW universe is given as

$$3H^2 = \rho_m + \rho_{de}. \quad (5.3)$$

Owing to the lack of knowledge about the microscopic origin of the interaction, three phenomenological forms of interaction are used in our analysis, $Q = 3bH(\rho_{de} + \rho_m)$, $Q = 3bH\rho_m$ and $Q = 3bH\rho_{de}$ [75, 78, 81]. The proportionality constant is b , known as the interaction parameter, which when positive ($b > 0$) implies dark energy decaying into dark matter and vice versa when b is negative. The ρ_{de} is the energy density of modified holographic Ricci dark energy which has

the expression[74],

$$\rho_{de} = \frac{2}{\alpha - \beta} \left(\dot{H} + \frac{3}{2}\alpha H^2 \right). \quad (5.4)$$

The expression for Ricci dark energy density is substituted in the Friedmann equation for various interaction terms to obtain the cosmological parameters defining the characteristics of holographic Ricci dark energy. In the next section we discuss the first interaction model with the interaction term $Q \propto H(\rho_{de} + \rho_m)$, its cosmology and later the thermodynamical behavior for a universe dominated by the modified holographic Ricci dark energy. In the work [74] Chimento et al., have studied the non-linear interaction of the modified holographic Ricci dark energy with dark matter.

5.2 Interacting modified holographic Ricci dark energy model with $Q = 3bH(\rho_{de} + \rho_m)$ -IMHRDE1

IMHRDE1 considers the interaction term $Q = 3bH(\rho_{de} + \rho_m)$ between Ricci dark energy and cold dark matter. Using the equation for the holographic Ricci dark energy as well as Friedmann equation, the expression for normalized Hubble parameter h is obtained as,

$$h^2 = \frac{\rho_m}{3H_0^2} + \frac{2}{3\Delta} \left(\frac{1}{2} \frac{dh^2}{dx} + \frac{3\alpha}{2} h^2 \right), \quad (5.5)$$

where $\Delta = \alpha - \beta$ and $x = \ln a$. When the above equation is differentiated again and substituting $\dot{\rho}_{de}$ from the conservation equation,

leads to a second order differential equation for h^2 as,

$$\frac{d^2 h^2}{dx^2} + 3(1 + \beta) \frac{dh^2}{dx} + 9(\beta + b\Delta) h^2 = 0. \quad (5.6)$$

The solution of this second order differential equation is found to be,

$$h^2 = c_1 e^{\frac{3}{2}m_1 x} + c_2 e^{\frac{3}{2}m_2 x}, \quad (5.7)$$

where

$$m_{1,2} = -1 - \beta \mp \sqrt{1 - 4b\alpha - 2\beta + 4b\beta + \beta^2}. \quad (5.8)$$

The coefficients c_1 and c_2 are calculated using the initial conditions,

$$h^2|_{x=0} = 1, \quad \frac{dh^2}{dx}|_{x=0} = 3\Omega_{de0}\Delta - 3\alpha. \quad (5.9)$$

where Ω_{de0} is the present value of the dark energy density, which for a flat universe become, $\Omega_{de0} = 1 - \Omega_{m0}$. Hence the coefficients become,

$$c_1 = \frac{2(\Omega_{de0}\Delta - \alpha) - m_2}{m_1 - m_2}, \quad c_2 = 1 - c_1. \quad (5.10)$$

The equation for the density parameter of dark energy using the solution for h^2 and the Friedmann equation turns out to be

$$\Omega_{de} = c_1 e^{\frac{3}{2}m_1 x} + c_2 e^{\frac{3}{2}m_2 x} - \Omega_{m0} e^{-3x}. \quad (5.11)$$

The general expression for the equation of state parameter for the holographic Ricci dark energy is[71],

$$\omega_{de} = -1 - \frac{1}{3} \frac{d \ln \Omega_{de}}{dx}. \quad (5.12)$$

After finding the derivative of Ω_{de} , the above equation becomes,

$$\omega_{de} = -1 - \frac{1}{2} \left(\frac{c_1 m_1 e^{\frac{3}{2} m_1 x} + c_2 m_2 e^{\frac{3}{2} m_2 x} + 2\Omega_{m0} e^{-3x}}{c_1 e^{\frac{3}{2} m_1 x} + c_2 e^{\frac{3}{2} m_2 x} - \Omega_{m0} e^{-3x}} \right). \quad (5.13)$$

For the case of non-interaction between the dark sectors, i.e. $b = 0$, at which, $m_1 = -2, m_2 = -2\beta, c_1 = 0$ and $c_2 = 1$ and the expression for ω_{de} reduces to

$$\omega_{de} = -1 + \beta. \quad (5.14)$$

This is in agreement with the non-interaction model studied by Titus et al.[71]. The co-evolution of the holographic Ricci dark energy density and dark matter density is plotted for $b = 0.001$ with parameter values $(\alpha, \beta) = (1.01, -0.01)$. It is found that for these parameter values, holographic Ricci dark energy and dark matter evolved together as shown in the figure 5.1 almost in a similar fashion in the past, but at later stage dark energy dominated over the dark matter. It is found that this domination of the dark energy is a recent phenomenon. The parameter set $(1.01, -0.01)$ is taken as the best fit parameters among different parameter sets by quantitative analysis, since it seems to give almost right values of the transition redshift.

The evolution of the equation of state parameter is plotted against redshift z for different model parameters, by taking $\Omega_{de0} = 0.7$, $\Omega_m = 0.3$ as shown in figure 5.2. The analysis of the characteristics of the ω_{de} showed that it's value starts from nearly zero in the remote past and evolves to negative value in the further evolu-

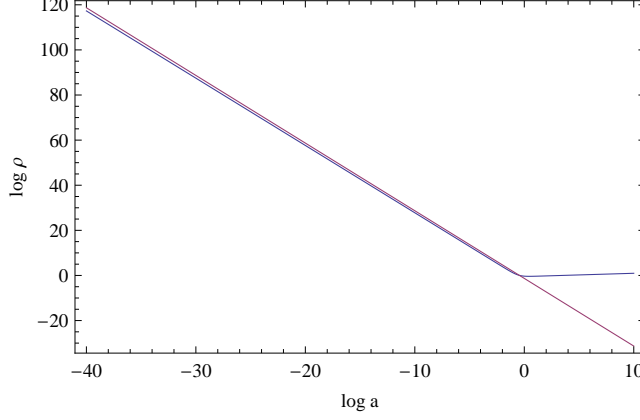


Figure 5.1: [Evolution of IMHRDE1 in comparison with the cold dark matter, with parameters $(\alpha, \beta) = (1.01, -0.01)$ and $b=0.001$. The continuous line which is deviating represents IMHRDE1 and the other one represents cold dark matter.]

tion. For the parameter values $(\alpha, \beta) = (1.01, -0.01)$, as $z \rightarrow -1$, the equation of state $\omega_{de} \rightarrow -1$. For the parameter sets $(1.15, 0.15)$, $(1.2, 0.1)$, $(4/3, 0.05)$, as $z \rightarrow -1$, the equation of state saturate to values higher than -1 , i.e., $\omega_{de} > -1$. For $(\alpha, \beta) = (1.2, -0.1)$, as $z \rightarrow -1$, $\omega_{de} < -1$. So it can be concluded that in the remote past of the evolution of the universe, the interacting holographic Ricci dark energy mimics the behavior of the cold dark matter. For certain parameters, as shown above, the equation of state is greater than -1 , i.e. $\omega_{de} > -1$, where dark energy shows a quintessence behavior. But for the model parameters, $(\alpha, \beta) = (1.2, -0.1)$, the equation of state crosses the phantom divide $\omega_{de} = -1$, the dark energy evolves in to a

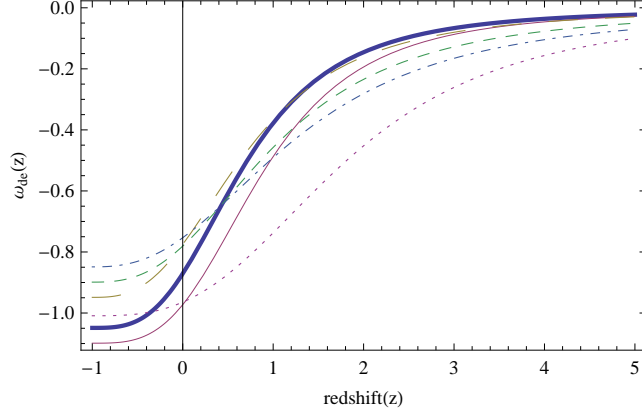


Figure 5.2: [Variation of the equation of state parameter ω_{de} with redshift z for the model parameters $(\alpha, \beta)=(1.2,-0.1)$ -thin continuous, first from the left bottom; $(4/3,-0.05)$ -thick continuous, 2nd from left bottom; $(1.01,-0.01)$ -dotted, 3rd from left bottom; $(1.2,0.1)$ -large dashed, 4th from left bottom; $(4/3,0.05)$ -small dashed, 5th from left bottom and $(1.15,0.15)$ -dot-dashed, 6th from left bottom; all with $b=0.001$.]

phantom nature. The present value of the equation of state parameter is found to be around ω_{de0} is -0.96 for $(\alpha, \beta) = (1.01, -0.01)$. WMAP observational value for the present equation of state parameter of dark energy is around $\omega_{de0} = -0.93$ [16]. Thus the predicted and observational values are in much concordance with each other. However some latest observational results, for instance the Planck result in which $\omega_{de} = -1.49 \pm^{+0.65}_{-0.57}$ [36], favors phantom behavior for the dark energy (but due to comparatively higher error ranges, a definite

conclusion regarding this remains still doubtful.)

Deceleration parameter q , is that which explains the nature of expansion of the universe i.e., whether the universe is decelerating or an accelerating one. For acceleration, $q < 0$. The deceleration parameter can be obtained using the expression[71],

$$q = -\frac{1}{2h^2} \frac{dh^2}{dx} - 1. \quad (5.15)$$

Using the expression for h^2 , from equation (5.7), q becomes,

$$q = -\frac{3 \left(c_1 m_1 e^{\frac{3}{2} m_1 x} + c_2 m_2 e^{\frac{3}{2} m_2 x} \right)}{4 \left(c_1 e^{\frac{3}{2} m_1 x} + c_2 e^{\frac{3}{2} m_2 x} \right)} - 1. \quad (5.16)$$

When the case of non-interaction is considered, i.e., $b = 0$, and also by avoiding the contribution from dark matter, the deceleration parameter, $q = (3\beta - 2)/2$, as shown in [71]. The evolution of q parameter is plotted with respect to redshift z as seen in figure 5.3. The plot shows the characteristics of q for different parameter sets. It starts from 0.5 and enters negative region at later stage of the expansion. The transition redshift z_T , at which the universe transits from an early decelerating phase to an accelerating one is found to be 0.47 for parameters $(4/3, -0.05)$, 0.55 for $(1.2, -0.1)$, 0.70 for $(1.01, -0.01)$, 0.44 for $(4/3, 0.05)$, 0.50 for $(1.2, 0.1)$ and 0.52 for $(1.15, 0.15)$. WMAP observations point to a transition redshift value in the range 0.45–0.73[82]. The present value of deceleration parameter is found to be $q_0 = -0.56$, for $(\alpha, \beta) = (1.01, -0.01)$, while WMAP observational value of q_0 is

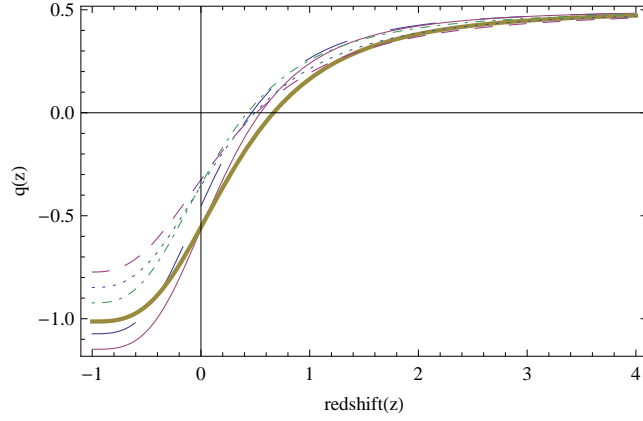


Figure 5.3: [Evolution of the q -parameter with redshift. The plots for $(\alpha, \beta)=(1.2, -0.1)$ -thin continuous, first from the bottom of the left side; $(4/3, -0.05)$ -large dashed line, 2nd from the bottom of the left side; $(1.01, -0.01)$ -thick continuous, third from the left bottom; $(4/3, 0.05)$ -dash-dot, 4th from the left bottom; $(1.2, 0.1)$ -dotted line, 5th from the left bottom and $(1.15, 0.15)$ - small dash line, 6th from left bottom, all with coupling constant $b = 0.001$.]

-0.60 [16]. Thus the predictions of the IMHRDE1 using the model parameters $(\alpha, \beta) = (1.01, -0.01)$, are in close agreement with the WMAP observational data.

Statefinder analysis

Statefinder method is a geometrical diagnostic tool, other than H and q , employed to characterize the properties of dark energy and also to contrast a given model with other dark energy models. Statefinder

parameters (r, s) are dimensionless parameters which are functions of the scale factor of the universe and its derivatives. It was introduced by Sahni et. al. [72, 73] and are defined as

$$r = \frac{1}{2h^2} \frac{d^2 h^2}{dx^2} + \frac{3}{2h^2} \frac{dh^2}{dx} + 1, \quad (5.17)$$

and

$$s = - \left(\frac{\frac{1}{2h^2} \frac{d^2 h^2}{dx^2} + \frac{3}{2h^2} \frac{dh^2}{dx}}{\frac{3}{2h^2} \frac{dh^2}{dx} + \frac{9}{2}} \right). \quad (5.18)$$

When the expression for h^2 is used, the above equations become,

$$r = 1 + \frac{9 \left(c_1 m_1^2 e^{\frac{3}{2} m_1 x} + c_2 m_2^2 e^{\frac{3}{2} m_2 x} \right)}{8 \left(c_1 e^{\frac{3}{2} m_1 x} + c_2 e^{\frac{3}{2} m_2 x} \right)} + \frac{9 \left(c_1 m_1 e^{\frac{3}{2} m_1 x} + c_2 m_2 e^{\frac{3}{2} m_2 x} \right)}{4 \left(c_1 e^{\frac{3}{2} m_1 x} + c_2 e^{\frac{3}{2} m_2 x} \right)}, \quad (5.19)$$

and

$$\begin{aligned} s = & - \left[(c_1 m_1^2 e^{\frac{3}{2} m_1 x} + c_2 m_2^2 e^{\frac{3}{2} m_2 x}) + 2(c_1 m_1 e^{\frac{3}{2} m_1 x} \right. \\ & \left. + c_2 m_2 e^{\frac{3}{2} m_2 x}) \right] / \left[2(c_1 m_1 e^{\frac{3}{2} m_1 x} + c_2 m_2 e^{\frac{3}{2} m_2 x}) \right. \\ & \left. + 4(c_1 e^{\frac{3}{2} m_1 x} + c_2 e^{\frac{3}{2} m_2 x}) \right]. \end{aligned} \quad (5.20)$$

In the case of non-interaction ($b=0$), the equations for r and s become $r = 1 + (9\beta(\beta - 1))/2$ and $s = \beta$, which is in quite correspondence with earlier results[71].

The evolution of $r - s$ parameters, of IMHRDE1 for the model parameters $(\alpha, \beta) = (4/3, -0.05)$, $(1.2, -0.1)$ and $(1.01, -0.01)$ is shown in figure 5.4. The plot depicts the nature of evolution which starts from right to left as the universe expands for the model parameters with

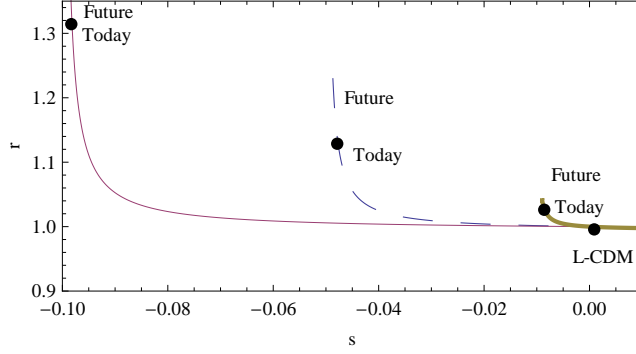


Figure 5.4: [$r - s$ evolutionary trajectories for the model for parameters, $(\alpha, \beta)=(1.2, -0.1)$ -the thin continuous line (extreme left), $(4/3, -0.05)$ -the dashed line (the middle one) and $(1.01, -0.01)$ -the thick continuous line (extreme right), all with $b=0.001$]

negative beta values. The present position of the universe as predicted by the IMHRDE1 model(IMHRDE1 point), the Λ CDM point which corresponds to $r = 1, s = 0$ and the future direction are noted. The present values (r_0, s_0) for the model parameters are, $(1.31, -0.098)$ for $(\alpha, \beta) = (1.2, -0.1)$, $(1.14, -0.048)$ for $(\alpha, \beta) = (4/3, -0.05)$, and $(1.03, -0.008)$ for $(\alpha, \beta) = (1.01, -0.01)$. It can be inferred from the plot that as the β value increases, the distance between the Λ CDM point and the IMHRDE1 point decreases and the r value increases. It is also seen that the trajectory progresses through the Λ CDM point. From the figure 5.5 for positive β values, it is seen that the trajectory evolves from right to left as the universe expands. The present position as predicted by the IMHRDE1 model(IMHRDE1 point) for

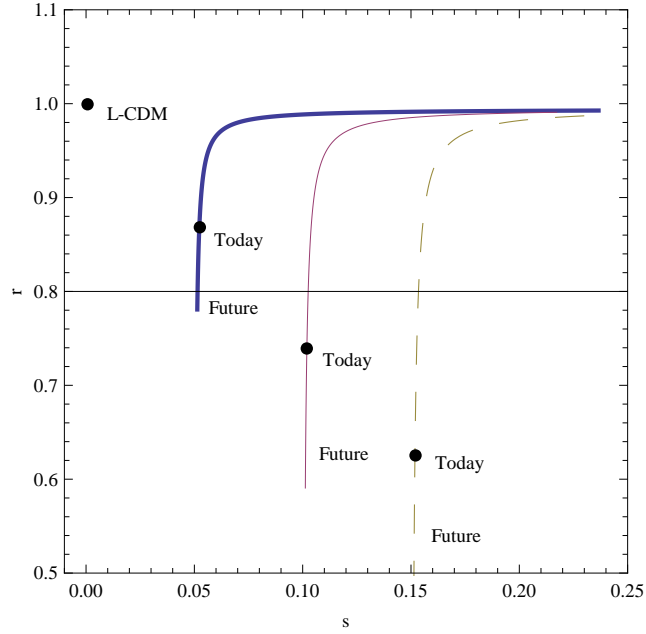


Figure 5.5: [Evolutionary trajectories of $r - s$ plane for parameters $(\alpha, \beta)=(4/3, 0.05)$ -thick continuous, left line; $(1.2, 0.1)$ -thin continuous, middle line and $(1.15, 0.15)$ -dashed, rightmost line; all with $b=0.001$]

positive values of β parameters, the Λ CDM point and the future point are noted. As β increases r value decreases. The Λ CDM point is out of the $r - s$ trajectory.

The statefinder diagnosis thus distinguishes IMHRDE1 model from other dark energy models. For example, for Quintessence model the statefinder parameters trajectory is in the region $r < 1, s > 0$, for Chaplygin gas model the parameters lie in the region $r > 1, s < 0$. For

holographic dark energy model with event horizon as the IR cut-off the $r - s$ trajectory evolves from $s = 2/3, r = 1$ to reach Λ CDM point at the end. In the present model it is found that $r > 1, s < 0$ for negative β values.

The characteristics of the $r - q$ parameters are also studied for IMHRDE1 model for the model parameters $(\alpha, \beta) = (1.01, -0.01)$ and is shown in the plot 5.6. From the plot it can be made out that the trajec-

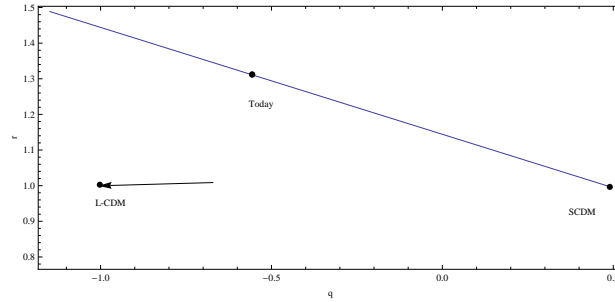


Figure 5.6: [$r - q$ plots for parameters $(\alpha, \beta) = (1.01, -0.01)$ with interaction constant $b=0.001$, the diagonal like line representing $r - q$ trajectory of IMHRDE1 and the horizontal line with arrow is for the Λ CDM as comparison]

tory starts from $q = 0.5, r = 1$ which is the SCDM point, then it evolves through present position of the universe, which has the value $(r_0, q_0) = (1.03, -0.56)$ for the model parameters $(1.01, -0.01)$. The present value of deceleration parameter $q_0 = -0.56$, is comparable to the WMAP value $q_0 = -0.60$. The Λ CDM point is out of the $r - q$

trajectory, which can be seen explicitly. Thus the statefinder analysis proves that the IMHRDE1 model differs from other models and the behavior of the holographic Ricci dark energy is almost in accordance with the observational results.

5.3 Thermodynamics of IMHRDE1 model

In the previous section the IMHRDE1 model is studied by analyzing its cosmological parameters and found that the model is almost satisfying with the values of WMAP observations. In this section we present the study on the thermodynamical aspects of the interacting dark energy model. The universe is assumed to be composed of dark energy and dark matter and is bounded by the horizon. The possible horizons taken for the study are apparent horizon and absolute horizon (event horizon). Study of thermodynamics comprises the analysis of generalized second law of thermodynamics, the evolution of entropies of the dark sectors in particular and the universe as a whole, in general. Generalized second law of thermodynamics(GSL) [62, 83] demands that the change in entropies of the components inside the universe when added together with that of the horizon bounding the universe must be greater than or equal to zero. In other words, the total entropy comprising that of the dark energy, dark matter

added with that of the horizon must not decrease. That is,

$$\dot{S}_{de} + \dot{S}_m + \dot{S}_h \geq 0, \quad (5.21)$$

where \dot{S}_{de} is the change in entropy of dark energy with respect to cosmic time, \dot{S}_m is the entropy change for dark matter and \dot{S}_h is the change in entropy of the horizon. The subsections below, consists of the analysis on the validity of GSL under thermal equilibrium and non-equilibrium conditions.

5.3.1 GSL validity under thermal equilibrium conditions

Thermal equilibrium condition means that the cosmic components were in thermal equilibrium with each other. So the temperatures of the dark energy and the dark matter are equal to each other, and are taken to be equal to the temperature of the horizon. That is,

$$T_{de} = T_m = T_h, \quad (5.22)$$

where T_{de}, T_m, T_h are the temperatures of dark energy, dark matter and horizon respectively. Under this condition we have studied the thermodynamics by first taking apparent horizon as the boundary of the universe, and in the second case we take event horizon as the boundary.

(i) Apparent horizon as the thermodynamic boundary: Apparent horizon is taken as the boundary of the universe. Then the

GSL demands that the entropy change of dark energy, dark matter when added together with that of the apparent horizon must increase. The apparent horizon distance, r_a is defined as[84, 85]

$$r_a = \frac{1}{\sqrt{H^2 + k/a^2}}, \quad (5.23)$$

where r_a is the apparent horizon radius. When $k = 0$, that is for a flat universe the expression becomes,

$$r_a = \frac{1}{H}, \quad (5.24)$$

which may be equivalent to Hubble horizon. The temperature of the horizon is given by $T_a = |\kappa|/2\pi$ where κ is known as the surface gravity. For a flat universe this reduces to

$$T_a = \frac{H}{2\pi}. \quad (5.25)$$

The entropy of the horizon is expressed as $S = A_a/4G$ [86] where $A_a = 4\pi r_a^2$ is the area of the horizon and G is the gravitation constant. Taking $8\pi G = 1$, it can be further shown that the equation of entropy takes the form,

$$S_a = \frac{8\pi^2}{H^2}, \quad (5.26)$$

For dark energy and dark matter, the entropy can be found using Gibb's relation given below,

$$TdS = dE + PdV, \quad (5.27)$$

where $V = \frac{4}{3}\pi r_a^3$ is the volume, $E = \frac{4}{3}\pi r_a^3(\rho_{de} + \rho_m)$ is the total energy of dark energy and dark matter. Using these expressions and conservation equations, the change in the total entropy in relation to $x = \log a$, is

$$S' = \frac{16\pi^2}{H^2} + \frac{16\pi^2}{H^2} \left(1 + \frac{3}{2}(1 + \omega_{de}\Omega_{de}) \right) q, \quad (5.28)$$

where prime denotes derivative with respect to x , thus for the GSL to be valid, $S' \geq 0$. It is clear from the expression that as $H^2 > 0$, the condition $q \geq \frac{-1}{(1+\frac{3}{2}(1+\omega_{de}\Omega_{de}))}$ must be satisfied for the GSL to be valid. The expression for S' can be simplified using the relation for q which is,

$$q = -1 - \frac{\dot{H}}{H^2} = \frac{1}{2} (1 + 3\omega_{de}\Omega_{de}). \quad (5.29)$$

The change in the total entropy will finally takes the form,

$$S' = \frac{16\pi^2}{H^2} (1 + q)^2. \quad (5.30)$$

From the above equation it can be seen that as all terms are squares there is no possibility for S' to become negative. Hence the condition $S' \geq 0$ is always valid for a universe with apparent horizon as the boundary. The plot showing the validity of GSL for the IMHRDE1 model with model parameters having positive β values is shown in figure 5.7. and that for negative values of β parameters is shown in figure 5.8 The plots showed that S' is positive for all model parameters. This implies that the condition for the validity of GSL is

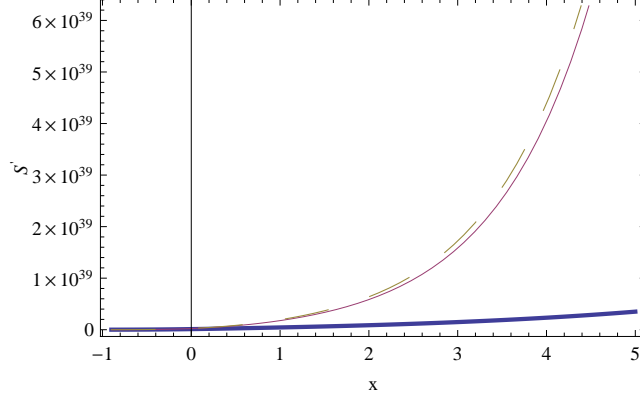


Figure 5.7: [The behavior of S' inside the apparent horizon under thermal equilibrium conditions for the parameters $(\alpha, \beta) = (1.2, 0.1)$ (thick continuous line), $(\alpha, \beta) = (1.3, 0.3)$ (thin continuous line), and $(\alpha, \beta) = (1.4, 0.3)$ (dashed line). The interaction coupling constant $b = 0.001$ for all the plots.]

satisfied. Conclusively, the GSL is always valid inside apparent horizon.

(ii)Event horizon as the thermodynamic boundary: Event horizon is a kind of absolute boundary beyond which no information can be received by an observer. Considering the FLRW universe with dark energy and dark matter bounded by event horizon, for the GSL to be valid, the entropy of dark energy, dark matter added with that of the event horizon must not decrease. The event horizon distance is given by

$$R_E = \frac{1}{1+z} \int_z \frac{dz}{H}. \quad (5.31)$$

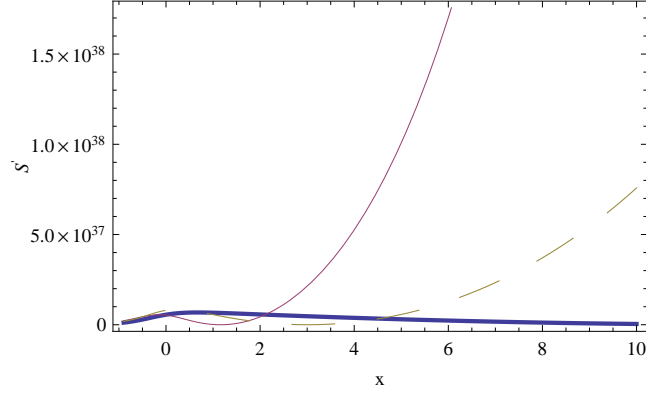


Figure 5.8: [The behavior of S' inside the apparent horizon under thermal equilibrium conditions for the parameters $(\alpha, \beta) = (1.01, -0.01)$ (thick continuous line), $(\alpha, \beta) = (1.2, -0.1)$ (thin continuous line), and $(\alpha, \beta) = (1.3, -0.05)$ (dashed line). The interaction coupling constant $b = 0.001$ for all the plots.]

where R_E is the event horizon radius. The integration is performed for the IMHRDE1 model and the result is

$$R_h = \frac{K_1(1+z)^{3m_2+1}}{c_1(1+z)^{\frac{3}{2}m_2-m_1}} {}_2F_1 \left[g_+, 0.5, 1+g_+, \frac{c_1}{c_2}(1+z)^{\frac{3}{2}m_2-m_1} \right], \quad (5.32)$$

for positive values of β and

$$R_h = \frac{K_2(1+z)^{3m_2+1}}{\sqrt{c_2}} {}_2F_1 \left[g_-, 0.5, 1+g_-, \frac{c_1}{c_2}(1+z)^{\frac{3}{2}m_2-m_1} \right], \quad (5.33)$$

for negative values of β . ${}_2F_1$ is the hypergeometric function which arises as the solution. The constants, K_1, K_2, g_+ , and g_- are having different values for different model parameters. The $g_+ = 0.185, 0.238,$

0.238 for $(\alpha, \beta) = (1.2, 0.1), (1.2, 0.3), (4/3, 0.3)$, respectively, and $K_1 = 8.484 \times 10^{17}$ for positive values of β . $g_- = 0.345, 0.349, 0.349$ for $(\alpha, \beta) = (1.01, -0.01), (1.2, -0.1), (4/3, -0.1)$, respectively and $K_2 = -4.227 \times 10^{17}$. The temperature and area of the event horizon are given by

$$\begin{aligned} T &= 1/4\pi R_E, \\ A &= 4\pi R_h^2. \end{aligned}$$

The Gibb's relation is used to find the rate of entropy of dark energy and dark matter as,

$$T (S'_{de} + S'_m) = H^{-1} (\rho_{de} + \rho_m + p_{de}) 4\pi R_E^2 (\dot{R}_E - H R_E). \quad (5.34)$$

In the above equation, the expression for temperature is substituted and considering $\dot{R}_E = H R_E - 1$, the equation become,

$$(S'_{de} + S'_m) = -H^{-1} (\rho_{de} + \rho_m + p_{de}) 8\pi^2 R_E^3. \quad (5.35)$$

When dominant energy condition $(\rho + p) > 0$ persists, the above sum of rate of entropies can be negative when $R_E > 0$. But when the rate of change of horizon entropy is added with these, the rate of total entropy is obtained as,

$$S' = H^{-1} \left[16\pi^2 R_E \left(\dot{R}_E - \frac{R_E^2}{2} (\rho_{de} + \rho_m + p_{de}) \right) \right]. \quad (5.36)$$

When the expression

$$\dot{H} = -(1/2)(\rho_{de} + \rho_m + p_{de}), \quad (5.37)$$

is used the equation (5.36) becomes

$$S' = H^{-1} \left[16\pi^2 R_E \left(\dot{R}_E + \dot{H} R_E^2 \right) \right]. \quad (5.38)$$

For the GSL to be valid $\dot{R}_E + \dot{H} R_E^2 \geq 0$, which in terms of Friedmann equation becomes,

$$\dot{R}_E \geq \frac{3}{2} (1 + \omega_{de} \Omega_{de}) H^2 R_E^2. \quad (5.39)$$

More clearly,

$$H R_E - 1 - \frac{3}{2} (1 + \omega_{de} \Omega_{de}) H^2 R_E^2 \geq 0. \quad (5.40)$$

The above condition is plotted in the figures 5.9 and 5.10. The

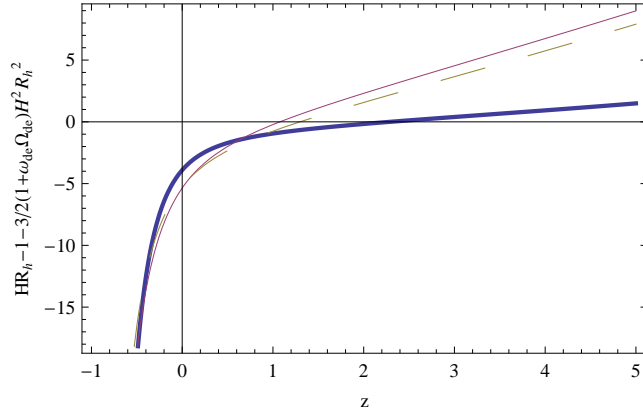


Figure 5.9: [Plot for the parameters $(\alpha, \beta) = (1.2, 0.1)$ (thick continuous line), $(\alpha, \beta) = (1.3, 0.3)$ (thin continuous line), and $(\alpha, \beta) = (4/3, 0.3)$ (dashed line), with the interaction coupling constant $b = 0.001$ inside the event horizon under thermal equilibrium conditions.]

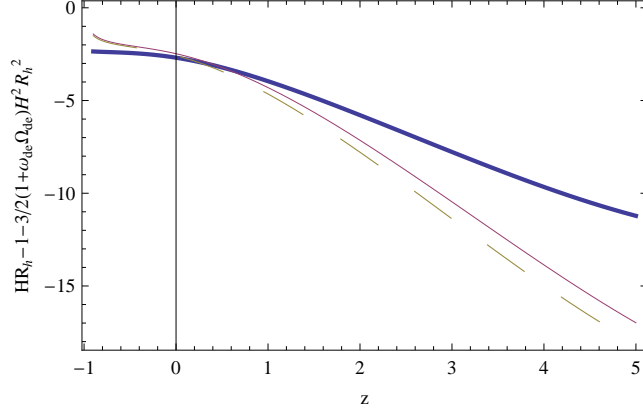


Figure 5.10: [Plot for the parameters $(\alpha, \beta) = (1.01, -0.01)$ (thick continuous line), $(\alpha, \beta) = (1.2, -0.1)$ (thin continuous line), and $(\alpha, \beta) = (4/3, -0.1)$ (dashed line), with the interaction coupling constant $b = 0.001$ inside the event horizon under thermal equilibrium conditions.]

figures show that the GSL is only partially satisfied in the case of positive β parameters, while the GSL is completely violated in the case of negative β parameters.

Substituting the relation for q , the above inequality for the validity of GSL becomes,

$$q \leq -1 + \frac{\dot{R}_E}{H^2 R_E^2}. \quad (5.41)$$

It is to be noted that the critical condition is satisfied for de-Sitter universe, for which $\dot{R}_E = 0$ resulting in $q = -1$.

5.3.2 GSL validity under thermal non-equilibrium conditions

Thermal non-equilibrium implies that the temperatures of the dark energy, dark matter and the horizon are different i.e. $T_{de} \neq T_m \neq T_h$. Here apparent horizon is taken as the viable thermodynamic boundary of the universe. Using Gibb's relation the total entropy change of the universe comprising of the dark energy, dark matter and apparent horizon in terms of deceleration parameter q can be expressed as,

$$S' = H^{-1} \left[\frac{4\pi}{H^2} \left(\frac{\rho_{de} + \rho_m + P_{de}}{T_{de}} \right) q + \frac{8\pi}{T_h} (1+q) \right] + \frac{8\pi}{T_h} (1+q), \quad (5.42)$$

which can be reduced to

$$S' = H^{-1} 8\pi (1+q) \left(\frac{q}{T_{de}} + \frac{1}{T_h} \right) + 12\pi q \Omega_m \left(\frac{1}{T_m} - \frac{1}{T_{de}} \right). \quad (5.43)$$

If one assumes that, equilibrium existing between dark energy and dark matter alone, then $T_{de} = T_m$, hence the second term in the above equation vanishes. When $(q+1) \geq 0$, which corresponds to the quintessence nature of dark energy, the GSL is valid if $\frac{T_{de}}{T_h} \geq -q$. This means that the temperature of dark energy must be greater than that of the horizon. On the other hand if $(1+q) \leq 0$, which corresponds to the phantom nature of dark energy, then the temperature of dark energy must be less than that of the horizon for the validity of GSL. Considering the second case in which the universe is completely dominated by the dark energy, and hence the dark matter density contri-

bution to the total energy density be neglected, then the equation for change of entropy becomes

$$S' = 8\pi(1+q) \left(\frac{q}{T_{de}} + \frac{1}{T_h} \right) - \frac{12\pi q \Omega_m}{T_{de}}. \quad (5.44)$$

It is clear from the above equation that the GSL will be satisfied only if,

$$\frac{T_{de}}{T_h} > -\frac{3(1+\omega_{de})\Omega_{de}}{2} \left(\frac{q}{1+q} \right). \quad (5.45)$$

For quintessence type of dark energy with $q < 0$, $(1 + \omega_{de}) > 0$ and $(1 + q) > 0$, the above condition demands that the temperature of the dark energy must be greater than that of the horizon. Even for the phantom type of universe with $(1 + \omega_{de}) < 0$ and $(1 + q) < 0$ the above said condition holds for the validity of GSL.

5.4 Entropy evolution of IMHRDE1

In the previous section we have shown that, the GSL is valid if the dark energy temperature is greater than that of the horizon. Here it is assumed that the dark energy temperature is proportional to the temperature of the horizon, $T_{de} \propto T_h$ and more specifically let $T_{de} = kT_h$, where k is a constant. The equation for entropy of the dark energy is obtained using the standard relation $S = \frac{(\rho+p)V}{T}$ [1]. On substituting the density, pressure and temperature of the dark

energy, the entropy become,

$$S_{de} = \frac{8\pi^2}{kH^2} \Omega_{de} (1 + \omega_{de}), \quad (5.46)$$

and the total entropy, which include the entropy of dark energy and that of the horizon, is

$$S = \frac{8\pi^2}{kH^2} \Omega_{de} (1 + \omega_{de}) + \frac{8\pi^2}{H^2}. \quad (5.47)$$

The evolution of the entropy of dark energy and total entropy with respect to $x = \ln a$ are plotted and are shown in the below figures (5.11) and (5.12). The figure 5.11 shows that the entropy of dark energy

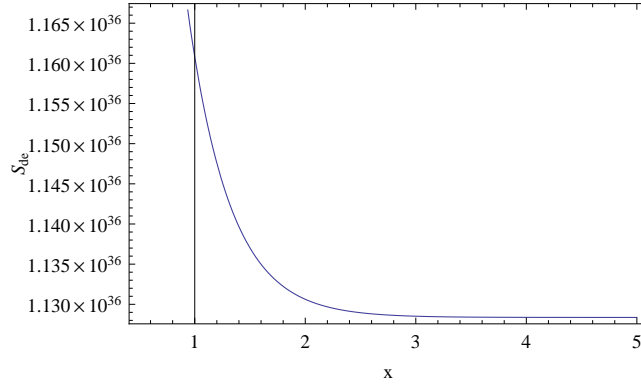


Figure 5.11: [Evolution of entropy of holographic Ricci dark energy against $x \ln a$]

decreases as the universe expands, while the second plot shows that the entropy of the horizon increases and total entropy also increases as universe expands. Thus it can be explained that the decrease in

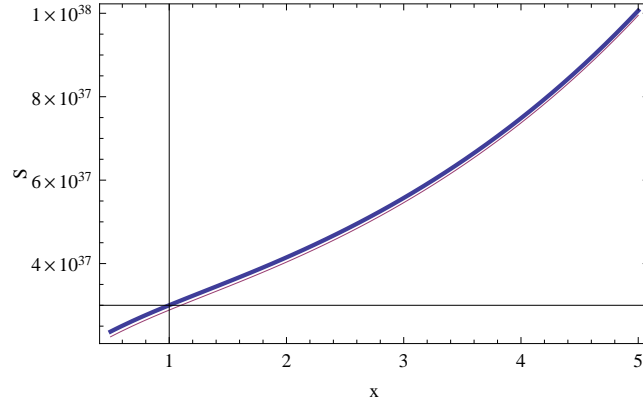


Figure 5.12: [Evolution of apparent horizon entropy and total entropy against $x = \ln a$. The thick continuous line represents the total entropy S_{tot} while the thin line represents the horizon entropy S_h .]

entropy of the dark energy is compensated by the increase in the entropy of the horizon. Hence the total entropy increases.

5.5 Conclusions

The interacting model of holographic Ricci dark energy is studied for a flat FLRW universe, in which the interaction between dark energy and dark matter is taken as proportional to $(\rho_{de} + \rho_m)$ (IMHRDE1). The evolution of the cosmological parameters and thermodynamics of the IMHRDE1 model are analyzed for different model parameters. We have shown that the model IMHRDE1 is explaining co-evolution of dark matter and dark energy with interaction parameter $b = 0.001$. At late stages, the dark energy dominates over the dark matter

and hence the universe transit into an accelerating phase of expansion. The evolution of the equation of state parameter shows that IMHRDE1 behaves almost like cold dark matter in the remote past. As the universe expands, it has evolved to negative values. For the best fit parameters $(1.01, -0.01)$, the equation of state $\omega_{de} \rightarrow -1$ as $z \rightarrow -1$. However, in general, the equation of state may cross the phantom divide for certain model parameters. The present value of the equation of state parameter is almost in agreement with the WMAP data.

The evolution of the deceleration parameter starts from the value 0.5 in the remote past, mimicking the behavior of dark matter. In the further stage of evolution, there occur transition into an accelerating phase for all parameter values. For the best fit parameters, $q \rightarrow -1$ as $z \rightarrow -1$. The present value of the deceleration parameter, q_0 is almost in agreement with the value of WMAP observation.

The validity of generalized second law of thermodynamics(GSL) is checked for a universe with dark energy, dark matter bounded by horizon (for both apparent horizon and event horizon), under thermal equilibrium and also under non-equilibrium conditions. When thermal equilibrium prevails between the entities inside the universe and the horizon, the GSL is valid only if apparent horizon is the boundary, while the GSL is violated if event horizon is the boundary. Many other works also support these results[87–90]. Under thermal

non-equilibrium case where the contents inside the universe are not in thermal equilibrium with the apparent horizon, the temperature of dark energy must be greater than that of the horizon for the GSL to be valid. Works like [91] show similar results.

Further the entropy evolution of the IMHRDE1 is examined in a universe dominated by dark energy. It is found that the entropy of the dark energy decreases while the horizon entropy increases leading to the increase in the total entropy.

6

Interacting modified holographic Ricci dark energy

model with interaction term

$$Q \propto H\rho_m\text{-IMHRDE2}$$

6.1 Interacting modified holographic Ricci dark energy model with interaction term $Q \propto H\rho_m$ - IMHRDE2

The IMHRDE2 model considers the interaction between dark energy and dark matter defined through the interaction term $Q = 3bH\rho_m$, where b is the interaction parameter, H is the Hubble parameter and ρ_m is the energy density of dark matter. The evolution of the densities is governed by,

$$\dot{\rho}_{de} + 3H(\rho_{de} + p_{de}) = -Q, \quad (6.1)$$

$$\dot{\rho}_m + 3H\rho_m = Q. \quad (6.2)$$

Interacting modified holographic Ricci dark energy model with interaction term

80

$Q \propto H\rho_m$ -IMHRDE2

where Q is the interaction term. The whole analysis presented in this section is based on the paper given by [79].

The Friedmann equation for a flat FLRW universe is,

$$3H^2 = \rho_m + \rho_{de}, \quad (6.3)$$

where ρ_{de} is the energy density of the dark energy. The expression for modified holographic Ricci dark energy [74] is,

$$\rho_{de} = \frac{2}{\alpha - \beta} \left(\dot{H} + \frac{3}{2}\alpha H^2 \right). \quad (6.4)$$

Using the Friedmann equation, the interaction equation and the expression for the dark energy density, the differential equation for normalized Hubble parameter h is found out to be

$$\frac{d^2 h^2}{dx^2} + 3(\beta - b + 1) \frac{dh^2}{dx^2} + 9\beta(1 - b)h^2 = 0, \quad (6.5)$$

which is a second order differential equation with respect to the variable $x = \ln a$. The general solution of the above differential equation is obtained as,

$$h^2 = k_1 e^{-3\beta x} + k_2 e^{3(b-1)x}, \quad (6.6)$$

where the constant coefficients k_1 and k_2 are evaluated using initial conditions

$$h^2|_{x=0} = 1, \quad \frac{dh^2}{dx}|_{x=0} = 3\Omega_{de0}\Delta - 3\alpha, \quad (6.7)$$

and thus,

$$k_1 = \frac{\Omega_{de0}(\alpha - \beta) - \alpha - b + 1}{1 - \beta - b}, \quad k_2 = 1 - k_1. \quad (6.8)$$

The dark energy density parameter Ω_{de} is then found to be,

$$\Omega_{de} = k_1 e^{-3\beta x} + k_2 e^{3(b-1)x} - \Omega_{m0} e^{-3x}. \quad (6.9)$$

The equation of state ω_{de} of the dark energy is found out, using the general expression given by

$$\omega_{de} = -1 - \frac{1}{3} \frac{d \ln \Omega_{de}}{dx}, \quad (6.10)$$

which becomes,

$$\omega_{de} = -1 + \left[\frac{k_1 \beta e^{-3\beta x} + k_2 (1-b) e^{-3(1-b)x} - \Omega_{m0} e^{-3x}}{k_1 e^{-3\beta x} + k_2 e^{-3(1-b)x} - \Omega_{m0} e^{-3x}} \right], \quad (6.11)$$

and the expression for pressure p whose basic expression is $p = \omega_{de} \times \rho_{de}$ is obtained as,

$$p_{de} = - \left[(1 - \beta) k_1 e^{-3\beta x} + b k_2 e^{-3(1-b)x} \right]. \quad (6.12)$$

If there is no interaction, i.e., $b = 0$, then the constants, $k_1 = 1$, and $k_2 = 0$, then the equation of state reduces to $\omega_{de} = -1 + \beta$, in a dark energy dominated universe and is in confirmation with the earlier result regarding a flat FLRW universe consists of non-interacting Ricci dark energy and dark matter[71]. An important fact is the co-evolution of the dark energy and dark matter. We have found that the present model with interaction between the dark sectors is very well explaining this. The co-evolution of the dark energy density given by equation(6.9) and dark matter density, $\Omega_m = \Omega_{m0} a^{-3}$ is studied

Interacting modified holographic Ricci dark energy model with interaction term

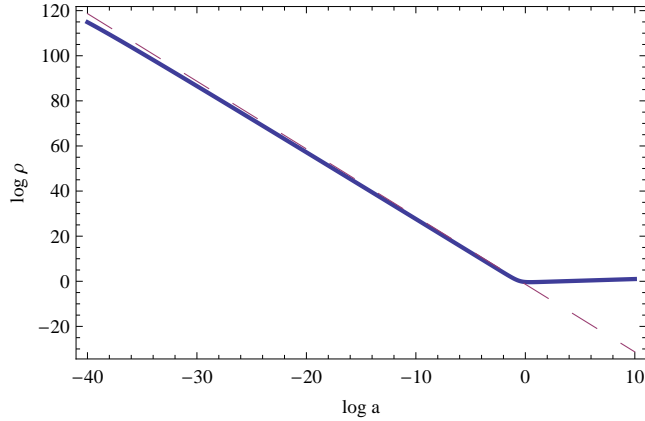


Figure 6.1: [Evolution of IMHRDE2 model with $Q = 3bH\rho_m$, for parameters, $(\alpha, \beta)=(1.01, -0.01)$ and $b=0.003$. Continuous line for interacting IMHRDE and dashed line is for dark matter.]

for the best fit of model parameters $(\alpha, \beta) = (1.01, -0.01)$ and interaction parameter, $b = 0.003$. The co-evolution is observed only when the interaction parameter $b \leq 0.003$. The plot shown in figure 6.1 is in logarithmic scale and it shows that the dark energy density and dark matter density is of the same order in the recent past and the dark energy is dominating only recently.

The evolution of the equation of state parameter, ω_{de} of IMHRDE2 with redshift z as given by the equation (6.11) is plotted for different sets of model parameters as shown in the below figure 6.2. From the plot it can be deduced that for the model parameters with $\beta > 0$, the equation of state, $\omega_{de} > -1$ as $z \rightarrow -1$, which corresponds to the quintessence nature of dark energy, while for the model param-

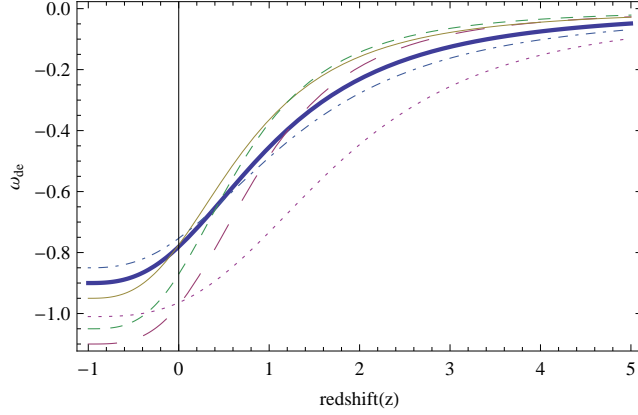


Figure 6.2: [Behavior of the ω_{de} of IMHRDE2 with $b=0.003$ for parameter $(\alpha, \beta)=(1.2, -0.1)$ -large dashed line, $(4/3, -0.05)$ -small dashed line, $(1.01, -0.01)$ -dotted line, $(1.2, 0.1)$ -thin continuous line, $(4/3, 0.05)$ -thick continuous line and $(1.15, 0.15)$ -dot-dashed line]

eters $(\alpha, \beta) = (1.2, -0.1), (4/3, -0.05)$, with $\beta < 0$, the equation of state, $\omega_{de} < -1$ as $z \rightarrow -1$, which corresponds to the phantom nature of dark energy in the future, and for $(\alpha, \beta) = (1.2, -0.1)$, the equation of state, $\omega_{de} \rightarrow -1$ as $z \rightarrow -1$ which corresponds to the de Sitter phase in the future. The present value of the equation of state parameter ω_{de0} is found to be -0.88 for $(\alpha, \beta) = (4/3, -0.05)$, -0.98 for $(\alpha, \beta) = (1.2, -0.1)$, -0.97 for $(\alpha, \beta) = (1.01, -0.01)$, -0.78 for $(\alpha, \beta) = (4/3, 0.05)$, -0.78 for $(\alpha, \beta) = (1.2, 0.1)$ and -0.76 for $(\alpha, \beta) = (1.15, 0.15)$. The ω_{de0} value for $(\alpha, \beta) = (1.01, -0.01)$ is very close to the WMAP value -0.93 [16].

The analytic expression for deceleration parameter q is obtained

Interacting modified holographic Ricci dark energy model with interaction term

as

$$q = -1 + \frac{3}{2} \left(\frac{k_1\beta e^{-3\beta x} - k_2(b-1)e^{-3(1-b)x}}{k_1 e^{-3\beta x} + k_2 e^{-3(1-b)x}} \right). \quad (6.13)$$

The evolution of deceleration parameter is studied with respect to redshift z and is shown in the figure 6.3. The trajectory of q param-

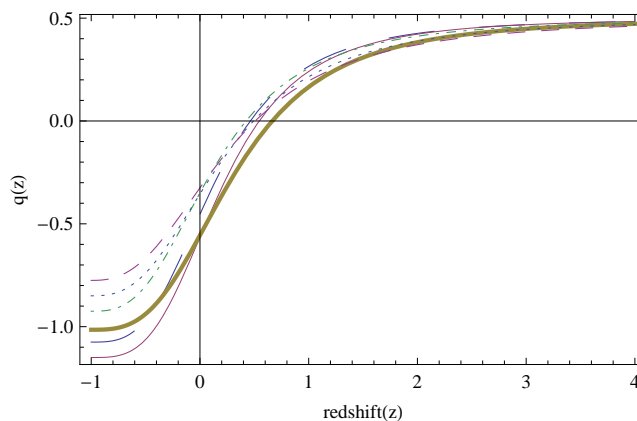


Figure 6.3: [Characteristics of q -parameter of IMHRDE2 with redshift for $(\alpha, \beta)=(1.2,-0.1)$ thin continuous line, $(4/3,-0.05)$ -large dashed line, $(1.01,-0.01)$ -thick continuous line, $(4/3,0.05)$ -dot dashed line, $(1.2,0.1)$ -dotted line and $(1.15,0.15)$ - small dashed line for coupling constant $b = 0.003$.]

ter starts from nearly 0.5 corresponds to cold dark matter region, at higher redshift, and then reaches negative value and enters the accelerating phase at a redshift $z < 1$. The early behavior of q gives an indication that the interacting holographic Ricci dark energy can be considered as a unifying candidate such that it behaves as cold dark

matter in the early epoch and later behaves as dark energy which causing the acceleration in the expansion of the universe. The present value of the deceleration parameter q_0 given by IMHRDE2 model for different model parameters are: -0.46 for $(4/3, -0.05)$, -0.57 for $(1.2, -0.1)$, -0.57 for $(1.01, -0.01)$, -0.34 for $(4/3, 0.05)$, -0.36 for $(1.2, 0.1)$, and -0.33 for $(1.15, 0.15)$. The q_0 value is -0.57 for the parameters $(\alpha, \beta) = (1.01, -0.01)$ which is very close to the WMAP observational value -0.60 . The transition redshift z_T , which is the redshift at which the q parameter crosses in to the negative region so that the universe enters the accelerating phase is found to be 0.68 for $(1.01, -0.01)$, 0.57 for $(1.2, -0.1)$ and 0.44 for $(4/3, -0.05)$. The z_T as per the observations is in the range $0.45 - 0.73$ [82]. The transition redshift, z_T values corresponding to the model parameters $(\alpha, \beta) = (1.01, -0.01)$ lies in the observational range range.

Statefinder Analysis

Statefinder diagnostic tool introduced by Sahni et al.[72, 73], is a geometric method used to discriminate different dark energy models. The statefinder parameters are denoted by (r, s) and the analytic expression of the statefinder parameters for IMHRDE2 is obtained

Interacting modified holographic Ricci dark energy model with interaction term

using the same way as in the previous chapter,

$$r = 1 + \frac{9k_1\beta^2 e^{-3\beta x} + 9k_2(1-b)^2 e^{-3(1-b)x}}{2(k_1 e^{-3\beta x} + k_2 e^{-3(1-b)x})} - \frac{9k_1\beta e^{-3\beta x} + 9k_2(1-b)e^{-3(1-b)x}}{2(k_1 e^{-3\beta x} + k_2 e^{-3(1-b)x})}, \quad (6.14)$$

and

$$s = -[9k_1\beta^2 e^{-3\beta x} + 9k_2(1-b)^2 e^{-3(1-b)x} - 9k_1\beta e^{-3\beta x} - 9k_2(1-b)e^{-3(1-b)x}] / [-9k_1\beta e^{-3\beta x} - 9k_2(1-b)e^{-3(1-b)x} + 9k_1 e^{-3\beta x} + 9k_2(1-b)e^{-3(1-b)x}]. \quad (6.15)$$

$$(6.16)$$

For non-interaction case with $b = 0$, the statefinder parameters in a dark energy dominated phase will be $r = 1 + 9\beta(\beta - 1)/2$ and $s = \beta$, which is in good terms with the results of earlier work[71]. The evolution of IMHRDE2 in the $r - s$ plane is plotted for model parameters with both positive and negative β values. For negative β the $r - s$ trajectories is shown in the below figure 6.4. The evolutionary trajectory in $r - s$ plane for IMHRDE2 model parameters with negative β values passes through $r = 1, s = 0$ which is the Λ CDM point, at the beginning. The present position of the universe in $r - s$ plane of IMHRDE2 model is noted and is closer to the Λ CDM point for the model parameters $(\alpha, \beta) = (1.01, -0.01)$ and the distance increases with the increase in β value. The present position of IMHRDE2 in the $r - s$ plane is noted as $(r_0, s_0) = (1.14, -0.048)$ for $(\alpha, \beta) =$

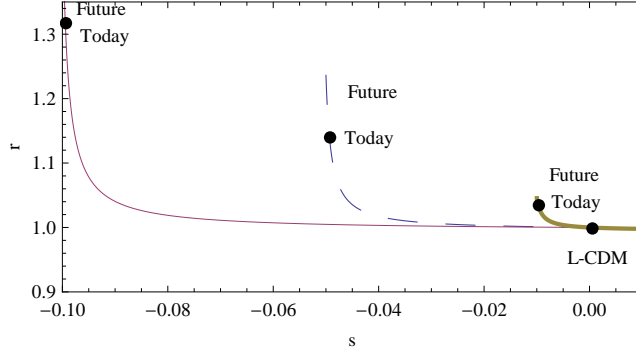


Figure 6.4: [Trajectory of the IMHRDE2 model in the $r - s$ plane $(\alpha, \beta) = (1.2, -0.1)$ -thin continuous, left line; $(4/3, -0.05)$ -dashed, middle line, $(1.01, -0.01)$ -thick continuous, right line, for $b = 0.003$. The evolution is from right to left]

$(4/3, -0.05)$, $(r_0, s_0) = (1.31, -0.099)$ for $(\alpha, \beta) = (1.2, -0.1)$ and $(r_0, s_0) = (1.03, -0.0096)$ for $(\alpha, \beta) = (1.01, -0.01)$.

The evolution of IMHRDE2 in the $r - s$ plane for positive β parameters is shown in the figure 6.5. The evolution shows that the trajectory starts from $r = 1$. The present position of the universe is marked, and the evolution of the whole trajectory is from right to left. The Λ CDM point lies out of the path. The present position noted is $(r_0, s_0) = (0.87, 0.05)$ for $(\alpha, \beta) = (4/3, 0.05)$, $(r_0, s_0) = (0.74, 0.10)$ for $(\alpha, \beta) = (1.2, 0.1)$ and $(r_0, s_0) = (0.62, 0.15)$ for $(\alpha, \beta) = (1.15, 0.15)$.

The present position of (r, s) parameters for the best fit parameters $(1.01, -0.01)$ has correspondence with that of the Chaplygin gas model for which $(r > 1, s < 0)$. The quintessence model of dark en-

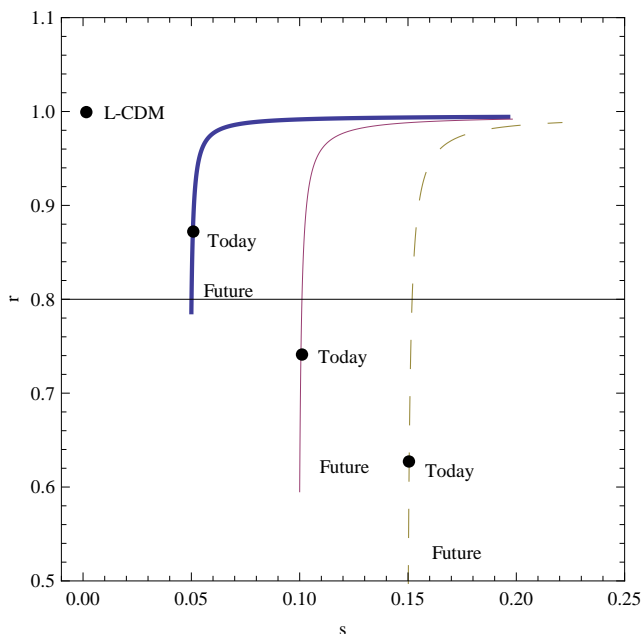


Figure 6.5: [Evolutionary path of IMHRDE2 in $r - s$ plane for parameters $(\alpha, \beta) = (4/3, 0.05)$ -thick continuous, left line; $(1.2, 0.1)$ -thin continuous, middle line and $(1.15, 0.15)$ -dashed, rightmost line; for $b = 0.003$]

ergy has $(r < 1, s > 0)$ and that for holographic dark energy model with event horizon as the IR cut-off, $(r, s) = (1, 2/3)$.

As a conformation of the above results, we have studied the evolution of IMHRDE2 in the $q - r$ plane also and is shown in the figure 6.6. The trajectory is drawn only for the model parameters $(\alpha, \beta) = (1.01, -0.01)$. The present value noted is $(r_0, q_0) = (1.03, -0.57)$.

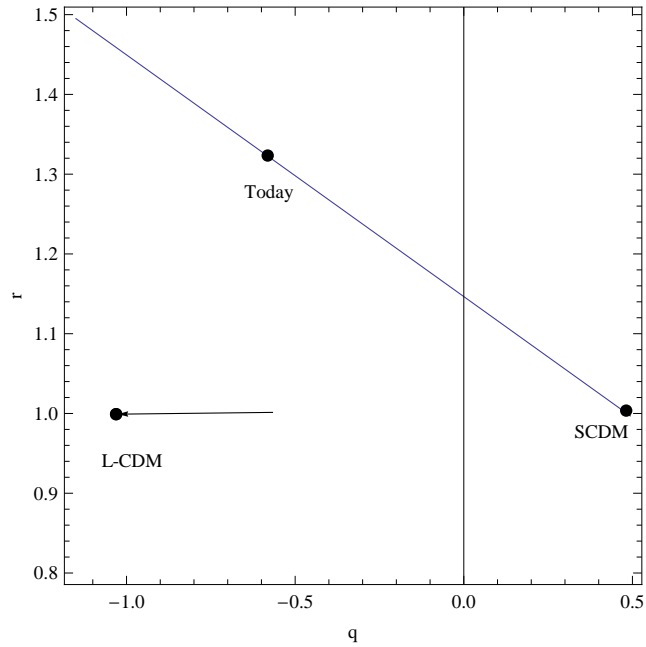


Figure 6.6: [Behavior of IMHRDE2 model in the $r - q$ plane for model parameters $(\alpha, \beta) = (1.01, -0.01)$ with $b=0.003$]

6.2 Study of the thermodynamics of IMHRDE2

In this section we analyze the thermodynamics of the model. The evolution of the entropy of both dark energy and dark matter and also the generalized second law are the main objectives of the study. The generalized second law (GSL) [62, 83] demands that the entropy of the contents inside the universe added with that of the horizon must never decrease. The behavior of entropy of IMHRDE2 is thus another aim of this study. The analysis is done under the conditions of thermal equilibrium existing between the contents inside the universe and

the horizon, with both apparent and event horizon bounding the universe and also for the case of non-equilibrium existing between them. Earlier works such as [87–90, 92, 93] showed that at the apparent the GSL is always valid, while it is violated at the event horizon for various dark energy models. The thermodynamical analysis described in the below subsections are written based on the earlier work [94].

6.2.1 Analysis of IMHRDE2 under thermal equilibrium

Thermal equilibrium means the condition in which the temperatures of the entities present inside the universe, dark energy and dark matter may have same temperature as a result of their interaction and due to that the horizon which is bounding them also acquires the same temperature. Thermal equilibrium condition is a most likely condition and can be mathematically defined as

$$T_{de} = T_m = T_h, \tag{6.17}$$

where T_{de}, T_m, T_h are the temperatures of dark energy, dark matter and horizon respectively. **(i)Thermal equilibrium for a universe with apparent horizon as the boundary:** Apparent horizon distance is defined as[84, 85],

$$r_A = \frac{1}{\sqrt{H^2 + k/a^2}}, \tag{6.18}$$

where k is the curvature parameter. For flat FLRW universe, $k = 0$, then the apparent horizon becomes the same as Hubble horizon,

$$r_A = \frac{1}{H}. \quad (6.19)$$

The apparent horizon has a temperature given by,

$$T_A = \frac{H}{2\pi}, \quad (6.20)$$

while its entropy is $S = A/4G$, [86] where $A = 4\pi r_A^2$ is its area and G is the gravitation constant. The entropy can be modified as

$$S_A = \frac{8\pi^2}{H^2}, \quad (6.21)$$

taking $8\pi G = 1$. The entropy of dark energy and dark matter is found using the Gibb's relation

$$TdS = dE + PdV, \quad (6.22)$$

where the volume $V = \frac{4}{3}\pi r_A^3$, and the total energy $E = \frac{4}{3}\pi r_A^3(\rho_{de} + \rho_m)$ which is that of the sum of dark energy and dark matter. The total change in entropy with respect to $x = \ln a$ by considering the above equations, is obtained as,

$$S'_{tot} = S'_{de} + S'_m + S'_A = \frac{2\pi}{H^2} + \frac{2\pi}{H^2} (1 + 12\pi(1 + \omega_{de}\Omega_{de})) q, \quad (6.23)$$

where

$$q = \frac{1}{2} (1 + 3\omega_{de}\Omega_{de}). \quad (6.24)$$

Interacting modified holographic Ricci dark energy model with interaction term

The total entropy change S'_{tot} is then plotted against x for the IMHRDE2 model parameters with negative β values and also for positive β values as shown in figure 6.7 and figure 6.8 respectively. From the two

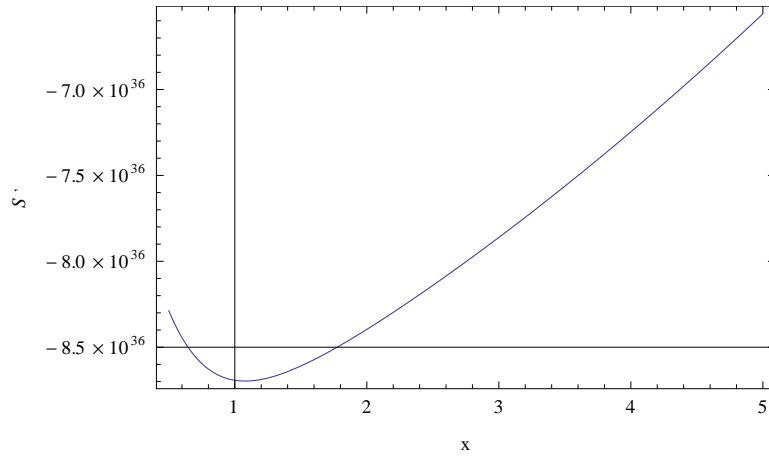


Figure 6.7: [Behavior of S'_{tot} with respect to x for the model parameter $(\alpha, \beta) = (1.01, -0.01)$ for $b = 0.003$.]

figures it can be deduced that the GSL is valid for model parameters with positive β parameters, while that for negative β , parameters, the total entropy change is always negative, which means that the GSL is invalid in this case. This is because the equation of state $\omega_{de} < -1$ for negative β parameters and hence is approaching phantom phase whereas for positive β parameter $\omega_{de} > -1$. Thus it can be inferred that the GSL is satisfied at the apparent horizon for an FLRW universe provided the Ricci dark energy is of quintessence in character. **(ii)Thermal equilibrium for a universe with event**

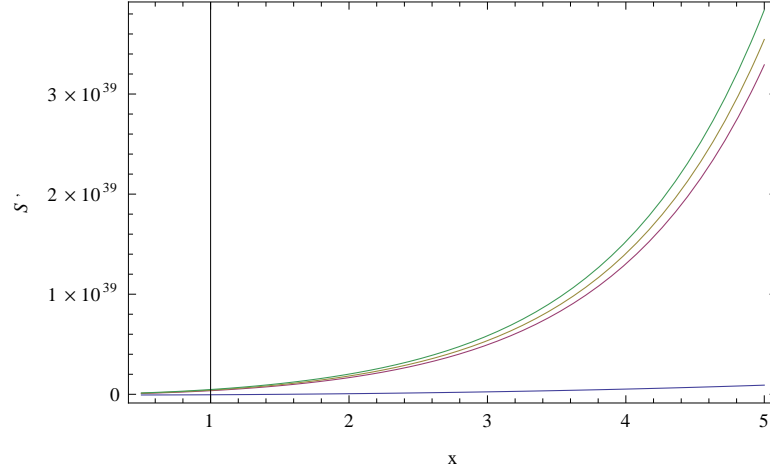


Figure 6.8: [Behavior of S'_{tot} with respect to x for model parameter $(\alpha, \beta) = (1.2, 0.1)$ -first line from the bottom, $(1.2, 0.3)$ -second line from the bottom, $(1.3, 0.3)$ -third line from the bottom, $(1.4, 0.3)$ -topmost line for $b = 0.003$.]

horizon as the boundary: Event horizon is considered to be the permanent boundary of the universe beyond which no information can be procured in the future. The distance of the event horizon is defined as,

$$R_E = a(t) \int_t^\infty \frac{dt'}{a(t')} = -\frac{1}{(1+z)H_0} \int_z^{-1} \frac{dz'}{h}. \quad (6.25)$$

The temperature of the event horizon is

$$T_E = \frac{1}{2\pi R_E}. \quad (6.26)$$

The analytic expression for the event horizon distance after performing the integration is,

Interacting modified holographic Ricci dark energy model with interaction term

$$R_E = \left(\frac{\gamma}{H_0}\right) \frac{1}{\sqrt{k_2(1+z)^{3(1-b)}}} \times {}_2F_1\left[0.5, -\frac{0.5}{3\beta - 3(1-b)}, 1 - \frac{0.5}{3\beta - 3(1-b)}, -\frac{k_1}{k_2}(1+z)^{3\beta-3(1-b)}\right] \quad (6.27)$$

where $\gamma = 2.0182$, and ${}_2F_1$ is the hypergeometric function. The rate of entropy change for dark energy and dark matter is obtained as,

$$S'_{de} + S'_m = -24\pi^2 (1 + \omega_{de}\Omega_{de}) H R_E^3. \quad (6.28)$$

Adding the entropy change of event horizon to this equation, the above expression becomes,

$$S'_{tot} = S'_{de} + S'_m + S'_E = -24\pi^2 (1 + \omega_{de}\Omega_{de}) H R_E^3 + 2\pi R_E^2 - 2\pi H^{-1} R_E, \quad (6.29)$$

with the help of the relation $\dot{H} = H R_E - 1$. The GSL is valid only if $S' \geq 0$, which in terms of the above expression(6.29) implies,

$$\omega_{de}\Omega_{de} \leq -1 + \frac{1}{12\pi H R_E} \frac{d \log R_E}{dx}. \quad (6.30)$$

From the above equation, it can be assessed that as $H > 0$, for $R_E \geq 0$, the equation of state becomes $\omega_{de} > -1$, for a dark energy dominated universe for which $\Omega_{de} \approx 1$. But if $R_E \leq 0$, then the equation of state ω_{de} will always be less than 1. The plot of S'_{tot} is drawn for model parameters with negative β values as shown in figure 6.9. The plot of S'_{tot} for positive β values is shown in the figure

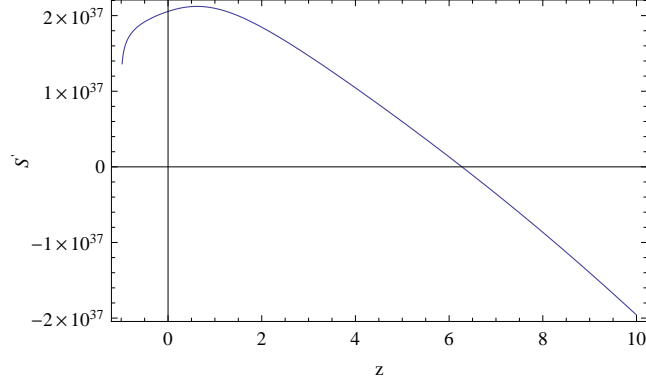


Figure 6.9: [Behavior of S'_{tot} in relation to x for the model parameters $(\alpha, \beta)=(1.01, -0.01)$ at the event horizon of the universe with $b=0.003$.]

6.10. The plots show that the rate of entropy is partially negative, hence the GSL is only partially satisfied for the model parameters of IMHRDE2 model for both positive and negative β values in a flat FLRW universe bounded by event horizon. From figure 6.9, it is seen that the trajectory of S'_{tot} transits from negative value to positive in the past at a redshift $z \sim 7$. The figure 6.10 for different model parameters also show similar behavior, but unlike in the previous case as $z < 4$, S'_{tot} becomes zero. Therefore, the IMHRDE2 with positive β values also support the result that the GSL is only partially satisfied by event horizon as the boundary, under thermal equilibrium conditions. Owing to this result, it is concluded that the event horizon cannot be taken as the thermodynamic boundary of the universe.

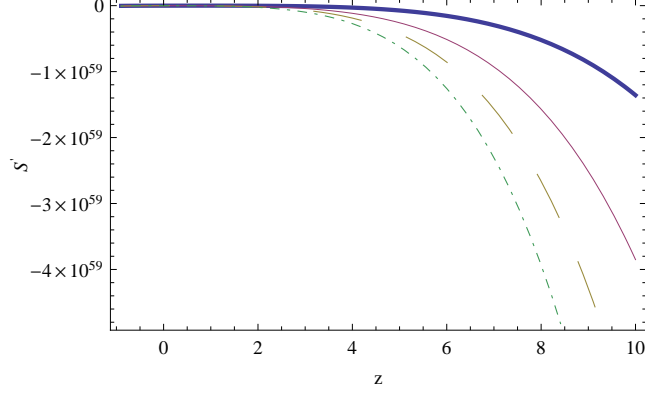


Figure 6.10: [Behavior of S'_{tot} with respect to x for model parameters $(\alpha, \beta)=(1.2,0.1)$ -thick continuous line, $(1.2,0.3)$ -thin continuous line, $(1.3,0.3)$ -dashed line, $(1.4,0.3)$ -dot-dashed line, for $b=0.003$.]

6.2.2 Analysis of IMHRDE2 under thermal non-equilibrium condition

The temperatures of dark energy, dark matter and the horizon will not be the same when thermal non-equilibrium exist, that is, $T_{de} \neq T_m \neq T_h$. Apparent horizon is considered to be the boundary for the present analysis. The change in total entropy of the universe is then obtained as below using the presumptions described in the previous cases,

$$S'_{tot} = \frac{12\pi}{H} \frac{\Omega_{de}}{T_{de}} (1 + \omega_{de})q + \frac{12\pi}{H} \frac{\Omega_m}{T_m} q - \frac{2\pi H'}{H^3}. \quad (6.31)$$

The above equation impose a condition for the validity of GSL as,

$$T_{de} \geq - \left(\frac{6q}{1+q} \right) (1 + \omega_{de})\Omega_{de}H. \quad (6.32)$$

When the temperature of apparent horizon can be approximated as $T_A \sim H$ with $H > 0$, then the above condition can be interpreted like this: as long as $q < 0$ for an accelerating universe and considering dark energy of quintessence nature with $\omega_{de} > -1$, the right hand side of the inequality relation will be always positive. Thus the condition implies that for the GSL to be valid the temperature of dark energy must be greater than that of the horizon bounding the universe.

As the temperature of dark energy is greater than the horizon, its entropy will be decreasing in nature. To evaluate this, a dark energy dominated universe is considered where the contribution from matter can be neglected. The temperature of dark energy is taken as proportional to the temperature of the horizon as,

$$T_{de} = kT_A, \quad (6.33)$$

where $k > 1$. The entropy of dark energy is then found out using the standard relation [1]

$$S_{de} = \left(\frac{\rho_{de} + p_{de}}{T_{de}} \right) V = \frac{8\pi^2(1 + \omega_{de})\Omega_{de}}{kH^2}. \quad (6.34)$$

The nature of the entropy evolution of dark energy is studied by drawing the characteristic curve of S_{de} with respect to $x = \ln a$ as shown in figure 6.11 The plot shows that the entropy of dark energy is decreasing as the universe expands. For the GSL to be valid the total entropy of the universe must increase. The total entropy comprises

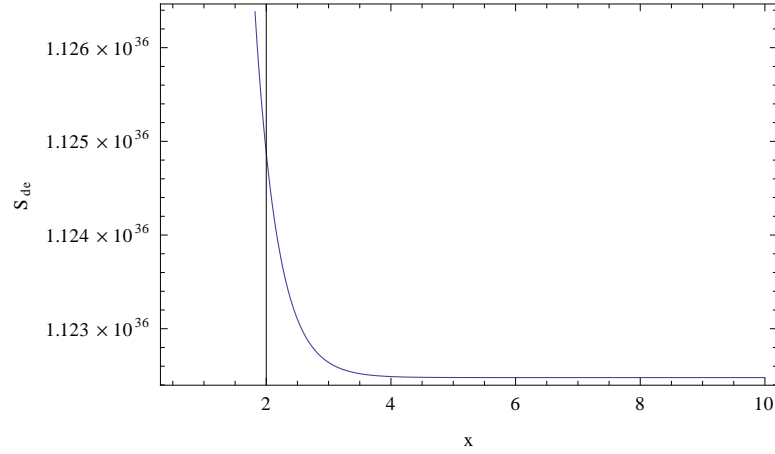


Figure 6.11: [Behavior of the entropy of dark energy with respect to x for the parameters (1.2,0.1)]

the entropy of the contents inside the universe and that of the horizon bounding the universe. Thus the entropy of the horizon and the total entropy is also plotted with respect to x which is shown in the figure 6.12. The plot shows that the entropy of horizon is increasing as x increases and the total entropy also increases. These results lead to the understanding that the loss of entropy of dark energy is compensated by the increase in the entropy of horizon so as to keep the total entropy of the universe at the increase. Hence the GSL is valid for a universe dominated by dark energy, which is bounded by the apparent horizon.

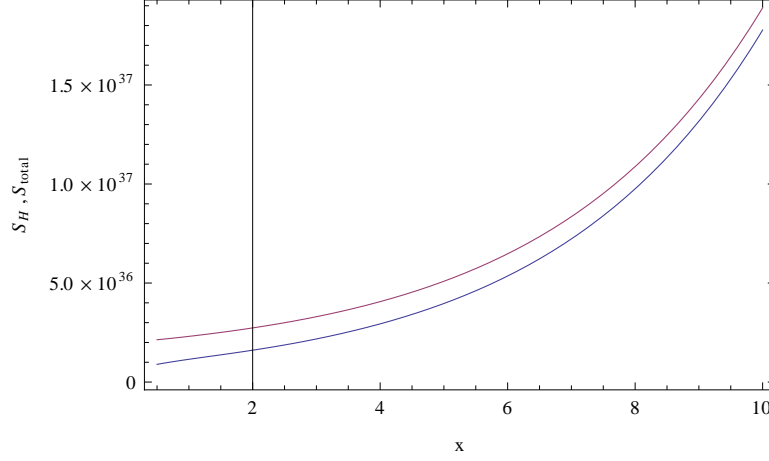


Figure 6.12: [Entropy characteristics of apparent horizon in relation to x (bottom line) and total entropy in relation to x (top line) for model parameters (1.2,0.1)]

6.3 Conclusion

The IMHRDE2 model is studied with interaction term $Q = 3bH\rho_m$ in a flat FLRW universe. The co-evolution of the energy densities of dark energy and dark matter is explained when the interaction parameter $b \leq 0.003$. The characteristics of IMHRDE2 which include the evolution of equation of state parameter ω_{de} and that of deceleration parameter q is studied. The evolution of both predicts that there occurred a transition into the accelerating phase of expansion at around a redshift of $z \sim 0.68$ for the best fit parameters of the model. The present values of these parameters, predicted by IMHRDE2 model, $\omega_{de0} \sim -0.97$, $q_0 \sim -0.57$, are found to be in close

Interacting modified holographic Ricci dark energy model with interaction term

agreement with the WMAP observational values for the model parameters $(\alpha, \beta) = (1.01, -0.01)$. Statefinder parameters are used for distinguishing the model from other dark energy models, and found the model is distinguishably different from other models, especially from Λ CDM model.

The study of the thermodynamics of the model is done by checking the validity of the generalized second law of thermodynamics(GSL) under both thermal equilibrium and non-equilibrium conditions in a universe consisting of dark energy and dark matter, bounded by apparent and event horizon. The evolution of entropy of dark energy is also analyzed. At thermal equilibrium, where the temperatures of the contents of the universe and the horizon are the same, the GSL is valid at the apparent horizon only if the dark energy is of quintessence nature, while the GSL is generally violated at the event horizon. For thermal non-equilibrium condition, the GSL is valid at the apparent horizon only when the temperature of dark energy is greater than that of the horizon. Works like [91, 95] showed that the GSL is valid at the apparent for the case of thermal non-equilibrium conditions under specific constraints.

The evolution of entropy of dark energy in a dark energy dominated universe is analyzed. The dark energy entropy is found to decrease as universe expands and this is compensated by the increase in the entropy of the horizon as a result total entropy of the universe

increases. Thus the IMHRDE2 model is a thermodynamically feasible model for a universe with apparent horizon as the boundary, provided the dark energy is of quintessence nature.

7

Interacting modified holographic Ricci dark energy
model with interaction term

$$Q \propto H\rho_{de}\text{-IMHRDE3}$$

7.1 Interacting modified holographic Ricci dark energy model with interaction term $Q \propto H\rho_{de}$ -IMHRDE3

The Interacting modified holographic Ricci dark energy model, IMHRDE3 is one which considers a flat FLRW universe with dark energy in interaction with dark matter via an interaction term $Q = 3bH\rho_{de}$, where b is the interaction parameter, H is the Hubble parameter and ρ_{de} is the density of dark energy. The interaction can be defined by the

Interacting modified holographic Ricci dark energy model with interaction term

equations,

$$\dot{\rho}_{de} + 3H(\rho_{de} + p_{de}) = -Q, \quad (7.1)$$

$$\dot{\rho}_m + 3H\rho_m = Q, \quad (7.2)$$

where p_{de} is the pressure of dark energy. The analysis that is described below in this section is in reference to article published earlier in [79].

The modified holographic Ricci dark energy[74] is given by

$$\rho_{de} = \frac{2}{\alpha - \beta} \left(\dot{H} + \frac{3}{2}\alpha H^2 \right), \quad (7.3)$$

where α and β are the model parameters. The Friedmann equation is

$$3H^2 = \rho_m + \rho_{de}. \quad (7.4)$$

Using equations(7.2, 7.3, 7.4) the normalized Hubble parameter h is found to satisfy the following differential equation

$$\frac{d^2 h^2}{dx^2} + 3(\beta + b + 1)\frac{dh^2}{dx} + 9(\alpha b + \beta)h^2 = 0, \quad (7.5)$$

where $h = \frac{H}{H_0}$, and $x = \ln a$. The solution is obtained as

$$h^2 = f_1 e^{\frac{u_1}{2}x} + f_2 e^{\frac{u_2}{2}x}, \quad (7.6)$$

where the constant coefficients f_1 and f_2 are found using the initial

conditions $h^2|_{x=0} = 1$, $\frac{dh^2}{dx}|_{x=0} = 3\Omega_{de0}\Delta - 3\alpha$. They are

$$\begin{aligned}
 f_1 &= [3 - 6\alpha + 3b + 3\beta \\
 &\quad - \sqrt{-36(\alpha b + \beta) + 9(1 + b + \beta)^2 + 6(\alpha - \beta)\Omega_{de0}}] \\
 &\quad / [2b - 2\sqrt{-36(\alpha b + \beta) + 9(1 + b + \beta)^2}], \\
 f_2 &= 1 - f_1.
 \end{aligned} \tag{7.7}$$

and

$$\begin{aligned}
 u_1 &= -3 - 3b - 3\beta - \sqrt{9(1 + b + \beta)^2 - 36(\alpha b + \beta)}, \\
 u_2 &= -3 - 3b - 3\beta + \sqrt{9(1 + b + \beta)^2 - 36(\alpha b + \beta)}.
 \end{aligned} \tag{7.8}$$

The energy density parameter Ω_{de} then becomes,

$$\Omega_{de} = f_1 e^{\frac{u_1}{2}x} + f_2 e^{\frac{u_2}{2}x} - \Omega_{m0}e^{-3x}. \tag{7.9}$$

The analytic expression for the equation of state parameter is thus obtained as

$$\omega_{de} = -1 - \left[\frac{f_1 \frac{u_1}{2} e^{\frac{u_1}{2}x} + f_2 \frac{u_2}{2} e^{\frac{u_2}{2}x} + 3\Omega_{m0}e^{-3x}}{3 \left(f_1 e^{\frac{u_1}{2}x} + f_2 e^{\frac{u_2}{2}x} - \Omega_{m0}e^{-3x} \right)} \right]. \tag{7.10}$$

If there is no interaction between dark energy and dark matter, i.e., $b = 0$, then the constants reduces to, $f_1 = 1$, $f_2 = 0$, $u_1 = -6\beta$ and $u_2 = -6$ for $\Omega_{de0} = 1$. The equation of state parameter then takes the value $\omega_{de} = -1 + \beta$. This result is complying with that in the earlier work[71].

Interacting modified holographic Ricci dark energy model with interaction term

The IMHRDE3 model can explain the coincidence of the energy densities of dark energy and dark matter for the value of interaction parameter $b = 0.009$. For $b > 0.009$, the coincidence is not observed in this model. The plot shown in figure 7.1 depicts the coincidence. The

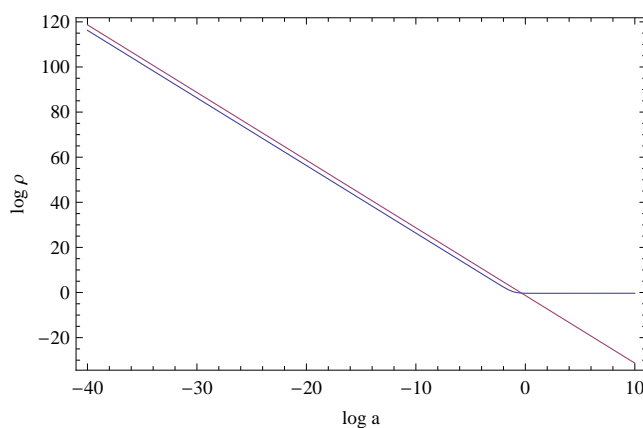


Figure 7.1: [Co-evolution of energy densities of dark energy(IMHRDE3) and dark matter for $(\alpha, \beta) = (1.01, -0.01)$ with $b = 0.009$. The continuous line which deviates represents dark energy and the other line represents dark matter.]

plot shows that the densities of dark energy and dark matter evolving together and dark energy dominating only recently. The co-evolution plot is drawn for IMHRDE3 model parameters $(\alpha, \beta) = (1.01, -0.01)$ which are the best parameters found as the result of quantitative analysis.

The evolution of equation of state can be obtained using the stan-

standard procedure using the expression,

$$\omega_{de} = -1 - \frac{1}{3} \frac{d \ln \Omega_{de}}{dx}. \quad (7.11)$$

The dynamics of the equation of state with respect to redshift is shown in the figure 7.2 The trajectory of the evolution the equation of state

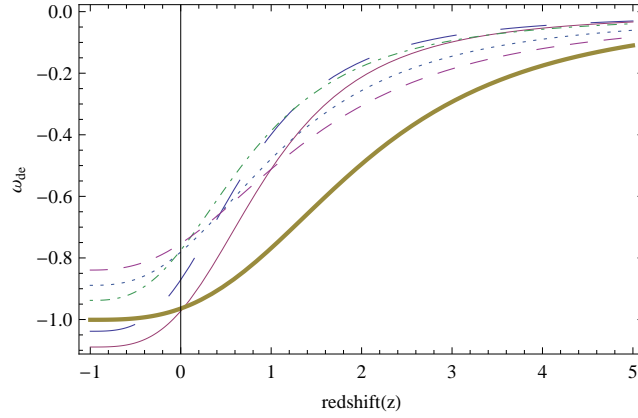


Figure 7.2: [Evolution of the equation of state parameter of IMHRDE3 with $b=0.009$, for parameters $(\alpha, \beta)=(1.2,-0.1)$ - thin continuous line, first from the left bottom; $(4/3,-0.05)$ -large dashed line, 2nd from left bottom, $(1.01,-0.01)$ -thick continuous line, 3rd from the left bottom; $(4/3,0.05)$ -dot-dashed line, 4th from left bottom; $(1.2,0.1)$ -dotted line, 5th from the left bottom and $(1.15,0.15)$ - small dashed line, 6th from the left bottom.]

starts from nearly zero at higher redshifts to $\omega_{de} > -1$ at lower redshifts particularly as $z \rightarrow -1$, for model parameters with positive values of β and to $\omega_{de} < -1$ for negative β values as $z \rightarrow -1$. The present

Interacting modified holographic Ricci dark energy model with interaction term

value of equation of state parameter, ω_{de0} for different parameter sets are: -0.86 for $(\alpha, \beta) = (4/3, -0.05)$, -0.97 for $(\alpha, \beta) = (1.2, -0.1)$, -0.97 for $(\alpha, \beta) = (1.01, -0.01)$, -0.78 for $(\alpha, \beta) = (4/3, 0.05)$, -0.78 for $(\alpha, \beta) = (1.2, -0.1)$ and -0.75 for $(\alpha, \beta) = (1.15, -0.15)$. The ω_{de0} corresponding to $(1.01, -0.01)$ is very much closer to the corresponding WMAP observational value $\omega_{de0} \sim -0.93$ [16].

The analytic expression for the deceleration parameter q is obtained as

$$q = -1 - \frac{1}{2} \left[\frac{\frac{u_1}{2} f_1 e^{\frac{u_1}{2}x} + \frac{u_2}{2} f_2 e^{\frac{u_2}{2}x}}{f_1 e^{\frac{u_1}{2}x} + f_2 e^{\frac{u_2}{2}x}} \right]. \quad (7.12)$$

If there is no interaction such that $b = 0$ and let $\Omega_{de} \sim 1$, then the expression for q reduces to $q = (3\beta - 2)/2$, which is in correspondence with the earlier result[71]. The evolution of q with respect to z is shown in the figure 7.3. The evolutionary path of deceleration parameter q starts from nearly 0.5, it then enters the negative region at lower redshift. The present value of deceleration parameter, q_0 for various model parameters are : -0.47 for $(\alpha, \beta) = (4/3, -0.05)$, -0.57 for $(\alpha, \beta) = (1.2, -0.1)$, -0.57 for $(\alpha, \beta) = (1.01, -0.01)$, -0.36 for $(\alpha, \beta) = (4/3, 0.05)$, -0.36 for $(\alpha, \beta) = (1.2, 0.1)$ and -0.34 for $(\alpha, \beta) = (1.15, 0.15)$. The value of q_0 corresponding to the model parameter sets $(\alpha, \beta) = (1.01, -0.01)$ is in close agreement with the WMAP observational value $q_0 \sim -0.60$ [16]. The transition redshift, z_T which is the redshift at which the universe enter the accel-

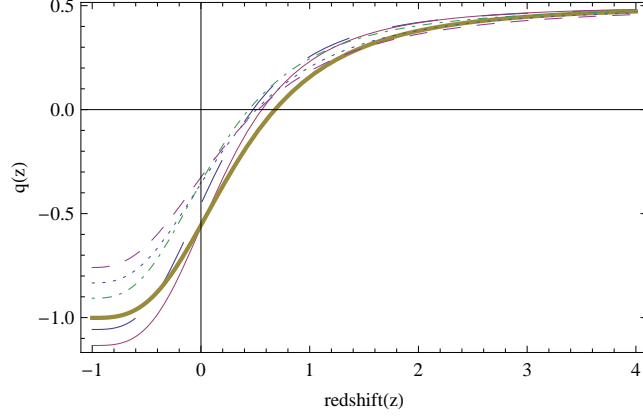


Figure 7.3: [Evolution of the q -parameter with redshift of IMHRDE3. The plots for $(\alpha, \beta)=(1.2,-0.1)$ thin continuous - first from the bottom of the left side, $(4/3,-0.05)$ -large dashed line, 2nd from the bottom of the left side, $(1.01,-0.01)$ -thick continuous, third from the left bottom, $(4/3,0.05)$ -dash-dot, 4th from the left bottom, $(1.2,0.1)$ -dotted line, 5th from the left bottom, $(1.15,0.15)$ - small dash line, 6th from left bottom, all with coupling constant $b = 0.009$.]

erating stage of the universe for different model parameters are : $z_T = 0.49$ for $(\alpha, \beta) = (4/3, -0.05)$, $z_T = 0.60$ for $(\alpha, \beta) = (1.2, -0.1)$, $z_T = 0.70$ for $(\alpha, \beta) = (1.01, -0.01)$, $z_T = 0.45$ for $(\alpha, \beta) = (4/3, 0.05)$, $z_T = 0.50$ for $(\alpha, \beta) = (1.2, 0.1)$ and 0.53 for $(\alpha, \beta) = (1.15, 0.15)$. The z_T values are in much accordance with the observational value of WMAP, which lies in the range $z_T \sim 0.45 - 0.73$ [82], particularly for best fit model parameters $(1.01, -0.01)$.

Interacting modified holographic Ricci dark energy model with interaction term

Statefinder Analysis

Statefinder parameters are used to differentiate the model from other dark energy models. The geometric diagnostic technique is introduced by Sahni et al.[72, 73]. The parameters used are (r, s) which are different from the usual parameters used such as H, q . The expression for the statefinder parameters is obtained as

$$r = 1 + \left[\frac{\frac{u_1^2}{4} f_1 e^{\frac{u_1}{2}x} + \frac{u_2^2}{4} f_2 e^{\frac{u_2}{2}x} + \frac{3}{2} u_1 f_1 e^{\frac{u_1}{2}x} + \frac{3}{2} u_2 f_2 e^{\frac{u_2}{2}x}}{2(f_1 e^{\frac{u_1}{2}x} + f_2 e^{\frac{u_2}{2}x})} \right], \quad (7.13)$$

and

$$s = - \left[\frac{\frac{u_1^2}{4} f_1 e^{\frac{u_1}{2}x} + \frac{u_2^2}{4} f_2 e^{\frac{u_2}{2}x} + \frac{3}{2} u_1 f_1 e^{\frac{u_1}{2}x} + \frac{3}{2} u_2 f_2 e^{\frac{u_2}{2}x}}{\frac{3}{2} u_1 f_1 e^{\frac{u_1}{2}x} + \frac{3}{2} u_2 f_2 e^{\frac{u_2}{2}x} + 9f_1 e^{\frac{u_1}{2}x} + 9f_2 e^{\frac{u_2}{2}x}} \right]. \quad (7.14)$$

If there is no interaction between the dark energy and dark matter i.e., $b = 0$ and $\Omega_{de} \approx 1$, then the above expression reduces to $r = 1 + 9\beta(\beta - 1)/2$ and $s = \beta$, which is their standard form. The evolution of the IMHRDE3 in the $r - s$ plane is analyzed for the model parameters with positive and negative β parameters. The figure 7.4 shows the trajectory for negative β parameters. The evolution is from right to left in the $r - s$ plane. The plot distinctly shows the present position of the universe predicted by the IMHRDE3 model, the Λ CDM point (with $r = 1, s = 0$) and the region corresponding to the future direction for the model parameter with negative β . The present position for the parameters are : $(r_0, s_0) = (1.1, -0.036)$ for $(\alpha, \beta) = (4/3, -0.05)$, $(1.28, -0.088)$ for $(\alpha, \beta) = (1.2, -0.1)$ and

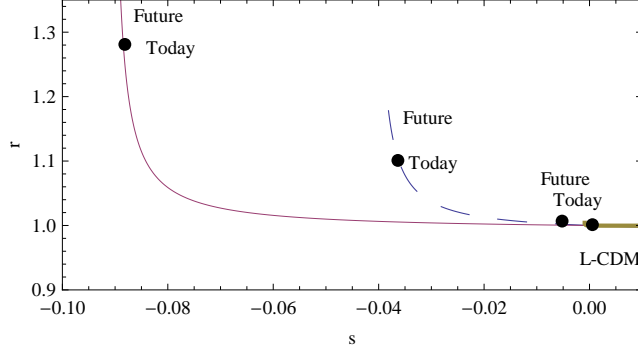


Figure 7.4: [$r - s$ plots of IMHRDE3 for parameters $(\alpha, \beta) = (1.2, -0.1)$ (thin continuous, extreme left trajectory), $(4/3, -0.05)$ (dashed, middle trajectory), $(1.01, -0.01)$ (thick continuous, extreme right trajectory), with $b = 0.009$]

$(r_0, s_0) = (1.003, -0.0008)$ for $(\alpha, \beta) = (1.01, -0.01)$. It is seen that the path evolves from right covering through Λ CDM in the past and evolves to the future.

The figure 7.5 describes the plot of the evolution of $r - s$ parameters for positive β values. The present position of the universe, the Λ CDM point and the future evolution of IMHRDE3 for model parameters with positive β are noted. The present values for (r, s) obtained are : $(r_0, s_0) = (0.83, 0.066)$ for $(\alpha, \beta) = (4/3, 0.05)$, $(r_0, s_0) = (0.70, 0.115)$ for $(\alpha, \beta) = (1.2, 0.1)$ and $(r_0, s_0) = (0.60, 0.16)$ for $(\alpha, \beta) = (1.15, 0.15)$. The trajectory evolves from right to left and the Λ CDM point lies out of the path. The (r_0, s_0) values predicted by IMHRDE3 model is different from other models for example for

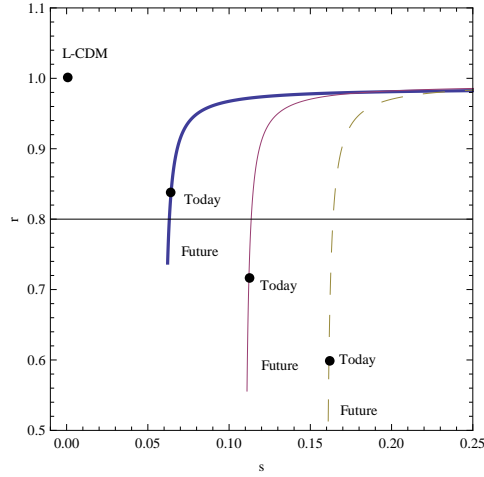


Figure 7.5: $[r - s]$ plots of IMHRDE3 for parameters $(\alpha, \beta) = (4/3, 0.05)$ (thick continuous, extreme left trajectory), $(1.2, 0.1)$ (thin continuous, middle trajectory), and $(1.15, 0.15)$ (dashed, extreme right trajectory) with $b = 0.009$

the case of Chaplygin gas model, $r > 1, s < 0$, for quintessence model $r < 1, s > 0$.

The evolution of IMHRDE3 in the $q - r$ plane is also studied. The figure 7.6 shows the $q - r$ trajectory for the model parameters $(\alpha, \beta) = (1.01, -0.01)$.

7.2 Thermodynamics of the IMHRDE3 model

In the previous section the study of cosmological characteristics of the IMHRDE3 is explained. The current section is meant for the description of the thermodynamic characteristics of the model especially the

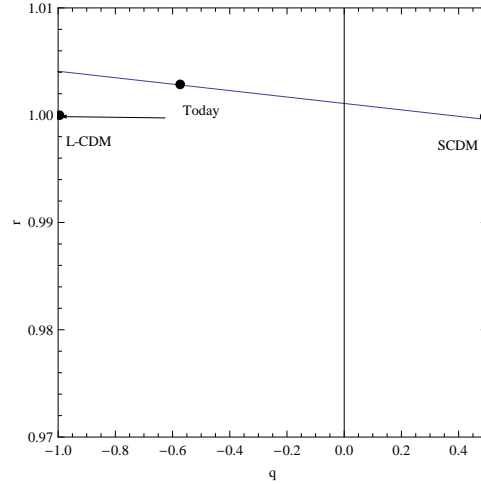


Figure 7.6: [$r - q$ behavior of the IMHRDE3 for the best fit parameter (1.01,-0.01) with $b=0.009$. The diagonal like line representing the trajectory of IMHRDE3 and the horizontal line representing Λ CDM for comparison.]

study of the generalized second law of thermodynamics(GSL) which states that the total entropy of the universe, which is the sum of the components of the universe and the horizon bounding it, must never decrease[62, 83] and the entropy evolution of the IMHRDE3 in such a universe. The analysis presented here is in reference to the work[96]. The study is done under thermal equilibrium and non-equilibrium conditions.

7.2.1 Analyzing the case of thermal equilibrium

A flat FLRW universe with dark energy, dark matter and the horizon surrounding it is considered. Thermal equilibrium implies that the temperatures of the contents inside the universe and the boundary are the same. That is $T_{de} = T_m = T_h$, where T_{de}, T_m and T_h are the temperatures of dark energy, dark matter and horizon respectively. Then the generalized second law(GSL) demands that the entropy of the contents added with that of the horizon must never decrease. Mathematically,

$$\dot{S}_{de} + \dot{S}_m + \dot{S}_h \geq 0, \quad (7.15)$$

where S_{de}, S_m and S_h means the entropy of dark energy, dark matter and horizon respectively. Over dot implies the derivative with respect to cosmic time. The analysis under thermal equilibrium is carried out for both apparent horizon as well as event horizon as thermodynamic boundary and are detailed below. Earlier works[87–90, 92, 93] showed that the GSL is valid at apparent horizon but not at event horizon.

(i) Apparent horizon as the boundary: The apparent horizon distance r_A is defined as[84],

$$r_A = \frac{1}{\sqrt{H^2 + k/a^2}}, \quad (7.16)$$

where k is the curvature parameter. For flat universe the above expression reduces to

$$r_A = \frac{1}{\sqrt{H^2}}, \quad (7.17)$$

which now became the same as Hubble radius. The temperature, entropy of the horizon is

$$T_A = \frac{H}{2\pi}, \quad (7.18)$$

and $S = A/4G$ [86], where area of the horizon $A = 4\pi r_A^2$ and G is the gravitational constant. Taking $8\pi G = 1$, the expression for entropy can be restructured to

$$S_A = \frac{8\pi^2}{H^2}. \quad (7.19)$$

The entropy of dark energy and dark matter are found using Gibb's relation,

$$TdS = dE + PdV, \quad (7.20)$$

where $V = \frac{4}{3}\pi r_A^3$, is the volume and $E = \frac{4}{3}\pi r_A^3(\rho_{de} + \rho_m)$ is the total energy which comprises the sum of the energy of dark energy and dark matter. GSL states that the sum of entropies of the dark energy, dark matter and the apparent horizon must not decrease.

The total change in entropy obtained with respect to $x = \ln a$, using the above said expressions

$$S' = \frac{16\pi^2}{H^2} + \frac{16\pi^2}{H^2} \left(1 + \frac{3}{2}(1 + \omega_{de}\Omega_{de}) \right) q, \quad (7.21)$$

where S' implies derivative with respect to $x = \ln a$, ω_{de} is the equation of state parameter of dark energy and Ω_{de} is the energy density

Interacting modified holographic Ricci dark energy model with interaction term

parameter of dark energy and q is the deceleration parameter. Using the expression $q = \frac{1}{2}(1 + 3\omega_{de}\Omega_{de})$, the expression for entropy change can be modified as,

$$S' = \frac{36\pi^2}{H^2}(1 + \omega_{de}\Omega_{de})^2. \quad (7.22)$$

The expression clarifies that as the term on the right hand side are perfect squares and hence the entropy change is always positive. The behavior of S' with respect to x is plotted for various model parameters of IMHRDE3 and is shown in figure 7.7. Thus it is inferred that the GSL is always valid when apparent horizon is taken as the thermodynamic boundary of the universe comprising IMHRDE3.

(ii)Event horizon as the boundary: The event horizon radius R_E is given by

$$R_E = \frac{1}{1+z} \int_z \frac{dz}{H}, \quad (7.23)$$

where z is the redshift. The validity of GSL insists that the sum of the entropy change of the contents inside the universe with that of the event horizon must never decrease. The integration in the expression for R_E is carried out for IMHRDE3 model and thus the R_E becomes

$$R_E = -4.2265 \times 10^{17} \left(I \sqrt{(1+z)^{\frac{u_2}{2}}} {}_2F_1\left[P, 0.5, 1+P, \frac{-f_1}{f_2}(1+z)^{\frac{u_2}{2}}\right] \right), \quad (7.24)$$

where I and P are constants which have distinct values for different IMHRDE3 model parameters. The respective I, P values for parameters with positive β are : 0.751, 0.626 for $(\alpha, \beta) = (1.2, 0.1)$,

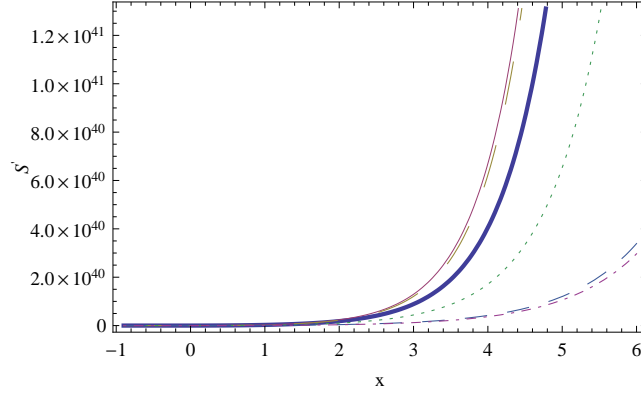


Figure 7.7: [The behavior of S' for the parameters $(\alpha, \beta) = (1.01, -0.01)$ the thick continuous line, $(\alpha, \beta) = (1.2, -0.1)$ the thin continuous line, $(\alpha, \beta) = (4/3, -0.1)$ the large dashed line, $(\alpha, \beta) = (1.2, 0.1)$ the dotted line, $(\alpha, \beta) = (1.2, 0.3)$ the small dashed line, and $(\alpha, \beta) = (4/3, 0.3)$ the dot-dashed line, with the interaction coupling constant $b=0.009$ inside apparent horizon under thermal equilibrium conditions]

0.780, 0.627 for $(\alpha, \beta) = (4/3, 0.1)$ and 0.838, 0.736 for $(\alpha, \beta) = (1.2, 0.3)$ and that for parameters with negative β are : 0.682, 0.583 for $(\alpha, \beta) = (1.01, -0.01)$, 0.683, 0.556 for $(\alpha, \beta) = (1.2, -0.1)$ and 0.704, 0.557 for $(\alpha, \beta) = (4/3, -0.1)$. ${}_2F_1$ is the hypergeometric function.

The temperature of the event horizon is

$$T_E = \frac{1}{2\pi R_E}, \quad (7.25)$$

while the area of the event horizon is $A = 4\pi R_E^2$. The total change

Interacting modified holographic Ricci dark energy model with interaction term

in entropy of dark energy and dark matter using the Gibb's equation with respect to $x = \log a$ is obtained as

$$T(S'_{de} + S'_m) = H^{-1}(\rho_{de} + \rho_m + p_{de})4\pi R_E^2(\dot{R}_E - HR_E). \quad (7.26)$$

The expression for temperature is substituted in the above expression. Using the relation $\dot{R}_E = HR_E - 1$, and adding the horizon entropy, the total entropy change is obtained as

$$S' = H^{-1}[16\pi^2 R_E(\dot{R}_E - \frac{R_E^2}{2}(\rho_{de} + \rho_m + p_{de}))]. \quad (7.27)$$

When the equation $\dot{H} = -\frac{1}{2}(\rho_{de} + \rho_m + p_{de})$ is used the expression for total entropy change turns out to be

$$S' = H^{-1}[16\pi^2 R_E(\dot{R}_E - \dot{H}R_E^2)]. \quad (7.28)$$

Since $H > 0, R_E > 0$ the condition for the validity of GSL with reference to the above expression is

$$\dot{R}_E \geq \frac{1}{2}(\rho + p)R_E^2. \quad (7.29)$$

In a prevailing dominant energy condition where $(\rho + p) > 0$, \dot{R}_E is substituted in terms of Hubble parameter and the densities of the fluid contents of the universe. Then the condition of validity turns out to be,

$$HR_h - 1 - \frac{3}{2}(1 + \omega_{de}\Omega_{de})H^2 R_h^2 \geq 0. \quad (7.30)$$

The above condition is checked for the validity of GSL by plotting the term on the left hand side of the equation against $x = \ln a$, for

IMHRDE3 model parameters. The figure 7.8 shows the evolution of the condition for the validity of GSL for model parameters with positive β values and figure 7.9 for negative β parameters. The

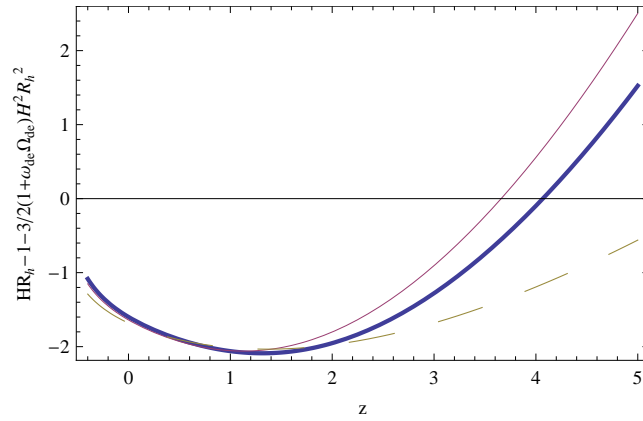


Figure 7.8: [The behavior of S' for the parameters $(\alpha, \beta) = (1.2, 0.1)$ thick continuous line, $(\alpha, \beta) = (4/3, 0.1)$ thin continuous line, $(\alpha, \beta) = (1.2, 0.3)$ dashed line, with the interaction coupling constant $b=0.009$ inside event horizon under thermal equilibrium conditions]

plot shows that the GSL is only partially satisfied for both negative and positive β values of the IMHRDE3 model parameters, which is in confirmation with earlier results. Thus it can be concluded that event horizon cannot be a feasible thermodynamic boundary of the universe.

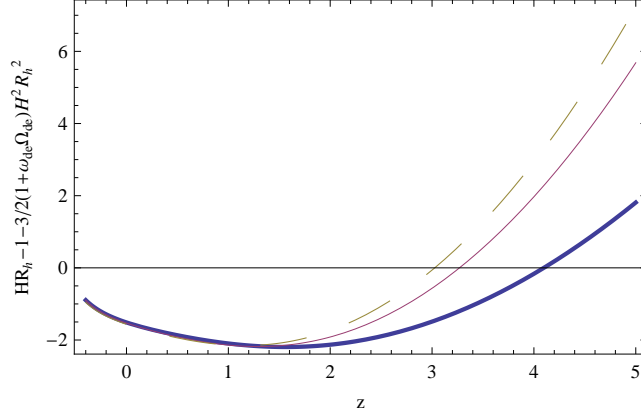


Figure 7.9: [The behavior of S' for the parameters $(\alpha, \beta) = (1.01, -0.01)$ thick continuous line, $(\alpha, \beta) = (1.2, -0.1)$ thin continuous line, $(\alpha, \beta) = (4/3, -0.1)$ dashed line, with the interaction coupling constant $b=0.009$ inside event horizon under thermal equilibrium conditions]

7.2.2 Analyzing the case of thermal non-equilibrium

In the above subsection the thermal equilibrium between the components of the universe with the horizon is considered. It is likely that thermal non-equilibrium can exist between the components and it implies,

$$T_{de} \neq T_m \neq T_h. \quad (7.31)$$

Taking apparent horizon as the feasible horizon, the total entropy change is found using Gibb's relation which is

$$S' = -H^{-1} \left(12\pi \left(1 + \frac{H'}{H} \right) \left(\frac{\Omega_{de}(1 + \omega_{de})}{T_{de}} + \frac{\Omega_m}{T_m} \right) + \frac{8\pi H'}{T_h H} \right). \quad (7.32)$$

Neglecting the contribution of dark matter i.e., $\Omega_m \sim 0$ for a dark energy dominated universe, then the above expression becomes

$$S' = -H^{-1} \left(12\pi \left(1 + \frac{H'}{H} \right) \left(\frac{\Omega_{de}(1 + \omega_{de})}{T_{de}} \right) + \frac{8\pi}{T_h} \frac{H'}{H} \right). \quad (7.33)$$

The validity of GSL requires that $S' \geq 0$. Using the expression $q = -1 - \frac{H'}{H}$, the condition for the validity of GSL is obtained as

$$\frac{T_{de}}{T_h} \geq -\frac{3}{2} \Omega_{de}(1 + \omega_{de}) \frac{q}{1 + q}. \quad (7.34)$$

The condition implies that as $(1 + q) > 0$ and $(1 + \omega_{de}) > 0$ for the dark energy of quintessence type the validity of GSL requires $T_{de} \geq T_h$, while if $(1 + q) < 0$, and $(1 + \omega_{de}) < 0$ which is the case of phantom type model, the validity of GSL requires $T_{de} \leq T_h$. Avoiding the phantom behavior which is unfavorable, the GSL validity insists that the temperature of the dark energy to be greater than that of the horizon.

The behavior of the temperature of the dark energy motivates to look into its entropy characteristics. For that, a universe dominated by dark energy is considered avoiding the contribution from dark matter. Let the temperature of dark energy is proportional to the temperature of the apparent horizon by a factor $k > 1$. That is,

$$T_{de} = kT_A, \quad (7.35)$$

The entropy of dark energy is found using the standard relation $S =$

Interacting modified holographic Ricci dark energy model with interaction term

$\frac{(\rho+P)V}{T}$ [1], as

$$S_{de} = \frac{8\pi^2}{kH^2}\Omega_{de}(1 + \omega_{de}). \quad (7.36)$$

The total entropy of the universe which includes the sum of the entropies of both dark energy and horizon is obtained as

$$S_{tot} = \frac{8\pi^2}{kH^2}\Omega_{de}(1 + \omega_{de}) + \frac{8\pi^2}{H^2}. \quad (7.37)$$

The behavior of the S_{de} and S_h, S_{tot} with respect to $x = \ln a$ is shown in figure 7.10 and figure 7.11 respectively. The figure 7.10 shows

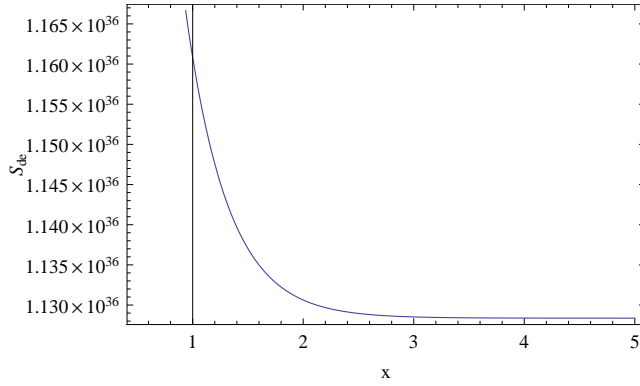


Figure 7.10: [The behavior of S_{de} against x for the parameters $(\alpha, \beta) = (1.2, 0.1)$ with $k = 1.25$ inside apparent horizon under thermal non-equilibrium condition]

that the entropy of dark energy is decreasing as the universe expands while figure 7.11 shows that the horizon entropy is increasing with x and the total entropy of the universe increases with x . Hence the GSL is valid at the apparent horizon of the universe dominated by dark energy under thermal non-equilibrium conditions.

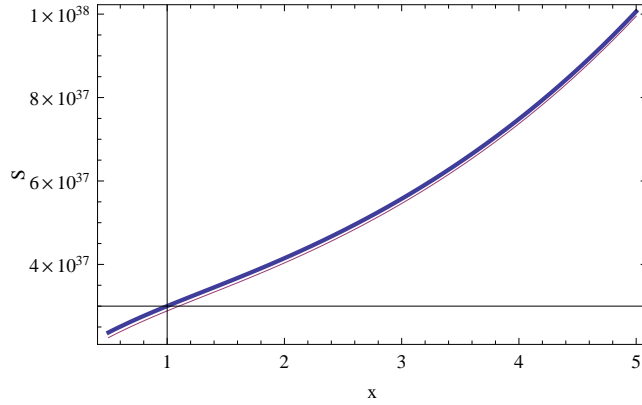


Figure 7.11: [The behavior of S_h along with S_{total} with x for the parameters $(\alpha, \beta) = (1.2, 0.1)$ inside apparent horizon under thermal non-equilibrium condition. The thick continuous line represents the total entropy S_{tot} and the thin line represents the entropy of the horizon S_h .]

7.3 Conclusion

The modified holographic Ricci dark energy in interaction with dark matter, with the interaction term $Q = 3bH\rho_{de}$, (IMHRDE3) in a flat FLRW universe is considered. The co-evolution of the energy densities of dark energy and dark matter is explained and evolution of the equation of state parameter and deceleration parameter is studied. The model predicts a late time acceleration of the universe. The statefinder parameters are used to distinguish the model from other dark energy models. The thermodynamics of the model is studied

Interacting modified holographic Ricci dark energy model with interaction term

which includes checking the validity of the GSL and the evolution of the entropy of the dark energy and the universe for a dark energy dominated universe.

First section include the study of the cosmological parameters of IMHRDE3. The co-evolution of the densities of dark energy and dark matter is explained for interaction parameter $b = 0.009$. The evolution of equation of state parameter shows that the present value of the parameter matches with the values of WMAP observations for the parameters $(1.01, -0.01)$ and $(1.2, -0.1)$. The characteristics of deceleration parameter shows that the present value of the parameter and the transition redshift z_T are very much closer to the SNe+CMB analysis results. Statefinder parameters (r, s) are used to find the present position of the universe predicted by the IMHRDE3 model which is quite different from other models.

Second section deals with the analysis of thermodynamics of IMHRDE3 model. The validity of GSL is checked assuming thermal equilibrium and non-equilibrium for a universe bounded by apparent horizon and event horizon separately. The thermal equilibrium study shows that the GSL is valid only when apparent horizon is taken as the boundary and not for event horizon. Hence apparent horizon can be the feasible thermodynamic boundary of the universe. This conclusion is in confirmation with the results of previous works on this subject for various other dark energy models. Under thermal non-

equilibrium condition, the validity of GSL demands that the temperature of dark energy to be greater than that of the apparent horizon, for a dark energy dominated universe. Studies such as [91, 95] showed that the GSL is valid for the case of thermal non-equilibrium conditions under particular constraints only. The evolution of the entropy of dark energy is studied for a universe dominated by dark energy and bounded by apparent horizon. The analysis shows that the entropy of dark energy decreases but the horizon entropy increase in such a way that the total entropy of the universe increases. As a result the GSL is valid for a dark energy dominated universe with apparent horizon as the boundary.

8

Extracting the model parameters

The study of the interacting modified holographic Ricci dark energy model(IMHRDE) well explained the acceleration of the universe. The model predicted better values for the present values of the equation of state parameter, deceleration parameter and transition redshift, also the co-evolution of dark energy and matter densities is accounted for. Statefinder parameters distinguishes the model from other dark energy models. The study of thermodynamics, which comprises analyzing the validity of GSL and the entropy evolution of the dark energy along with the entire universe, also favors the model. The whole analysis are done for different values of the IMHRDE model parameters (α, β) . For the theory to be effective it is necessary to know the best fit parameters for which the predictions made by the model to be much closer to the observations. This led to the need for

quantitative analysis. In fact the best fit model parameters we have used in the previous chapters are the result of our analysis which is described in the following section.

8.1 Statistical Methods

The parameter estimation were done using the Type Ia supernovae data. We have used modified chi square fitting method[97–102] to estimate the best fit parameters. To find out the best fit parameters of the model the method of least squares is used. The least squares is defined in simple form as

$$\chi^2 = \sum w_i [D_i - y_i], \quad (8.1)$$

where χ^2 is the function which quantify how much the data and the model agrees with and the minimum value of the function χ^2 is associated with the best fit parameters of the model, D_i are the data points, y_i represents the model points corresponding to its parameters and w_i is the weight and the minimum variance weight is $w_i = \frac{1}{\sigma_i^2}$, σ_i is the error on the data point i .

8.1.1 Determining the best fit parameters using Union2 compilation-SNLS+ESSENCE data

Union2 compilation-SNLS+ESSENCE data[104] (307 data points) is used for parameter extraction and fitting. The theoretical distance

modulus $\mu_{th}(z)$ is defined as

$$\mu_{th}(z_i) = 5 \log_{10} D_L(z_i) + 25, \quad (8.2)$$

where z is the redshift, and

$$D_L(z) = (1 + z) \int_0^z \frac{dz'}{h(z')}, \quad (8.3)$$

where $h(z) = \frac{H(z)}{H_0}$. The μ_{th} is calculated for each IMHRDE model.

The corresponding χ^2 function for the SNe 307 data is

$$\chi_{SN}^2 = \sum \frac{[\mu_{obs}(z_i) - \mu_{th}(z_i)]^2}{\sigma^2(z_i)}, \quad (8.4)$$

where $\mu_{obs}(z_i)$ is the observed value of the distance modulus of the supernova corresponding to redshift z_i . The χ_{SN}^2 is found for each data point corresponding to redshift in the range $0.01 < z < 1.6$ and the minimum value of χ^2 with respect to the model parameters is estimated. For the IMHRDE model, the minimum value of χ^2 and the best fit parameters corresponding to each model are respectively given below :

- IMHRDE1 : $\chi_{min}^2 = 312.411$, for $\alpha = 0.97$, $\beta = -0.01$, $H_0 = 70.01$,
- IMHRDE2 : $\chi_{min}^2 = 312.42$, for $\alpha = 0.97$, $\beta = -0.01$, $H_0 = 70.01$,
- IMHRDE3 : $\chi_{min}^2 = 431.935$, for $\alpha = 1.5$, $\beta = -0.01$, $H_0 = 75.47$.

Thus the best fit parameters for IMHRDE1 and IMHRDE2 are found to be corresponding with each other while a difference is seen in the case of IMHRDE3. To determine the precision of the parameters, error has to be estimated. This is done by drawing confidence contours.

8.1.2 Confidence Contours

Confidence regions are those which are drawn around best fit parameters. Plausibly, a region of parametric space of m -dimension (m corresponds to the number of parameters) which contain a probability distribution is to be selected. Compact regions around the best fit parameters are preferred. If parameter values are disturbed from the best fit, then the χ^2 value increases. The variation in the value of χ^2 is given by $\Delta\chi^2$. The confidence regions in the $\alpha - \beta$ plane are drawn in terms of the minimum value of χ^2 and $\Delta\chi^2$. That is, confidence regions are drawn by taking,

$$\chi^2 \leq \chi_{min}^2 + \Delta\chi^2. \quad (8.5)$$

For m number of parameters, n number of data points, the value of $\Delta\chi^2$ corresponding to the confidence limit p are given in the table 8.1

p(confidence limit)	$\Delta\chi^2$ for m=2
68.3%	2.30
95.4%	4.61
99.73%	11.8
99.99	18.4

Table 8.1: The $\Delta\chi^2$ value for various confidence limits for two parameters

8.1.3 Drawing confidence regions and error estimation for IMHRDE best fit model parameters

The confidence regions are drawn for each IMHRDE model for the parameters (α, β) fixing H_0 . The plot for IMHRDE1 best fit parameters as is shown in figure 8.1, the best fit parameters are,

- $\alpha = 0.97_{-0.22}^{+0.27}$,
- $\beta = -0.01_{-0.16}^{+0.21}$.

The confidence regions of IMHRDE2 are shown in figure 8.2. The best fit parameters of IMHRDE2 are found to be,

- $\alpha = 0.97_{-0.22}^{+0.26}$,
- $\beta = -0.01_{-0.16}^{+0.20}$.

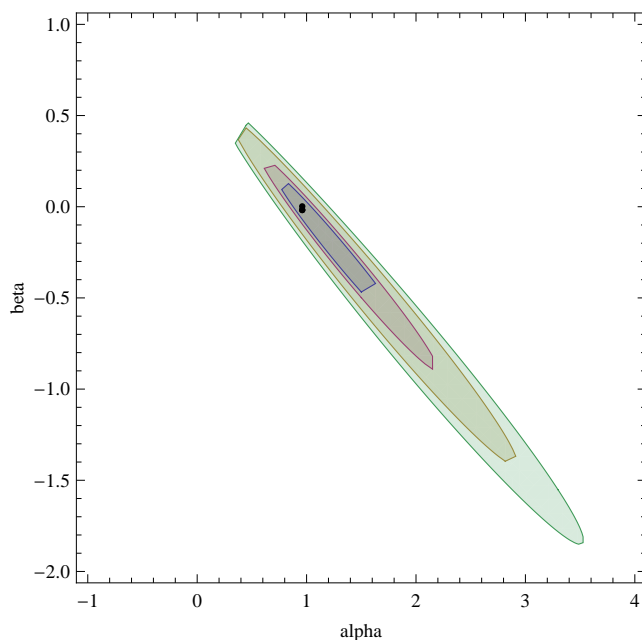


Figure 8.1: [confidence region of IMHRDE1 best fit parameters, outer contour represent 99.99% confidence region, the immediate next contour represent 97.3% confidence region, the next contour to it represent 95.4% confidence region and the inner most contour represent 68.3% confidence region.]

The confidence regions for the parameters of IMHRDE3 are shown in figure 8.3. The best fit parameters are obtained as.

- $\alpha = 1.5^{+0.95}_{-0.09}$,
- $\beta = -0.01^{+1.69}_{-0.33}$.

The IMHRDE1 and IMHRDE2 parameters corresponds to each other very well, while IMHRDE3 parameters are considerably different com-

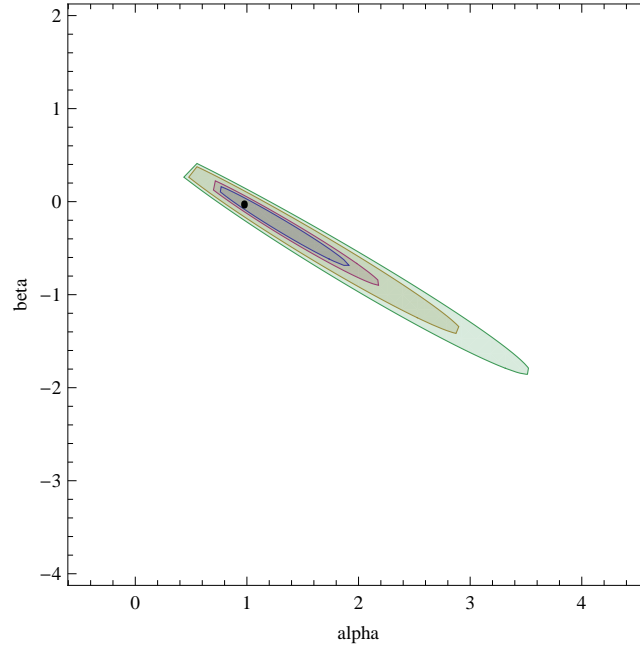


Figure 8.2: [confidence region of IMHRDE2 best fit parameters. Outer contour represent 99.99% confidence region, the immediate next contour represent 97.3% confidence region, the next contour to it represent 95.4% confidence region and the inner most contour represent 68.3% confidence region.]

pared with that of IMHRDE1 and IMHRDE2. For the analysis of both cosmology parameters and thermodynamics of IMHRDE, we adopt the parameter as obtained for IMHRDE1 and IMHRDE2. For practical purposes, we have found the average of both α and β by considering the error bars, and hence found the best estimates of the parameters as $(1.01, -0.01)$.

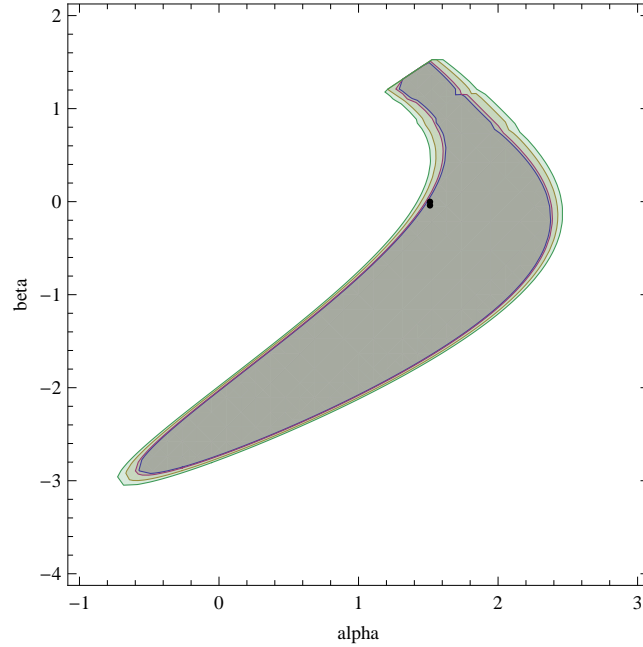


Figure 8.3: [confidence region of IMHRDE3 best fit parameters. Outer contour represent 99.99% confidence region, the immediate next contour represent 97.3% confidence region, the next contour to it represent 95.4% confidence region and the inner most contour represent 68.3% confidence region.]

8.1.4 Variation of distance modulus- comparison of theory and observation

Using the best fit parameters, the μ_{th} for each interacting model of IMHRDE is calculated and compared with the observational data for corresponding redshift values. The plot for IMHRDE1 is shown in figure(8.4). The plot shows that for IMHRDE1, the theory matches

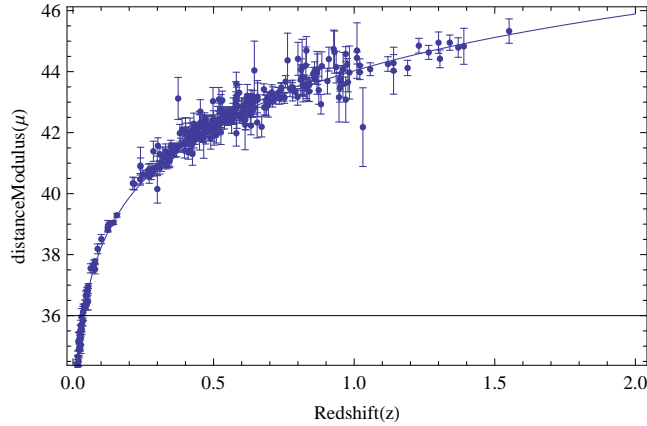


Figure 8.4: [IMHRDE1:continuous line represents theory, dots with error bars represent observation]

very well with the data.

The plot for IMHRDE2 is shown in figure(8.5). The figure shows that the theory and observation matches very well.

The plot of comparison for IMHRDE3 is shown in figure(8.6). The plot reveals that the theory and observation shows a poor match.

8.2 Conclusion

The quantitative statistical techniques are used to estimate best fit parameters of the model so that its predictions matches quite well with the observations quite. The χ^2 method is used to determine best fit parameters $(\alpha, \beta,)$ and H_0 for each IMHRDE model. The best fit parameters corresponds to that values which make χ^2 minimum. The

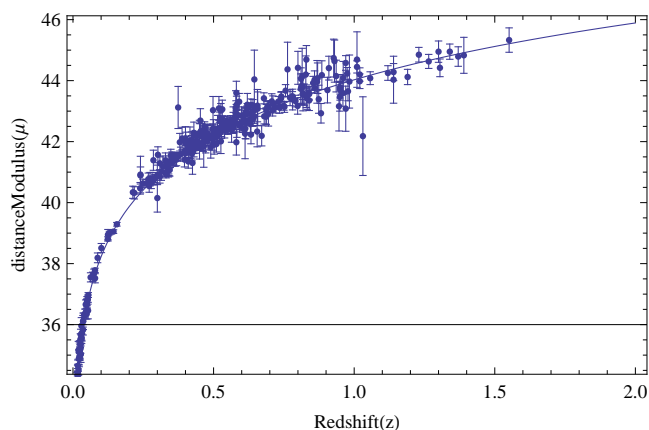


Figure 8.5: [IMHRDE2:continuous line represents theory, dots with error bars represents observation]

confidence regions are drawn corresponding to the limits 68.3%(1σ), 95.4%(2σ), 99.7%(3σ) and 99.99%(4σ). The correction factors for the best fit parameters are obtained in the case of each model. The parameters of IMHRDE1 and IMHRDE2 corresponds to each other very well, but not so with that of IMHRDE3.

The comparison of theory and observation of the distance modulus is carried out, in which the theoretical value is calculated using the best fit parameters. The plot of comparison clearly shows that the theory and data matches very well for IMHRDE1 and IMHRDE2, while that for IMHRDE3, it matches very poorly.

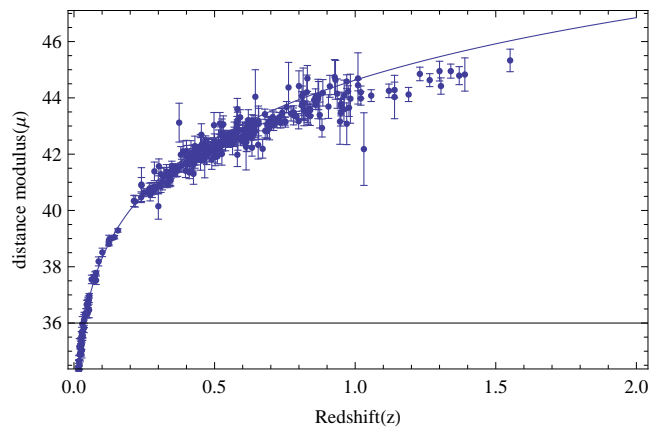


Figure 8.6: [IMHRDE3:continuous line represents theory, dots with error bars represents observation]

9

Conclusion

9.1 Major findings and conclusion

Discovery of the recent acceleration of the universe, has led to speculations that it is dark energy which causes the acceleration. But the nature and evolution of dark energy is still an unsettled problem. Various models have been proposed in the recent literature. Holographic Ricci dark energy model have been much discussed recently due to its promising nature. Since the dark energy and dark matter co-exist together they may possibly interact with each other. In this thesis we have analyzed both the cosmology and thermodynamics of holographic Ricci dark energy which is interacting with dark matter. The interaction of modified holographic Ricci dark energy(IMHRDE) with dark matter through a linear, non-gravitational interaction in a

flat FLRW universe is studied. The interaction is defined through the conservation equations with an additional interaction term Q , which has three phenomenological forms, $Q = 3bH(\rho_m + \rho_{de})$, $Q = 3bH\rho_m$ and $Q = 3bH\rho_{de}$, where b is the interaction parameter. The qualitative as well as quantitative analysis of the IMHRDE model with the three interaction terms are separately carried out.

The IMHRDE1 model is the one with interaction term

$Q = 3bH(\rho_m + \rho_{de})$. The co-evolution of dark energy and dark matter is studied for the interaction parameter $b = 0.001$, and found that the model is reasonably explaining it. But for $b > 0.001$ this coincidence cannot be explained. The best fit parameters are found to be $(\alpha, \beta) = (1.01, -0.01)$ in reference to the statistical analysis done which is described in chapter 8. The evolution of the equation of state parameter is studied and its present value given by $\omega_{de0} = -0.96$ for $(\alpha, \beta) = (1.01, -0.01)$ is very much closer to the WMAP value -0.93 . The dynamics of deceleration parameter is examined and its present value is obtained as $q_0 = -0.56$, very much in correspondence with the WMAP value -0.60 . The model is predicting the late time acceleration of the universe. The transition redshift, z_T is found to be 0.70 while the SNe+CMB analysis constraints it in the range $z_T \sim 0.45-0.73$. The statefinder analysis shows that the present value of the parameters are $(r_0, s_0) = (1.003, -0.0008)$ and when compared with the Λ CDM model points $(r, s) = (1, 0)$, it can be made out that

the model is not far from the Λ CDM model and has correspondence with the Chaplygin gas model which has $(r > 1, s < 0)$. On the other hand the IMHRDE1 seems to be different from other models for example from quintessence model, for which $(r < 1, s > 0)$ and the holographic dark energy model with event horizon as the IR cut off having $(r, s) = (1, 2/3)$.

The study of thermodynamics of the universe with IMHRDE1 is carried out and it comprised checking the validity of the generalized second law(GSL) of thermodynamics under both thermal equilibrium and non-equilibrium conditions existing between the contents of the universe, mainly IMHRDE1, dark matter, and the horizon limiting it. The analysis have shown that the model is viable only when the universe is bounded by the apparent horizon rather than the event horizon, so that the apparent horizon can be treated as a viable thermodynamic boundary. Further the evolution of entropy of dark energy is studied in a dark energy dominated universe, and it is found that the entropy of dark energy decreases, but the entropy of the apparent horizon is seen increasing and as a result there is an increase in the total entropy, which safeguard the validity of GSL.

The IMHRDE2 model is characterized by the interaction term $Q = 3bH\rho_m$. The coincidence between dark energy and dark matter is explained for $b = 0.003$. The evolution of equation of state ω_{de} and deceleration parameter q as a function of redshift is studied. In

this case also the universe is found to be showing a recent acceleration. The present value of equation of state parameter is obtained as $\omega_{de0} = -0.96$, which is close to the WMAP value -0.93 for the best fit parameters $(\alpha, \beta) = (1.01, -0.01)$. The present value of the deceleration parameter is found to be $q_0 = -0.55$, whereas the WMAP value is $q_0 = -0.60$, while the transition redshift is found to be $z_T = 0.68$, perfectly lying in the SNe+CMB observational range, $z_T \sim 0.45-0.73$. Statefinder parameters (r, s) are used to characterize the uniqueness of the model and the present value of the parameters are obtained as $(r_0, s_0) = (1.03, -0.0096)$. The Λ CDM point corresponds to $(r_0, s_0) = (1, 0)$. Thus even though the model is distinguishable from Λ CDM, its present position is close to it. This surely tells that the IMHRDE2 model is nearer in quality to the Λ CDM model and have parameters in the range similar to the Chaplygin gas model with $(r > 1, s < 0)$ and is different from other dark energy models such as the quintessence model which has $(r < 1, s > 0)$ and the holographic dark energy model with event horizon as the IR cut off with $(r, s) = (1, 2/3)$.

The validity of generalized second law(GSL) is checked for a universe with IMHRDE2 bounded by apparent horizon and event horizon separately, under both thermal equilibrium and non-equilibrium conditions. The study revealed that the GSL is valid only for the universe bounded by apparent horizon. Another result is that in a dark en-

energy dominated universe, the entropy of the dark energy is seen to be decreasing which gets compensated by the increase in entropy of the apparent horizon so that the total entropy gets increasing. Thus the GSL is again valid for such a universe.

The IMHRDE3 model have the interaction term $Q = 3bH\rho_{de}$. The co-evolution of dark energy and dark matter is explained satisfactorily in this model also for the interaction parameter $b = 0.009$. The coincidence is not seen for values greater than this. The evolution of equation of state parameter ω_{de} , deceleration parameter q as a function of redshift is studied. The present value of equation of state parameter is obtained as $\omega_{de0} = -0.97$ which is close to the WMAP value -0.93 , for the best fit parameters $(\alpha, \beta) = (1.01, -0.01)$. The present value of the deceleration parameter is found to be $q_0 = -0.57$, whereas the WMAP value is $q_0 = -0.60$. The transition redshift z_T is found to have the value 0.70 which lies in the observational range of $z_T \sim 0.45 - 0.73$. The analysis using statefinder parameters have shown that the present position of the universe have the parameter values $(r_0, s_0) = (1.003, -0.0008)$ which is close to the Λ CDM point $(r, s) = (1, 0)$, and the Chaplygin gas model with $(r, s) = (r > 1, s < 0)$, but different from other dark energy models such as the holographic dark energy model with event horizon as the IR cut off which has $(r, s) = (1, 2/3)$, quintessence model with $(r < 1, s > 0)$.

The thermodynamic characteristics for a universe consisting of IMHRDE3 is studied. It included checking the validity of the generalized second law of thermodynamics(GSL) and the evolution of entropy of the dark energy. The analysis is done for the universe bounded by apparent horizon, as well as by event horizon separately, assuming the cases of both thermal equilibrium and non-equilibrium existing between the contents of the universe and the horizon bounding them. The inference is that the GSL is valid for the universe surrounded by apparent horizon. The entropy of IMHRDE3 is seen to decrease in an IMHRDE3 dominated universe, but the entropy of the apparent horizon increase in such a way that the total entropy is seen increasing thus validating the GSL for such a universe.

We have used the χ^2 method to determine the best fit parameters. We have used Union2 data on Type Ia supernovae for this, the results are summarized below:

- The best fit parameters are those which corresponding for the minimum value of the χ^2 and they are:
 1. For IMHRDE1 : $\chi_{min}^2 = 312.411$, corresponding to $\alpha = 0.97$, $\beta = -0.01$, $H_0 = 70.01$
 2. For IMHRDE2 : $\chi_{min}^2 = 312.42$, corresponding to $\alpha =$

$$0.97, \beta = -0.01, H_0 = 70.01$$

3. For IMHRDE3 : $\chi_{min}^2 = 431.935$, corresponding to $\alpha = 1.5, \beta = -0.01, H_0 = 75.47$

Since the values corresponding to IMHRDE1 and IMHRDE2 are satisfying with both the cosmological and thermal evolution of the model, we have adopted these values predominantly in our work. However, in taking the values of α and β , we took the corresponding averages including the error bars. Hence the parameters (1.01, -0.01) becomes the best fit.

- The correction in best fit parameters are found out from confidence contours for a fixed Hubble parameter H_0 . They are :

1. $\alpha = 0.97_{-0.22}^{+0.27}$ and $\beta = -0.01_{-0.16}^{+0.21}$, fixing $H_0 = 70.01$ for IMHRDE1

2. $\alpha = 0.97_{-0.22}^{+0.26}$ and $\beta = -0.01_{-0.16}^{+0.20}$, fixing $H_0 = 70.01$ for IMHRDE2

3. $\alpha = 1.5_{-0.09}^{+0.95}$ and $\beta = -0.01_{-0.33}^{+1.69}$, fixing $H_0 = 75.47$ for IMHRDE3

- The parameters of IMHRDE1 and IMHRDE2 corresponds to each other while do not match with that of IMHRDE3.

- Plot showing comparison of theoretical and observational values of distance modulus points to the fact that IMHRDE1 and IMHRDE2 shows a good match of theoretical and observational values while IMHRDE3 shows a poor match.

Thus it is be inferred that IMHRDE1 and IMHRDE2 are preferred more when compared to IMHRDE3.

9.2 Scope for further study

The exact nature of the physical origin of Ricci dark energy is not known. It can only be explained by constructing a proper Lagrangian through the field theoretical formulation which will be a challenging work in the future.

The IMHRDE model explains an early decelerating era in the evolution of the universe, which is of course the recent matter dominated phase, from which the transition to the accelerating period which is the present period has been explained clearly by the model. But the radiation dominated era is not accounted for and this also can be a task for the further study.

The effect of the IMHRDE on the structure formation and on the CMB radiation is another significant work that can be pursued in future. Regarding the effect on CMB, it will be a challenging task to obtain the effect of IMHRDE on the late time evolution of CMB like

Integrated Sachs-Wolfe (ISW) effect.

Studies regarding the nature of interaction has scope. For our study, we have considered the interaction in a phenomenological way and is non-gravitational in nature. Only a quantum mechanical treatment will reveal the exact nature of interaction between the dark sectors.

A suitable method for such an analysis is studying the phase space structure of the model.

References

- [1] Edward W Kolb and Michael S Turner, "The Early Universe", Addison-Wesley Publishing Co., (1990).
- [2] Unsold A and Bodo B, "The New Cosmos, An Introduction to Astronomy and Astrophysics (5th ed.)", SpringerVerlag, 485, (2002).
- [3] Tegmark et.al., Phys. Rev. D, **74**, 123507, (2006).
- [4] Colless M et al., arXiv:astro-ph/0306581.
- [5] Sanchez A G et al., Mon. Not. R. Astron. Soc., **366**, 189, (2006).
- [6] Peacock J A et al., Nature, **410**, 169, (2001).
- [7] Perlmutter S et al., Astrophys. J., **517**, 565, (1999).
- [8] Riess A et al., Astron. J., **116**, 1009, (1998).
- [9] Spergel D N et al., [WMAP Collaboration], arXiv:astro-ph/0603449.
- [10] Seljak U et al., Phys. Rev. D, **71**, 103515, (2005).
- [11] Friedmann A, Z. Phys. ,**10**, 377, (1922).
- [12] Lamaitre G, Mon. Not. R. Astron. Soc., **91**, 483, (1931).

-
- [13] Robertson H P, " Kinematics and world-structure", ApJ, **82**, 284, (1935).
- [14] Walker A G, "On the milne's theory of world-structure", Proc.London.Math.Soc., **s2-42**, 90, (1937).
- [15] Weinberg S, "Gravitation and Cosmology", John Wiley and Sons, Inc., (1972).
- [16] Komatsu E et al., Astrophys. J Suppl. , **192**, 18, (2011).
- [17] Larson D et al., Astrophys. J Suppl. , **192**, 16, (2011).
- [18] Percival W J, et al., Mon. Not. Roy. Astron. Soc., **401**, 2148, (2010).
- [19] Leavitt H S, Annals of Harvard College Observatory, **60**, 87, (1908).
- [20] Copeland E J, Sami M and Tsujikawa S, Int. J. Mod. Phys. D, **15**, 1753, (2006).
- [21] Reichardt C L et al., astro-ph/ 0801.1491, 801, (2008).
- [22] Eisenstein et al., Astrophys. J., **633**, 560, (2005).
- [23] Frieman J A, Turner M S and Huterer D, Ann. Rev. Astron. Astrophys., **46**, 385, (2008).

-
- [24] Krauss L M and Chaboyer B, *Science*, **299**, 65, (2003).
- [25] Weinberg S, *Rev. Mod. Phys.*, **61**, 1, (1989).
- [26] Bousso R, *Gen. Relativ. Gravit.*, **40**, 607, (2008).
- [27] Einstein A, *Sitzungsber. K. Akad.*, **6**, 142, (1917).
- [28] Luca Amendola and Shinji Tsujikawa, "Dark Energy: Theory and Observations", cambridge University press, (2010).
- [29] Bamba K, Capozziello S, Nijori S and Odintsov S D, *Astrophys. Space Sci.*, **342**, 155, (2012).
- [30] Wetterich C, *Nuc. Phys. B*, **302**, 668, (1988).
- [31] Peebles P J E and Ratra B, *Astrophys. J.*, **325**, L17, (1988).
- [32] Chiba T, Okabe T and Yamaguchi M, *Phys. Rev. D*, **62**, 023511 (2000).
- [33] Armendariz-Picon C, Mukhanov V F and P J Steinhardt, *Phys. Rev. Lett.*, **85**, 4438, (2000).
- [34] Armendariz-Picon C, Mukhanov V F and P J Steinhardt, *Phys. Rev. D*, **63**, 103510, (2001).
- [35] Corasanati P S, Kunz M, Parkinson D, Copeland E J and Basset B A, *Phys. Rev. D*, **70**, 083006, (2004).

-
- [36] Knop R A, et al., *Astrophys. J.*, **598**, 102, (2003).
- [37] Alam U, Sahni V, Saini T D and Starobinski A A, *Mon. Not. Roy. Astron. Soc.*, **354**, 275, (2004).
- [38] Singh P and Dadhich N, *Phys. Rev. D* ,**68**, 023522, (2003).
- [39] Sami M and Toporensky A, *Mod. Phys. Lett. A*, **19** , 1509, (2004).
- [40] Caldwell R R, *Phys. Lett. B*, **545**, 23, (2002).
- [41] Nojiri S and Odintsov S D, *Phys. Lett. B*, **562**, 147, (2003).
- [42] Nojiri S and Odintsov S D, *Phys. Lett. B*, **565**, 1, (2003).
- [43] Carroll S M, Hoffman M and Trodden M, *Phys. Rev. D*, **68**, 023509, (2003).
- [44] Caldwell R R, Kamionkowski M and Weinberg N N, *Phys.Rev.Lett.*, **91**, 071301, (2003).
- [45] Kamenshchik A, Moschella U and Pasquier V, *Phys. Lett. B*, **511**, 265 (2001).
- [46] Bento M C, Bertolami O and Sen A A, *Phys. Rev. D*, **66**, 043507 (2002).
- [47] Li M, Li X.-D, Wang S and Wang Y, *Commun. Theor. Phys.*, **56**, 525, (2011).

-
- [48] Wang F Y and Dai Z G, *Mon. Not. R. Astron. Soc.*, **368**, 371, (2006).
- [49] Melchiorri A et al., *Phys. Rev. D*, **76**, 041301, (2007).
- [50] Fa-Yin Wang, Zi-Gao Dai and Shi Qi, *Research in Astron. Astrophys.*, **9**, 547, (2009).
- [51] Amendola L, Finelli F, Burigana C and Carturan D, *JCAP*, **0307**, 005, (2003).
- [52] Bilic N, Tupper G B and Viollier R D, *Phys. Lett. B*, **535**, 17, (2002).
- [53] Bento M C, Bertolami O and Sen A A, *Phys. Rev. D*, **67**, 063003, (2003).
- [54] Gerard 't Hooft, arXiv:gr-qc/9310026, (1993).
- [55] Susskind L, *J. Math. Phys.*, **36**, 6377, (1995).
- [56] Miao Li, *Phys. Lett. B*, **603**, 1, (2004).
- [57] Fischler W and Susskind L, hep-th/9806039.
- [58] Hawking S W, *Phys. Rev. Lett.*, **26**, 1344, (1971).
- [59] Hawking S W, *Commun. Math. Phys.*, **25**, 152, (1972).
- [60] Bekenstein J D, *Nuovo Cim. Lett.*, **4**, 737, (1972).

-
- [61] Bekenstein J D, Phys. Rev. D, **7**, 2333, (1973).
- [62] Bekenstein J D, Phys. Rev. D, **9**, 3292, (1974).
- [63] Hawking S W, Nature, **248**, 30, (1974).
- [64] Andrew G Cohen, David B Kaplan and Ann E Nelson, Phys. Rev. Lett., **82**, 4971, (1999).
- [65] Hsu S D H, Phys. Lett. B, **594**, 13, (2004).
- [66] Kim H -C , Lee J -W and Lee J, epl, **102**, 29001, (2013).
- [67] Granda L N and Oliveros A, Phys. Lett. B, **669**, 275, (2008).
- [68] Gao C, Wu F, Chen X and Shen Y -G, Phys. Rev. D, **79**, 043511, (2009).
- [69] Wei H and Zhang S N, Phys. Rev. D, **76**, 063003, (2007).
- [70] Cai R G, Phys. Lett. B, **657**, 228, (2007).
- [71] Titus K Mathew, Jishnu Suresh and Divya Divakaran, Int. J. Mod. Phys. D, **22**, 1350056, (2013).
- [72] Sahni V, Saini T D, Starobinsky A A and Alam U, JETP Lett., **77**, 201, (2003).
- [73] Sahni V and A. A. Starobinsky, Int. J. Mod. Phys. D, **9**, 373, (2000).

-
- [74] Chimento L P and Richarte M G, Phys. Rev. D, **84**, 123507, (2011).
- [75] Chattopadhyay S, Eur. Phys. J. Plus, **126**, 130, (2011).
- [76] Setare M R, Phys. Lett. B, **666**, 111, (2008).
- [77] Setare M R, Eur. Phys. J. C, **52**, 689, (2007).
- [78] Fu T -F, Zhang J -F, Chen J -Q and Zhang X, Eur. Phys. J. C, **72**, 1932, (2012).
- [79] Praseetha P and Titus K Mathew, Int. J. Mod. Phys. D, **23**, 1450024 , (2014).
- [80] Praseetha P and Titus K Mathew, Class. Quantum Grav., **31**, 185012, (2014).
- [81] Sheykhi A, Phys. Lett. B, **682**, 329, (2010).
- [82] Alam U, Sahni V and Starobinsky A A, J. Cosmol. Astropart. Phys., **406**, 008, (2004).
- [83] Bekenstein J D, Phys. Rev. D, **12**, 3077, (1975).
- [84] Bak D and Rey S J, Classical Quantum Gravity, **17**, L83, (2000).
- [85] Cai R -G, Cao L -M, Hu Y -P, Class. Quantum Gravity, **26**, 155018, (2009).

-
- [86] Hawking S W, Nature, **248**, 30, (1974).
- [87] Karami K, Ghaffari S and Soltanzadeh M M, Class. Quantum Grav., **27**, 205021, (2010).
- [88] Wang B, Gong Y and Abdalla E, Phys. Rev. D, **74**, 083520, (2006).
- [89] Wang B, Gong Y and Abdalla E, Phys. Lett. B, **624**, 141, (2005).
- [90] Jamil M, Saridakis E N and Setare M R, Phys. Rev. D, **81**, 023007, (2010).
- [91] Debnath U, Chattopadhyay S, Hussain I, Jamil M and Ratbay Myrzakulov, Eur. Phys. J. C, **72**, 1875, (2012).
- [92] Sheykhi A, Class. Quantum Grav., **27**, 025007, (2010).
- [93] Sheykhi A, Eur. Phys. J. C, **69**, 265, (2010).
- [94] Titus K Mathew and Praseetha P , Mod. Phys. Lett., **29**, 1450023, (2014).
- [95] Sadjadi H M and Jamil M, Eur. Phys. Lett., **92**, 69001, (2010).
- [96] Praseetha P and Titus K Mathew , Pramana-J.Phys.(accepted), (2015).
- [97] Alan Heaven, arXiv:0906.664, (2009).

-
- [98] Licia Verde, Lecture Notes in Physics Volume, **800**, 147, (2010).
- [99] Press et al., Numerical Recipes: the art of scientific computing, Cambridge University Press, (1992).
- [100] Wall J P and Jenkins C R, Practical Statistics for Astronomers, Cambridge University Press, (2003).
- [101] Fisher R A, J. Roy. Stat. Soc., **98**, 39, (1935).
- [102] Schwarz G, Annals of Statistics, **5**, 461, (1978).
- [103] O' Hagan A, Kendall's Advanced theory of statistics, Volume 2b, Bayesian Inference, Arnold, (1994).
- [104] Kowalski M et al., Astrophys. J., **686**, 749, (2008).

Appendix

List of Publications

1. Praseetha P and Titus K Mathew, "Interacting modified holographic Ricci dark energy model and statefinder diagnosis in flat universe", *Int. J. Mod. Phys. D*, **23**, 1450024 ,(2014). (arXiv no: 1309.3136)
2. Titus K Mathew and Praseetha P, "Holographic dark energy and generalized second law", *Mod.Phys.Lett.A*, **29**, 1450023, (2014). (arXiv no: 1311.4661)
3. Praseetha P and Titus K Mathew, "Entropy of holographic dark energy and the generalized second law", *Class. Quant. Grav.*, **31**, 185012, (2014). (arXiv no: 1401.8117)
4. Praseetha P and Titus K Mathew, "Evolution of holographic dark energy with interaction term $Q \propto H\rho_{de}$ and generalized second law", *Pramana-J.Phys.*(accepted for publication), (2015).